Stony Brook University

In search of miRNA function in the mouse neocortex and cerebellum

A Dissertation Presented

by

Miao He

to

The Graduate School

in Partial Fulfillment of the

Requirements

for the Degree of

Doctor of Philosophy

in

Genetics

Stony Brook University

August 2011

Stony Brook University

The Graduate School

Miao He

We, the dissertation committee for the above candidate for the
Doctor of Philosophy degree, hereby recommend
acceptance of this dissertation

Dr. Z. Josh Huang. Dissertation advisor
Professor, Cold Spring Harbor Laboratory

Dr. Joshua Dubnau. Chairman of Defense
Associate Professor, Cold Spring Harbor Laboratory

Dr. Gregory Hannon.
Professor, Cold Spring Harbor Laboratory

Dr. Michael Zhang
Professor, Cold Spring Harbor Laboratory
(Currently: Cecil H. and Ida Green Distinguished Chair, UT Dallas)

Dr. Howard Sirotkin
Associate Professor, Stony Brook University

Dr. Oliver Höbert
Professor, Columbia University

This dissertation is accepted by the Graduate School

Lawrence Martin
Dean of the Graduate School

Abstract of the Dissertation

In search of miRNA function in the mouse neocortex and cerebellum

by

Miao He

Doctor of Philosophy

in

Genetics

Stony Brook University

2011

MicroRNAs (miRNA) are implicated in brain development and function, but the underlying mechanisms have been difficult to study in part due to the cellular heterogeneity in neural circuits. The cellular diversity of the brain necessitates studies at the level of individual neuron types. During my thesis research, I have taken two complementary approaches to study miRNA function in mouse neocortex and cerebellum. One is to analyze cell type specific miRNA expression profiles, and the other is to disrupt miRNA production in subpopulations of cortical GABAergic neurons.

To establish genetic access of diverse interneuron subtypes, our laboratory has initiated the first round of a systematic effort to generate and characterize knockin Cre or CreER driver lines that target major classes and lineages of GABAergic neurons. I have contributed significantly to this effort by generating and characterizing several Cre lines that target several interneurons classes.

The main component of my thesis research is the invention of a miRNA-tagging and affinity purification method, miRAP, which can be targeted to cell types through the Cre-loxP binary system in genetically engineered mice. Using this method, my miRNA profiling study of several neuron types in the neocortex and cerebellum revealed the expression of a large fraction of known miRNAs with distinct profiles in glutamatergic and GABAergic neurons, and in subtypes of GABAergic neurons. I have further detected putative novel miRNAs and miRNA editing in subset of neuron types. Our method thus will facilitate a systematic analysis of miRNA expression and regulation in specific neuron types in the context of neuronal development, physiology, plasticity, pathology and disease models, and is generally applicable to other cell types and tissues.

Furthermore, I have used cell type specific knockout of Dicer to examine of role of miRNAs in interneuron development and physiology. My studies show that loss of miRNAs affects the intrinsic properties of cortical VIP neurons but not those of PV or SST neurons, while cell survival was not affected in any of the three interneuron subtypes. Thus my current results suggest that depletion of miRNAs has rather subtle effects on cortical interneurons. It is likely that miRNAs are involved in regulating the function and plasticity of interneurons in physiological and pathological conditions that are yet to be defined by future studies.

Table of Contents

List of Figures

List of tables

Acknowledgments

I would like to first give my greatest gratitude to my thesis advisor, Dr. Z. Josh Huang, for his continuous support during my PhD research. He has provided invaluable scientific guidance and warm encouragement to my work. His enthusiasm has been my inspiration to strive on the path of science.

I thank Dr. Michael Zhang for collaboration and discussion. His student Yu Liu is my main collaborator, who did most of the bioinformatic analysis for me in the miRAP project.

I thank Dr Gregory Hannon for guidance and suggestions. I spent a lot of time in the Hannon lab hot room, where I had sweet and bitter memories. I am grateful to a number of people in his lab: Ingrid, Astrid, Sihem, Antoine, Ted, Marek and Gordy, who taught me the small RNA cloning technique, initial analysis of deep sequencing result, and had helpful discussions with me on the miRAP project.

I thank Dr Joshua Dubnau, Howard Sirotkin, and Oliver Hobert for being part of my thesis committee, giving me critical feedback and insightful comments.

I thank all the present and past members of Huang lab, especially the following people. Graziella Di Cristo, who advised me during my rotation and introduced me to the field of neuroscience. Priscilla Wu, who is an indispensible person in Huang lab to make our lab function so well and so smoothly; we have had wonderful collaboration on the Cre driver project, as well as a few small side projects. Hiroki Taniguich, who is a great

scientist, always keeps the scientific goal in mind and finds his way to achieve it, no matter how difficult it could be; I admire his attitude towards science, and benefited a lot from discussing and collaborating with him. Anirban Paul, who opened the door of miRNA research for me; his braveness in trying outing new methods and exploring new ideas encouraged me to step into a new field. Yu Fu and Xiaoyun Wu, who are my best friends in the lab; I envy their optimistic attitude toward everything, which brought so much fun to my life inside and outside the lab. Jiangteng Lu, who did all the electrophysiology work in Dicer KO project for me. Keerthi Krishnan, who developed the FACS sorting protocol and provided some mice for my experiment. Ying Lin, Matt Lazarus, Jason Tucciarone, Caizhi Wu and others who gave me kind support and helpful suggestions.

I thank my classmates in SBU Genetics program, Mike, Azad, Mary, Kinga, Nadine, Joe, and Ruei-ying. My first year in US would be miserable without your friendship. I always miss the time we spent together to discuss homework, play games, have dinner and wonder how time flies. It feels like we just started our first year yesterday, but now some of you already graduated and started a new chapter of life. I wish the best to all of you, and wish one day we will get together again.

I thank people in the Genetics program in Stony Brook University, especially the program coordinator, Kate Bell, and the previous and current program directors, Dr. Gerald Thomsen, Peter J. Gergen and Turhan Canli, for their help and support.

I thank all my friends in SBU and CSHL, to name a few, Rui, Ying, Qiaojie, Wanhe and Yang. I am not a very social person and always afraid of challenges in life. Your friendship and support kept me going when times are rough. I enjoy the time we make dumplings, singing karaok, playing volleyball, gardening and doing so many other things together. I wish we will be good friends forever!

Last but not least, I would like to thank my mom and dad, who have only one child but still let me go so far away to chase my dream. Although you always say you cannot help me much due to the long distance, your love and support is the dearest to my heart and the best I could get. I also thank my husband for his understanding and support. I love you all dearly.

Chapter 1. Introduction

Brain function relies on the operation of neural circuits which often consist of diverse neuron types with stereotyped location, connectivity patterns, and physiological properties. To a large extent, the identity and physiological state of neuron types are determined by their patterns of gene expression (Nelson, Hempel et al. 2006)(Hobert, Carrera et al. 2010). In addition to gene transcription which dictates mRNA production, the stability and translation of mRNAs are regulated by microRNAs (miRNAs) (Bartel 2004), the class of 20~23nt small noncoding RNAs. miRNAs can also influence transcription by regulating the expression transcriptional factors (Hobert 2004). As main regulators of gene expression, miRNAs can play very important roles in the generation and maintenance of cellular diversity of the brain.

The mammalian brain is a prominent site of miRNA expression, often with specific spatial and temporal expression patterns (Landgraf, Rusu et al. 2007; Bak, Silahtaroglu et al. 2008). Recent studies begin to reveal diverse role of miRNAs in neural patterning (Ronshaugen, Biemar et al. 2005), neural stem cell differentiation (Kuwabara, Hsieh et al. 2004; Krichevsky, Sonntag et al. 2006), cell type specification (Chang, Johnston et al. 2004; Poole and Hobert 2006), synaptic plasticity (Schratt, Tuebing et al. 2006), and also in neurological disorders (Shafi, Aliya et al. 2010; Wu, Tao et al. 2010; Liu and Xu 2011). However, the mechanism and logic by which miRNAs regulate

neuronal development, function, plasticity and pathology are not well understood, partially due to the heterogeneity of neurons in the brain.

The cellular complexity of the brain necessitates miRNA research on cellular resolution. Individual cell types are the building blocks of neural circuits as well as the basic units of gene regulation (Monyer and Markram 2004). In order to study miRNA function at the level of cell type, I utilized Cre-loxP binary system in genetically modified mice to profile miRNA expression and disrupt miRNA maturation in specific neuron types and subtype of GABAergic neurons. The knowledge gained through my study will help to advance our knowledge and direct functional studies of miRNA in the brain.

1.1 miRNA function and biogenesis

MicroRNAs(miRNAs) are a group of endogenous expressed 20~23nt small noncoding RNAs, which can directly regulate mRNA stability or translation in a sequence specific manner by incomplete base pairing at the 3'UTR of target mRNA (Bartel 2004), or indirectly affect transcriptional network by regulating transcription factors (Hobert 2004). As key regulators of gene expression, miRNAs are involved in the control of diverse developmental and physiological processes, including embryogenesis, differentiation, developmental timing, organogenesis, growth control, and programmed cell death (He and Hannon 2004). Aberrant miRNA expression profiles have been observed in many pathological conditions, including cancers (Calin and Croce 2006), psychiatric diseases (Schratt 2009), virus infection(Skalsky and Cullen 2010), etc.

The discovery of miRNAs added a new layer to gene regulation network. The first miRNA, Lin-4, was discovered in C. elegans. It regulates cell lineage through recognizing the binding site in 3' UTR of Lin-14 mRNA (Lee, Feinbaum et al. 1993). Since then, increasing number of miRNAs are discovered in multiple species, a lot of which are highly conserved during evolution. To date, there are nearly 20,000 miRNAs deposited in miRbase in 153 species (miRbase V17), and the number is still increasing. One miRNA could regulate several to hundreds of mRNAs. In multicellular organisms, miRNAs are estimated to regulate half of the coding RNAs by bioinformatic predictions. miRNAs could work as binary switches (Reinhart, Slack et al. 2000; Cohen, Brennecke et al. 2006; Li, Wang et al. 2006) or fine turning controllers (Karres, Hilgers et al. 2007), depends on the level of target repression and the relative abundance of miRNA and their targets.

miRNAs biogenesis is a multi-step process (He and Hannon 2004). The canonical maturation pathway starts from transcription of miRNA genes by RNA polymerase II to generate long primary transcripts (pri-miRNA) harboring one or more miRNA stem-loops. RNA polymerase III (Pol III) transcribes some miRNAs, especially those with upstream Alu sequences, transfer RNAs (tRNAs), and mammalian wide interspersed repeat (MWIR) promoter units (Faller and Guo 2008). The "Microprocessor" complex formed by Drosha, an RNase III endonuclease, and DGCR8, recognize the double-stranded RNA structure of the hairpins in pri-miRNA, cleaves it to produce precursor-miRNA (pre-miRNA). Pre-miRNA has a two-nucleotide overhang at its 3' end; it has 3' hydroxyl and 5' phosphate groups (Gregory, Chendrimada et al. 2006). Some pre-

miRNAs, known as “Mirtrons” are spliced directly out of introns, bypass this step (Berezikov, Chung et al. 2007). Pre-miRNAs are transported by Exportin-5 to the cytoplasm, where the RNase III enzyme Dicer cuts away the loop joining the 3’ and 5’ arms, yielding miRNA::miRNA* duplexes (Lund and Dahlberg 2006). Usually, one strand of the duplex is preferably incorporated into the RNA-induced silencing complex (RISC complex) to regulate mRNA stability and translation.

RISCs reside in cytoplasmic RNA processing bodies (P bodies), which contain untranslated mRNAs and can serve as sites of mRNA degradation and storage (Liu, Rivas et al. 2005; Sen and Blau 2005). Members of the Argonaute (Ago) protein family are at the core of RISC complex. Two conserved RNA binding domains, PAZ and PWI are essential for Argonautes function. PAZ binds the single stranded 3’ end of the mature miRNA, while PIWI interacts with the 5’ end of the guide strand to orient it for interaction with a target mRNA. (Mourelatos, Dostie et al. 2002). In human and mouse genome, there are eight argonaute proteins divided into two sub-families: AGO (with four members present in all mammalian cells), and PIWI (found in the germ line and hematopoietic stem cells) (Pratt and MacRae 2009). If there is complete complementation between miRNA and the target RNA sequence, Ago2, one member of the Ago subfamily, can cleave the RNA target and lead direct RNA degradation. If there is incomplete complementation, the silencing can be achieved by repressing translation or decrease RNA level by means independent of target cleavage (Lim, Lau et al. 2005; Pillai 2005). For example, it can speed up deadenylation to increase the rate of RNA degradation (Eulalio, Huntzinger et al. 2009). Occasionally, some miRNAs can also cause histone

modification and DNA methylation of promoter sites to modulate gene expression on the transcriptional level (Hawkins and Morris 2008; Tan, Zhang et al. 2009).

Target recognition of miRNA requires conserved Watson–Crick pairing to the 5′ region of the miRNA centered on nucleotides 2–7, which is called the miRNA "seed" region (Brennecke, Stark et al. 2005). The remainder of the miRNA usually supplements seed pairing to enhance binding specificity and affinity, such as 3′-supplementary sites which optimally centers on miRNA nucleotides 13–16 and the UTR region directly opposite this miRNA segment, providing additional base pairing, and sometimes compensate the single-nucleotide bulge or mismatch in the seed region (Grimson, Farh et al. 2007).miRNA binding sites usually reside in the 3'-UTR of target mRNAs, although recent studies reveal binding sites within 5' UTR, open reading frame and introns (Chi, Zang et al. 2009).

1.2 miRNA and neuronal system

Recent studies demonstrate critical role of miRNAs in neural patterning (Ronshaugen, Biemar et al. 2005), neural stem cell differentiation (Kuwabara, Hsieh et al. 2004; Krichevsky, Sonntag et al. 2006), cell type specification (Chang, Johnston et al. 2004; Poole and Hobert 2006), synaptic plasticity(Schratt, Tuebing et al. 2006), neuron degeneration (Schratt, Tuebing et al. 2006; Bushati and Cohen 2008; Nelson, Wang et al. 2008) and apoptosis (Baehrecke 2003; De Pietri Tonelli, Pulvers et al. 2008).

At the neural patterning level, neural miRNAs are important for segmentation and differentiation or maintenance of tissue identity but not essential for tissue fate

establishment in zebra fish and mice (Bernstein, Kim et al. 2003; Giraldez, Cinalli et al. 2005). At the cellular level, miRNA can regulate specification of individual cell types in a tissue and in the maintenance of cell fate identity. The best characterized example is in the development of left–right asymmetry in C. elegans ASE neurons. ASEL (ASE left) and ASER (ASE right) neurons share many bilaterally symmetrical features, but express distinct sets of chemoreceptors. This asymmetry is determined by a double-negative feedback loop constituted by two miRNAs, *lsy-6* and miR-273, and one transcription factor *die-1* (Johnston and Hobert 2003; Chang, Johnston et al. 2004; Johnston, Chang et al. 2005). The recent discovery that the expression of miR-9/9* and miR-124 in human fibroblasts in causes their conversion into neurons, further proves the their essential role of miRNAs in neural fate determination in mammals (Yoo, Sun et al. 2011). At the synaptical level, miRNAs regulate neural dendritogenesis (eg, miR-124, 132 and 124) , synapse formation and synapse maturation (eg, miR-134 and 138) (Schratt 2009). On the other hand, neuronal activity could modulate the expression of some miRNAs thus the expression of their target mRNAs (Christensen and Schratt 2009). For example, miR-134 expression could be activated after neuronal activation in a Myocyte enhancing factor 2 (Mef2) dependent manner (Fiore, Khudayberdiev et al. 2009), while expression of miR-132 can be induced by light in a CREB dependent manner (Cheng, Papp et al. 2007).

miRNA dysfunction has been linked to neurological disorders (Shafi, Aliya et al. 2010; Wu, Tao et al. 2010; Liu and Xu 2011) and brain cancer (Chan, Krichevsky et al. 2005; Papagiannakopoulos, Shapiro et al. 2008). Profiling studies show change of miRNA expression in traumatic spinal cord or brain injury (Liu, Wang et al. 2009; Redell,

Liu et al. 2009; Redell, Moore et al. 2010). Changes in miRNA expression are also associated with neurodegenerative disorders, such as Alzheimer's disease (Cogswell, Ward et al. 2008), Parkinson's disease (Minones-Moyano, Porta et al. 2011) and Huntington's disease (Lee, Chu et al. 2011), and neurodevelopment disorders, such as schizophrenia (Burmistrova, Goltsov et al. 2007; Perkins, Jeffries et al. 2007) and autism (Abu-Elneel, Liu et al. 2008). A few miRNAs were found to be able to regulate Amyloid precursor protein (APP) expression level in vitro and in vivo (Hebert, Horre et al. 2009; Smith, Al Hashimi et al. 2011). Gain-of-function mutations in leucine-rich repeat kinase 2 (LRRK2), which cause familial as well as sporadic Parkinson's disease, was shown to negatively regulate miRNA-mediated translational repression (Gehrke, Imai et al. 2010). Huntington's disease (HD) is characterized by widespread changes in neuronal gene expression (Hodges, Strand et al. 2006). Dysregulation of miRNA expression and the negative feedback loop between REST and the REST-regulated miRNAs could be one of the causes of HD pathology (Packer, Xing et al. 2008). miRNA may also control drug addiction and provide new therapeutic targets (Dreyer 2010). microRNA-212 is suggested to play pivotal role in regulating cocaine intake in rats and perhaps in vulnerability to cocaine addiction (Hollander, Im et al. 2010).

Despite accumulating studies in this field, our understanding of the mechanism and logic of miRNAs function in the CNS is still limited. Expression profiling of miRNA can provide basis for functional studies. Indeed, miRNA profiling studies on different anatomical structures of the brain revealed interesting expression pattern (Miska, Alvarez-Saavedra et al. 2004; Landgraf, Rusu et al. 2007; Bak, Silahtaroglu et al. 2008;

Ling, Brautigan et al. 2011). However, these studies, like the vast majority of genomic studies in the brain, prepared miRNAs from tissue homogenates where the distinction among cell types is lost. As a result, both the detection of miRNA in minor cell populations and the interpretation of data in the context of relevant neural circuits are problematic. Cell type specific information of miRNA expression in the mammalian brain did not exist, largely due to the cellular complexity of the system.

1.3 Cellular diversity of the brain

The mammalian brain contains an enormous variety of neuron types, each with unique morphology, connectivity, physiology and function.The cerebral cortex is the newest addition to the vertebrate brain during evolution and supports the increasingly sophisticated sensory, motor, and cognitive functions in mammals (Allman 1999). A major obstacle to understanding the basic organization and function of neural circuits in cerebral cortex is the daunting diversity and heterogeneity of inhibitory interneurons (Markram, Toledo-Rodriguez et al. 2004). Compared with glutamatergic projection neurons, GABAergic interneurons constitute approximately 20% of cortical neurons; yet these interneurons are crucial in regulating the balance, flexibility, and functional architecture of cortical circuits (Markram, Toledo-Rodriguez et al. 2004; Klausberger and Somogyi 2008). GABAergic interneurons consist of a rich array of cell types with distinct physiological properties, connectivity patterns, and gene expression profiles. Their diverse intrinsic, synaptic, and dynamic properties allow interneurons to generate a rich repertoire of inhibitory outputs (Jonas, Bischofberger et al. 2004); their distinct connectivity patterns ensure differential recruitment of interneurons by appropriate inputs

as well as strategic distribution of their outputs to stereotyped locations (e.g. specific cellular and subcellular targets) in cortical network (Somogyi, Tamas et al. 1998; Buzsaki, Geisler et al. 2004; Huang, Di Cristo et al. 2007). GABA interneurons further generate and maintain various forms of network oscillations that provide spatial-temporal frameworks to dynamically organize functional neural ensembles (Buzsaki 2001; Bartos, Vida et al. 2007; Klausberger and Somogyi 2008).

The assembly of cortical GABAergic circuits begins during mid-gestation and continues well into the postnatal period (Huang, Di Cristo et al. 2007). GABAergic neurons are generated mainly in the medial and caudal ganglionic eminences (MGE and CGE) of the basal ganglia and the preoptic area (POA) (Batista-Brito and Fishell 2009; Gelman and Marin 2010). MGE and CGE express different sets of transcription factors and give rise to distinct classes of interneurons (Gelman and Marin 2010; Hernandez-Miranda, Parnavelas et al. 2010). Parvalbumin (PV), somatostatin (SST) and calbindin (CB) positive interneurons have been found to be produced by MGE; cholecystokinin (CCK), neuropeptide Y (NPY), or vasoactive intestinal peptide(VIP) positive interneurons are mainly produced from CGE. Transplantation experiments suggested that, depending on the donor age, MGE progenitors at different embryonic stage could produce different types of interneurons (Butt et al., 2008). Moreover, early-born MGE-derived GABAergic neurons usually locate in deep layers, while late-born MGE-derived GABAergic neurons reside in superficial layers in adult cortex, and thus show an inside-out pattern (Miyoshi et al., 2007). In contrast, the CR positive interneurons generated in CGE have an outside-in pattern (Rymar and Sadikot, 2007), and the VIP positive neurons

do not have obvious correlation of the final cortical layer and the birth time (Cavanagh and Parnavelas, 1989). Postmitotic GABAergic neurons navigate towards the developing neocortex through a remarkable process of long distance tangential migration (Marin and Rubenstein 2001; Hernandez-Miranda, Parnavelas et al. 2010). How interneurons subsequently disperse into appropriate cortical areas, settle in appropriate layers, establish specific connectivity patterns, and acquire distinct physiological properties is largely unknown.

Although an exhaustive classification of neocortical interneuron subtypes may not ever be possible, there are several general accepted features commonly used by researchers (Markram, Toledo-Rodriguez et al. 2004; Ascoli, Alonso-Nanclares et al. 2008). The first salient feature to classify GABAergic interneurons is their morphology. Based on subcellular targeting onto pyramidal neurons, interneurons could be classified into axon-targeting, soma- and proximal dendrite-targeting, dendrite-targeting, and dendrite- and tuft-targeting interneurons. These types could be further divided into subtypes base on their soma size, axon and dendrite organization. Soma- and proximal dendrite-targeting type includes nest basket cells, small basket cells, and large basket cells. Dendrite-targeting type includes double bouquet cells, bipolar cells, bitufted cells, and neuro-gliaform cells. Dendrite- and tuft-targeting type includes Cajal Retzius cells and Martinotti cells. Chanderlier cells target axon initial segment, forming very characteristic axon cartridges. Another feature useful for interneuron classification is the expression of molecular markers. With the expanding of knowledge, the number of molecular features one could measure or characterize is constantly growing. Nevertheless,

several groups were more commonly used: transcription factors, neurotransmitters or their synthesizing enzymes, neuropeptides, Ca2+-binding proteins, neurotransmitter receptors, structural proteins, ion channels, connexins, pannexins and membrane transporters. Physiological and biophysical features, including passive and subthreshold properties, action-potential measurements, firing pattern, and postsynaptical responses are also often used to classify interneurons.

1.4 Genetic targeting of neuron subtypes by Cre-loxP system

The phenotypic properties of different cell types are largely acquired and maintained by unique combinations of expressed genes (Monyer and Markram 2004). . To establish reliable experimental access that allow precise and reliable identification and manipulation of distinct cell types, genetic targeting techniques were developed which engage the intrinsic gene regulatory mechanisms that generate and maintain cell type identity and phenotypes. The most commonly used system in mice is Cre-loxP system.

First developed by Dr. Brian Sauer, the Cre-loxP binary system has been widely explored in biological studies (Sauer and Henderson 1989). The Cre protein is a site-specific DNA recombinase, which can recognize specific DNA sequences (LoxP sites), and catalyze the recombination of DNA between them. The outcome of recombination depends on the orientation of loxP sequences. If two loxP sites orient at the same direction, the DNA sequence between them will be excised; if they orient at the opposite directon, the DNA sequence between them will be inverted. Making use this

characteristics, researchers could control gene expression and modify chromosome architecture in genetically modified organisms (Dymecki and Kim 2007).

To use this system in a cell type specific manner, the key component is to express Cre recombinase in genetically defined cell populations, either by transgenic strategy or by gene knock-in strategy. Both strategies utilize the endogenous gene regulatory mechanism, but have different pros and cons respectively. Recently, collaborative effort has been made in the neuroscience field to generate Cre driver lines which can target specific cell type in the mouse brain.

As an added layer of regulation, CreER, an inducible form of Cre, can be used to allow temporal regulation of Cre activity and achieve sparse labeling of cells (Hayashi and McMahon 2002). CreER is a fusion protein between Cre and a mutated form of the ligand binding domain of the estrogen receptor. The mutation prevents binding of its natural ligand, but renders it responsive to Tamoxifen(TM). The ER domain leads to ER-dependent cytoplasmic sequestration of Cre by Hsp90, while binding by TM relieve the sequestration, permitting Cre activity in the neucleus.

Depending on the architecture of Cre-dependent responder (reporter) lines, this system can be used to visualize cell morphology, regulate neuron activity, inactivate endogenous gene expression and immune-purify nucleic acid through epitode-fused proteins. In my studies, I used this system to purify miRNAs and to knock-out Dicer in specific neuron types.

1.5 Cell type specific affinity tagging of nucleic acids

The key obstacle in genome-wide analysis of the brain is cell type complexity. Individual neuron types are building blocks of neural circuits as well as units for gene regulation. However, different neuron types in the brain are highly intermingled, makes it difficult to study genome and epigenome in a cell type specific way.

Previous profiling studies in individual cell type has relied on physically isolate the cell of interest from tissue, and then extract RNA for profiling. In terms of miRNAs, an additional size fractional step is required to enrich small RNA populations. These traditional techniques for purify individual cell types, including laser capture microdissection (LCM) (Meguro, Lu et al. 2004), fluorescence-activated cell sorting (FACS) (Tomomura, Rice et al. 2001; Lobo, Karsten et al. 2006), and ex vivo differentiation (Nave 2010; Zhao, He et al. 2010), involve extensive tissue manipulation, cause disruption of cell morphology, and are often of low yield and throughput.

Recently, several new techniques were developed to immune-purify mRNA from tissue homogenates by tagging mRNA binding protein, such as ribosome components (Heiman, Schaefer et al. 2008; Sanz, Yang et al. 2009) and polyA binding protein (Yang, Edenberg et al. 2005). Using transgenic technique (Heiman, Schaefer et al. 2008) or Cre-loxP system (Sanz, Yang et al. 2009), the tagged proteins were expressed in specific neuron types to achieve cell type specificity. Exploring similar idea, we developed miRNA affinity purification (miRAP) technique using a Cre-responsive epitope fused Argonaute2 allele in genetically engineered mouse.

1.6 Cell type specific miRNA expression profiling

miRNA expression has a higher level of diversity than mRNA in different tissue and cell types (Lu, Getz et al. 2005). miRNA expression profiling is not only an essential step toward further elucidation of miRNA function and miRNA-related gene regulatory network, but also a useful tool for cell type classification , disease diagnosis and therapy development (Hernando 2007). For example, hierarchical clustering of miRNA profiles from poorly differentiated tumor samples paralleled the developmental origins of the tissues, while mRNA profiles from the same samples failed to do so (Lu, Getz et al. 2005). Another example is that profiling studies in mouse model revealed miRNAs important for addiction which could be potential drug targets (Dreyer 2010).

Several general platforms can be used to detect miRNA expression: deep sequencing (Lu, Meyers et al. 2007), array based detection (Nelson, Baldwin et al. 2004), bead based detection (Siva, Nelson et al. 2009), qPCR based detection (Lu, Read et al. 2005) and in situ hybridization (Wienholds, Kloosterman et al. 2005). Among these techniques, deep sequencing is the most comprehensive one and has the highest throughput. Unlike the other techniques, it is not limited by prior knowledge of miRNA sequences, therefore is the only one which can detect novel miRNAs.

Systematical exploration of miRNA profiles in a cell type specific manner in the mouse brain by deep sequencing using our miRAP method may help to elucidate the cellular diversity, discover novel neuronal miRNAs, provide basis for detailed studies of individual miRNAs, their target genes and the miRNA-related regulatory networks, and reveal potential clinical targets from neurological disorders.

Chapter 2. Development of GABA Cre and CreER driver lines

2.1 Introduction

A major obstacle in understanding the basic organization and function of neural circuits in cerebral cortex is the daunting diversity and heterogeneity of inhibitory interneurons (Markram, Toledo-Rodriguez et al. 2004). Different classes of GABAergic neurons are distinct in terms of morphology, electrophysiology, and connectivity, and contribute to specific aspects of circuit operation

Based on morphological properties, cortical interneurons could be grouped into basket cells, chandelier cells, Martinotti cells, bipolar cells, double bouquet cells, neurogliaform cells etc. Based on subcellular targeting, they could be classified into axon-targeting, soma- and proximal dendrite-targeting, dendrite-targeting, and dendrite- and tuft-targeting interneurons. Based on discharge responses at steady-state, they could be classified as non-accommodating (NAC), accommodating (AC), stuttering (STUT), irregular spiking (IS) and bursting (BST); within which, subgroups can be further defined according to the onset response, with bursts, delays or being indistinguishable from the steady state. They could also be classified based on the expression of chemical markers, such as neuropeptides (neuropeptide Y (NPY), cholecystokinin (CCK), somatostatin (SST),calretinin (CR), vasoactive intestinal peptide (VIP),etc) and/or calcium binding protein(calbindin (CB), parvalbumin (PV), etc). These diverse intrinsic, synaptic, and dynamic properties allow interneurons to generate a rich repertoire of inhibitory outputs (Markram, Toledo-Rodriguez et al. 2004; Klausberger and Somogyi 2008).

Genetic approaches promise to significantly facilitate the study of the cortical GABAergic circuitry because they engage the intrinsic gene regulatory mechanisms that generate and maintain cell type identity and phenotypes (Haubensak, Kunwar et al. 2010). Using mouse genetic engineering, our lab initiated a systematic effort to genetically target cortical GABAergic neurons. For the practical purpose of genetic targeting, we parse cortical GABAergic populations based on their gene expression.

Two main strategies were available to engage gene transcription in targeting cell types in mice: transgenesis and knock-in. In order to faithfully engage the biological mechanisms that specify and maintain cell identity, it is necessary to generate driver lines in which Cre activity precisely and reliably recapitulates endogenous gene expression. We therefore used the gene knockin strategy to target GABAergic neurons. Cre and CreER cassettes are inserted by homologous recombination at endogenous gene loci, either at the translation initiation codon (*ires-Cre* or *2A-Cre*) or immediately after the translation STOP codon (*CreER*) of an endogenous gene, which are embedded in their native chromatin environment with largely intact regulatory elements

I have been actively involved in this project and devoted most of my time during the first two years of PhD research to it. I have generated three CreER driver lines (*PV-CreER, SST-CreER* and *CR-CreER*), and designed and supervised the generation of several other Cre and CreER driver lines (*Gad2-ires-Cre, CST-2A-Cre* and *nNos-CreER*). RCE reporter, Ai9 reporter, or H2B-GFP reporter were bred to these lines for characterization. The basic information of these lines is summarized in table2.1.

Driver lines	ES cells	Vector construction	Targeting efficiency	Recomb. Specificity (cortex)	Recomb. Efficiency (cortex)
Gad2-ires-Cre	V6.5	recombineering	15 %	~92.2%	~91%
SST-CreER	Bruce4	Long PCR	0.5%	~100%	Very low *
PV-CreER	Bruce4	recombineering	~10%	~100%	Very low*
CR-CreER	Bruce4	recombineering	~ 60%	>70%	Medium
CST-2A-Cre	V6.5	recombineering	30%	n.d.	n.d.
nNOS-CreER	V6.5	Long PCR	3.9%	~100%	Medium

Table 2.1 Summary of Cre/CreER driver lines.

*: <5 cells in cortex in a 50μm sagittal section. n.d. not determined due to lack of specific antibodies.

2.2 *Gad2-ires-Cre*

The defining feature of all GABAergic neurons is their synthesis of γ-aminobutyric acid. In mammalian brains, GABA is synthesized from glutamate via a single decarboxylation step catalyzed by two isoforms of glutamic acid decarboxylases GAD67 and GAD65, which are encoded by the *Gad1* and *Gad2* genes, respectively (Pinal and Tobin 1998; Soghomonian and Martin 1998). In most brain regions (with the notable exception of certain cells in amygdala, retina, and spinal cord) Gad1 and Gad2 are co-expressed in individual neurons and jointly contribute to complementary spatial and temporal pattern of GABA synthesis (Pinal and Tobin 1998; Soghomonian and Martin 1998). In most GABAergic neurons, GAD67 is the rate limiting enzyme that accounts for ~90% of GABA synthesis (Asada, Kawamura et al. 1997), whereas GAD65 is more engaged during increased synaptic activity (Kash, Tecott et al. 1999).

Although the ires startgy is believed to retain endgoneous gene expression, we have observed reduction of expression in other existing ires line(data not shown). As *Gad1* heterozygoous show altered development of inhibitory synapses (Chattopadhyaya, Di Cristo et al. 2004) and homozygous KO causes mouse death, whereas *Gad2* heterozygote and KO has less discernable phenotypes, we chose to target *Gad2* locus to generate a pan-GABA driver line. Cre is co-expressed with *Gad2* throughout development in GABAergic neurons and also in certain none-neuronal cells. Because Cre/loxP recombination converts transient CRE activity to permanent reporter allele activation, reporter expression is a spatial and temporal (i.e. developmental) integration of all Cre activities up to the time of analysis. In almost all brain regions, Cre-activated reporter expression is restricted to GABAergic neurons and appears to include all GABAergic neurons (Figure 2.1).

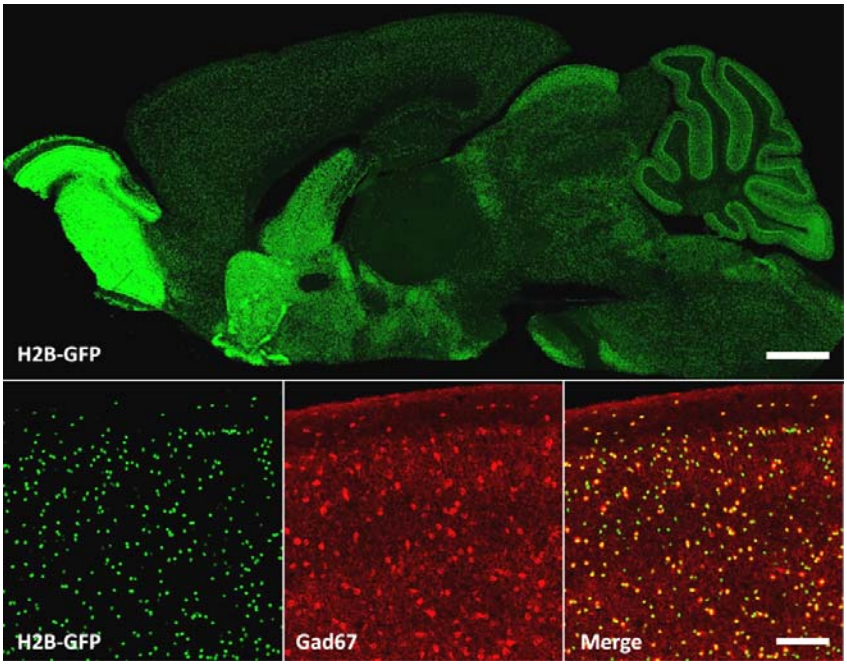

Figure 2.1 The *Gad2-ires-Cre* driver allows genetic access to GABAergic neurons throughout the brain.

Upper panel: GFP immunostaining of a sagittal section from an adult *Gad2-ires-cre;H2B-GFP*mouse brain. Scale bar: 1mm. Lower panels: Immunostaining shows co-localization of GFP and Gad67 in this line. Scale bar: 100 μm

2.3 *PV-CreER*

Expression of chemical markers is commonly used to classify interneuron subtype. Parvalbumin is a calcium binding protein expressed in ~40% of neocortical GABAergic interneurons (Gonchar, Wang et al. 2007). The large majority of PV cells are fast-spiking large basket interneurons (LBCs) which innervate the soma and proximal dendrites of pyramidal neurons. LBCs innervate the neurons across different layers and distant columns, and are proposed to provide the major source of lateral inhibition. Indeed, the perisomatic targeting basket cells are found to limit the repetitive firing of sodium-dependent spikes of target neurons and regulate efferent signaling, and thus are proposed to strongly influence the output of target neurons Single GABAergic interneuron may innervate up to a thousand pyramidal neurons, and thus provide a structural basis for synchronizing circuit activity both locally and across long distance.

The *PV-CreER* line has extremely low recombination efficiency, with no labeling in the cortex. In cerebellum, PV is expressed in Purkinje cells, basket cells and stellate cells (Celio and Heizmann 1981). *PV-CreER* could be used to label these cells at single cell level and high resolution. Using this line, we could visualize characteristic pinceau synapse at Purkinje cell axon initial segment made by basket cells (Figure 2.2).

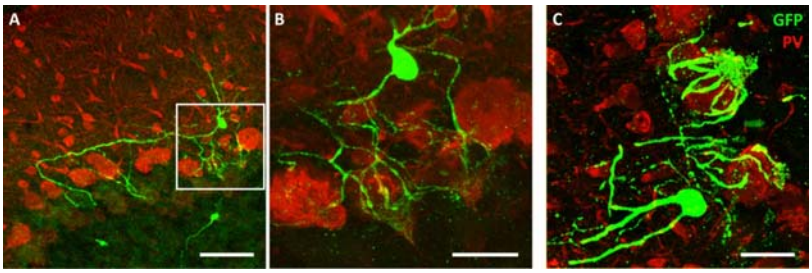

Figure 2.2 *PV-CreER* labels cerebellum basket cells, allowing visualization of pinceua synapses at Purkinje cell axon initial segment.
GFP and PV duel immunostaining in *PV-CreER;RCE* mouse cerebellum. A. Scale bar 50 μm B.C Scale bar 20 μm

2.4 *SST-CreER*

The dendrites of pyramidal neurons are innervated by multiple classes of inhibitory interneurons which regulate local processing and integration of synaptic inputs, back-propagating action potentials, and dendritic calcium spikes, and control synaptic plasticity (Klausberger 2009). Somatostatin (SST) is a neuropeptide expressed in a sub-population of dendrite-targeting interneurons that are derived from the MGE (Miyoshi, Butt et al. 2007; Xu, Guo et al. 2008). A subset of SST interneurons, the Martinotti cells in neocortex (Buzsaki, Geisler et al. 2004; Wang, Toledo-Rodriguez et al. 2004) , selectively innervates the distal dendrites of pyramidal neurons. Martinotti cells mediate frequency dependent di-synaptic inhibition among neighboring layer 5 pyramidal neurons and control their synchronous spiking (Berger, Perin et al. 2009). However, the mechanism underlying their synaptic specificity is unknown.

In the *SST-CreER* line, tamoxifen-induced recombination is restricted to SST neurons but the efficiency is also very low as assayed with both the RCE and Ai9 reporters. The *SST-CreER* driver allows imaging and reconstruction of single cortical SST interneurons and single cell genetic manipulation (Figure2.3). CreER in this line is also active in many other brain regions including: olfactory bulb, striatum, reticular nucleus of the thalamus, superior colliculus, brain stem, as well as cerebellar Purkinje cells (data not shown). The labeling efficiency in these regions is relatively higher.

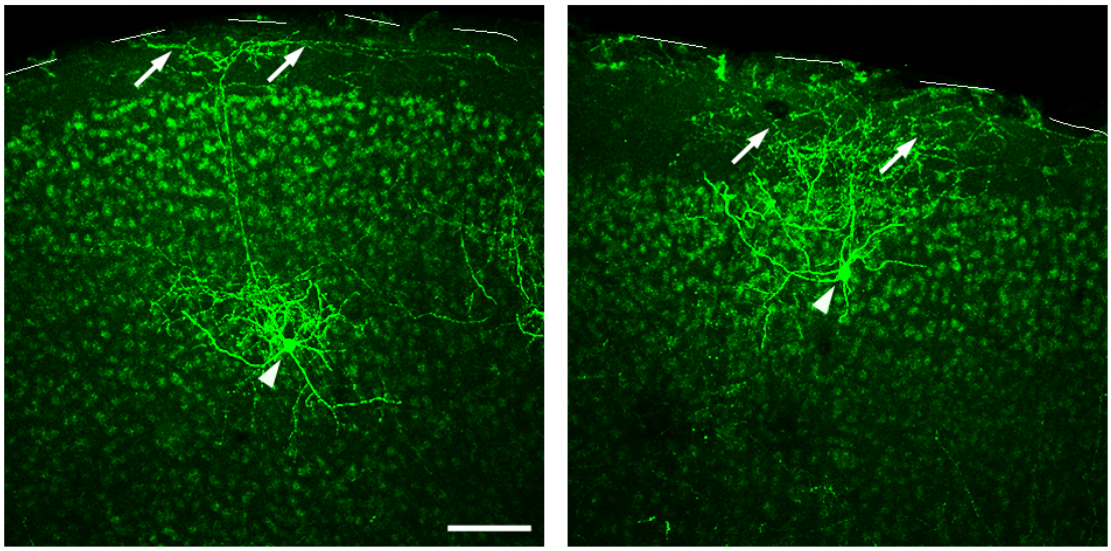

Figure 2.3 Low frequency recombination in the *SST-CreER* driver labeled single Martinotti cells (green, arrow heads) in layer 5 (left) and layer2 (right).

Note the characteristic axon arborization in layer1 (arrows). The background green puncta were non-specific signals from GFP antibody staining which were commonly seen when brain sections contained very small number of GFP expressing cells. Scale bar: 100 μm

2.5 *CR-CreER*

The calcium binding protein calretinin (CR) is expressed in a subpopulation of GABAergic neurons throughout the brain. In cerebral cortex, CR+ interneurons include layer 1 GABA neurons and several subpopulations that co-express SST and VIP (Xu, Roby et al. 2010). Labeling mediated by *CR-CreER* driver lines recapitulate endogenous CR expression. This line shows modest recombination efficiency in neocortex, but relatively high frequency in several other brain regions such as olfactory bulb (Figure 2.4).

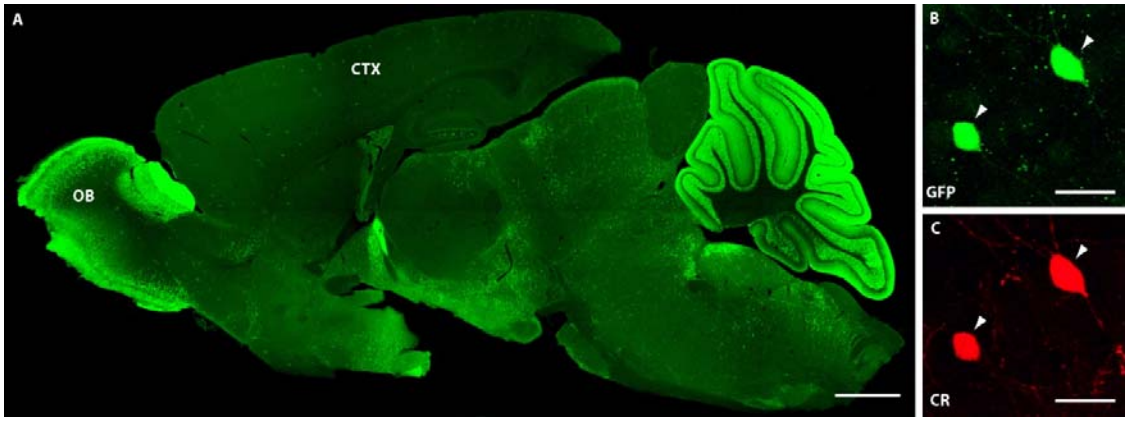

Figure 2.4 Tamoxifen administration induces moderate level of recombination in the *CR-CreER* driver.

(A) GFP immunostaining of a sagittal section from an induced adult *CR-CreER::RCE* mouse brain. Tamoxifen was administrated by intraperitoneal injection every other day for 5 days at 8mg/d dosage. Mouse was perfused 9 days after last injection. Scale bar: 1mm. OB: olfactory bulb. NTX:neocortex

(B) (C) Co-localization of GFP and calretinin immune- fluorescence (red) in induced neurons. Arrowheads: GFP and CR double positive cells. Scale bar: 20 μm.

2.6 *CST-2A-Cre*

Cortistatin (CST) is a neuropeptide that shares 11 of its 14 amino acids with somatostatin (de Lecea 2008). CST is predominantly expressed in cerebral cortex, a subset of GABA interneurons with partial overlap to SST (de Lecea, del Rio et al. 1997). Although CST and SST share several pharmacological properties, including binding to same set of somatostatin receptors in vitro, they show distinct functional properties in vivo: in contrast to SST, CST administration in brain ventricles enhances EEG synchronization by selectively promoting slow-wave sleep (de Lecea, Criado et al. 1996). Steady-state levels of CST mRNAs oscillate during the light: dark cycle and are upregulated upon sleep deprivation(Bourgin, Fabre et al. 2007). However, little is known about the connectivity, physiology, and regulation of CST interneurons, and their hypothesized function in sleep homeostasis and cortical synchronization remain to be tested.

The *CST-2A-Cre* driver appears to selectively target this interneuron population. Cre activity is restricted to subpopulation of GABA interneurons in cortex and hippocampus and shows a partial overlap with SST and PV interneuron populations (data not shown). This driver line thus enables more thorough study of CST interneurons in regulating cortical states.

2.7 *nNOS-CreER*

Nitric oxide (NO) is a signaling molecule in the brain synthesized by the neuronal isoform of nitric oxide synthase (nNOS). In cerebral cortex, nNOS is broadly expressed

during development(Bredt and Snyder 1994) and is subsequently restricted to subsets of GABAergic neurons(Jinno and Kosaka 2002; Kubota, Shigematsu et al. 2011). In hippocampus, nNOS neurons include neurogliaform cells (NGFCs) and ivy cells(Fuentealba, Begum et al. 2008), which together constitute the largest cohort of hippocampal interneurons. The most unique feature of NGFCs, including those in the neocortex, is their regulation of local neurons through non-synaptic GABA release and volume transmission (Olah, Fule et al. 2009). Thus in contrast to the highly specific targeting of other inhibitory synapses, the output of neurogliaform cells appears to lack spatial specificity and may lead to long-lasting network hyperpolarization and widespread suppression in local circuit. NO release from these neurons may also regulate blood vessels and local hemodynamics(Cauli and Hamel 2010). Although these unusual features of NGFCs have been discovered from studies in brain slice, their inputs, function, and modulation in vivo are poorly understood, and their development to date remains unexplored.

In the neocortex, nNOS+ GABA neurons appear to include two types: large Type I cells with intense nicotinamide adenine dinucleotide phosphate-diaphorase (NADPH-d) staining, and small Type II cells with weak NADPH-d staining(Kilduff, Cauli et al. 2011). Whereas Type II cells likely include NGFCs, Type I nNOS+ cells represent another highly unusual population of GABAergic neurons. First, Type I nNOS+ neurons project axons over long distance to other cortical areas, contralateral cortex, and subcortical regions; and they are conserved from rodent to primate neocortex(Tomioka, Okamoto et al. 2005; Higo, Akashi et al. 2009). Second, whereas most cortical neurons

exhibit reduced firing during slow wave sleep (SWS), Type I neurons in cortex, but not nNOS+ in any other subcortical regions, are selectively activated during SWS. Notably, the extent of activation is proportional to homeostatic sleep 'drive' (Gerashchenko, Wisor et al. 2008).These features suggest that Type I nNOS+ neurons might be positioned to influence neuronal activity and network state across widespread brain areas, and may provide a long-sought anatomical link for understanding homeostatic sleep regulation (Kilduff, Cauli et al. 2011). However, the connectivity pattern, physiological properties, function, and regulation of Type I nNOS+ neurons are at present unknown.

The *nNOS-CreER* driver provides a genetic means to label nNOS+ neurons in the brain. CreER recombination pattern induced by tamoxifen matched almost perfectly with known nNOS neuron profiles throughout the brain. However, the extent of labeling varied in the two reporter lines, as they display different sensitivity and expression levels, especially in neocortex. Whereas the less sensitive RCE reporter specifically labeled only the type I cells, the more sensitive Ai9 reporter labeled both type I and type II cells in cortex. In the hippocampus, *nNOS-CreER* efficiently labeled neurons whose somata were located in the stratum lacunosum molecular and stratum pyramidale, which likely correspond to NGFCs and ivy cells. In addition to the cerebral cortex and hippocampus, the *nNOS-CreER* driver efficiently labeled nNOS neurons in olfactory bulb, striatum, amygdala, superioculicullus and hypothalamus. (Figure2.5)

Genetic access to nNOS GABAergic projection neurons will facilitate the study of their: 1) projection pattern (e.g. cortico-cortical, contralateral, subcortical) and cellular

targets, 2) input source, 3) physiological properties, 4) function in regulating sleep and cortical state, and 5) role in regulating blood vessel and hemodynamics. Similarly, genetic access to nNOS neurogliaform and ivy cells in hippocampus will facilitate studying their connectivity, in vivo function, and development.

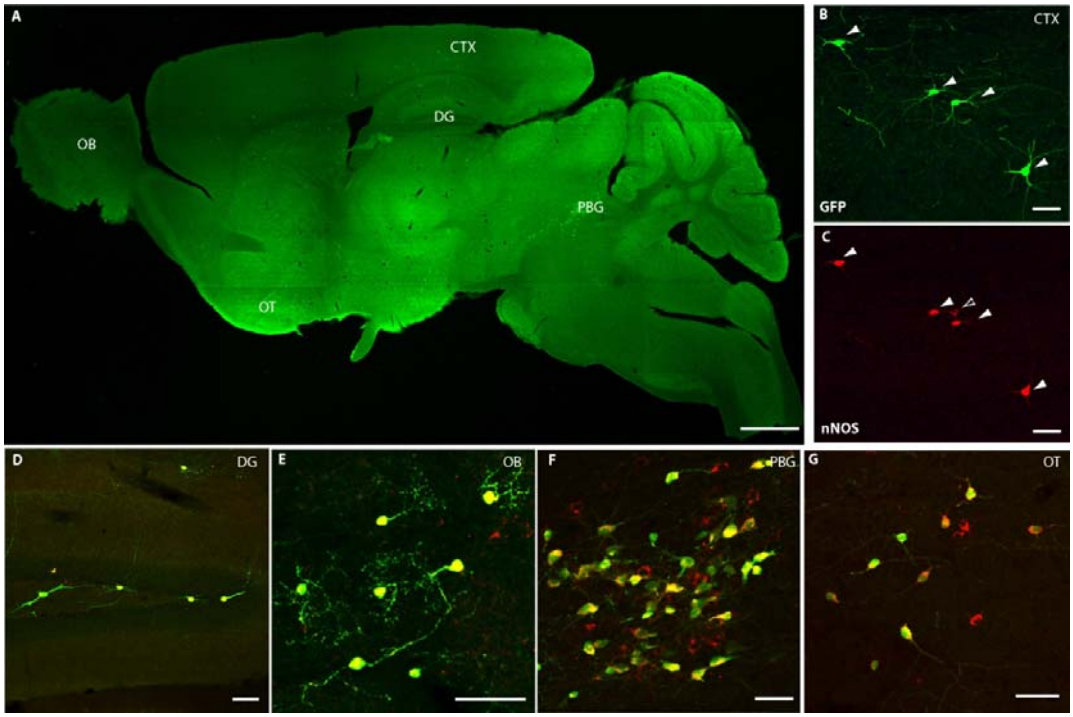

Figure 2.5 Tamoxifen administration efficiently induces Cre activity in nNOS expressing neurons.

(A) GFP immunostaining of a sagittal section from an induced adult *nNOS-CreER::RCE* mouse brain. Tamoxifen was administrated by intraperitoneal injection once at 8mg/d dosage. Mouse was perfused 9 days after injection Brain regions with high number of GFP positive cells are indiated. OB: olfactory bulb. CTX: cortex. DG: Denate gyrus. PBG: Parabigemenal neuclus. OT: Olfactory tubercle. Scale bar: 1mm.

(B) (C) Immunostaining shows colocalization of GFP and nNOS in induced neurons. Arrow heads: GFP and nNOS double positive cells. Scale bar: 20 μm.

(D) – (G) Higher magnification image of labeled cells in different brain region as indicated in (A). Scale bar: 50 μm.

2.8 Discussion

Since Cajal's study of cortical neurons using the Golgi stain more than a century ago(Cajal, 1899), a major obstacle in understanding the organization and function of neural circuits in cerebral cortex has been the lack of methods that allow precise and reliable identification and manipulation of specific cell populations. Genetic targeting is probably the best strategy to systematically establish experimental access to cortical cell types because it engages gene regulatory mechanisms that specify, maintain or correlate with cell types. Combined with modern molecular, optical, and physiological tools, genetic targeting enables labeling of specific cell populations with markers for anatomical analysis, expression of genetically encoded indicators to record their activity, and activation or inactivation of these neurons to examine the consequences in circuit operation and behavior (Luo, Callaway et al. 2008). Genetic analysis therefore promises to provide the fine scalpel for dissecting cortical circuits.

The effort made by our lab and others to genetically target neuron subtypes by establishing Cre-mediated genetic switches in different cell populations made it possible to systematically apply genetic analysis to neural circuits of the cerebral cortex. An increasing array of Cre-dependent responder lines and viral vectors have been generated that express genetically encoded markers, sensors and transducers. Reliable genetic access and the combinatorial power of the Cre/loxP binary system will integrate modern physiology, imaging and molecular tools to provide a systematic analysis of the neuronal system; they will further enable a comprehensive study of the connectivity, physiology, function, and plasticity in cortical circuitry.

Although the link between genes and cortical circuit function is indirect, it is increasingly evident that gene regulatory programs orchestrate many aspects of circuit assembly, from cell fate specification to synaptic connectivity. Given that the cell type is the basic unit of neural circuit function as well of gene regulation, a cell type-targeted genetic analysis will likely contribute to revealing the logic of cortical circuit assembly and organization. Combined with genetic etiological models in mice, such cell type-based approaches may further contribute to understanding the genetic architecture and pathogenic mechanisms of neurodevelopmental and psychiatric disorders

2.9 Materials and methods

2.9.1 Generation of GABA driver lines

2.9.1.1 Knockin vector construction

General scheme: Gene targeting constructs were generated using BAC recombineering and, in a few cases, PCR-based molecular cloning approach. For constitutive Cre lines, either an ires-Cre was inserted immediately after the STOP codon or a 2A-Cre cassette was inserted in frame just before the STOP codon of the targeted gene. For inducible lines, CreER was inserted at the translation initiation site of the targeted gene. If the ATG codon of the targeted gene is in the first coding exon, a CreER-intron-polyA cassette was used; if the ATG codon is not in the first coding exon, a CreER-polyA cassette was used. 2 to 5kb upstream or downstream regions of the targeted loci were cloned into targeting vector as 5' and 3' homologous arms, respectively. All targeting constructs include an frt-Neo-frt cassette, and a tyrosine kinase

cassette or diphtheria toxin cassette for positive and negative selection in ES cells, respectively. Detailed information on targeting constructs for each line is available at http://www.credriver.org.

BAC clones: For each gene of interest, 2 partially overlapping BAC clones from the RPCI-23&24 library were chosen from the Mouse Genome Brower. BAC DNA was transferred from DH10B strain to SW105 strain by electroporation. SW105 is a further improved EL250 strain which allows highly efficient recombineering using galK selection. The identity and integrity of these BAC clones were verified by a panel of PCR primers and restriction digestions. One clone was selected for recombineering.

Building vectors and BAC targeting vectors: We constructed a series of "building vectors" containing the essential elements for different strategies of BAC targeting. These elements were inserted into P451B (gift of Dr. Pentao Liu), a modified version of PL451 without a loxP site in front of the frt-Neo-frt cassette. The Neo gene is driven by both the PGK promoter for G418 selection in ES cells and the EM7 promoter for Kan selection in E.coli. A BAC targeting vector was generated for each gene by cloning appropriate 5' and 3' homology arms from a gene of interest into a building vector, flanking the CreERT2frt-Neo-frt cassette. For targeting to the ATG initiation codon, we typically use 300-500 bp DNA fragments immediate upstream and shortly downstream for 5' and 3' homology arms, respectively.

BAC recombineering and generation of knockin constructs: We used the PL253 or pBS-DT7 retrieval vector as the backbone of our knockin vectors. PL253 contains the

HSV-TK gene and pBS-DT7 contains a diphtheria toxin cassette for negative selection in ES cells, flanked by multi-cloning sites. Knockin cassette was retrieved from the modified BAC clones into retrieval vector by recombineering. For recombineering BAC targeting cassettes was excised by restriction digestion, purified to ~100ng/µl, and electroporated into competent SW105 cells containing the BAC clone of interest. Targeted BAC clones was selected for KanR, and confirmed by a panel of PCR primers and restriction digestions. A correctly targeted BAC clone was used for generating the knockin construct by the BAC retrieval method The 5'r and 3'r in the retrieval vector was designed such that between 2-5 kb DNA segment flanking the CreERT2-frt-PGK-EM7-Neo-frt cassette in the BAC clone will be subcloned into PL253. The total length of homology (2-5kb on either side) was sufficient for gene targeting in ES cells. The shorter homology arm was used to design PCR-based screens for targeted ES cells.

2.9.1.2 Generation of mouse lines

Targeting vectors were linearized by NotI or SalI and transfected into either a C57/black6 ES line (Bruce4, generously provided by Dr. Collin Stewart) or a 129SVj/B6 F1 hybrid ES cell line (V6.5, Open Biosystems). G418-resistant ES clones were first screened by PCR and then confirmed by Southern blotting using appropriate probes. PCR primers and conditions were first tested on targeted BAC clone, which was used as positive control for ES cell screening. Southern probes were generated by PCR, subcloned, and tested on wild type genomic DNA and modified BAC DNA to verify that they give clear and expected results. Gene targeting rate varied from ~0.5% to over 60%, depending on the targeted loci. For Bruce4 ES cells, positive ES clones were injected

into blastocysts from the albino C57BL/6J-Tyrc2j mice to obtain chimeric mice following standard procedures. Chimeric mice were bred with C57BL/6J-Tyrc2j mice mice to identify germline transmission. For V6.5 ES cells, positive ES cell clones were used for tetraploid complementation to obtain male heterozygous mice following standard procedures. The frt-Neo-frt cassette in the founder line was removed by breeding with Actin-FLPe transgenic mice (gift of Dr. Susan Dymecki). All experimental procedures were approved by the Institutional Animal Care and Use Committee (IACUC) of CSHL in accordance with NIH guidelines.

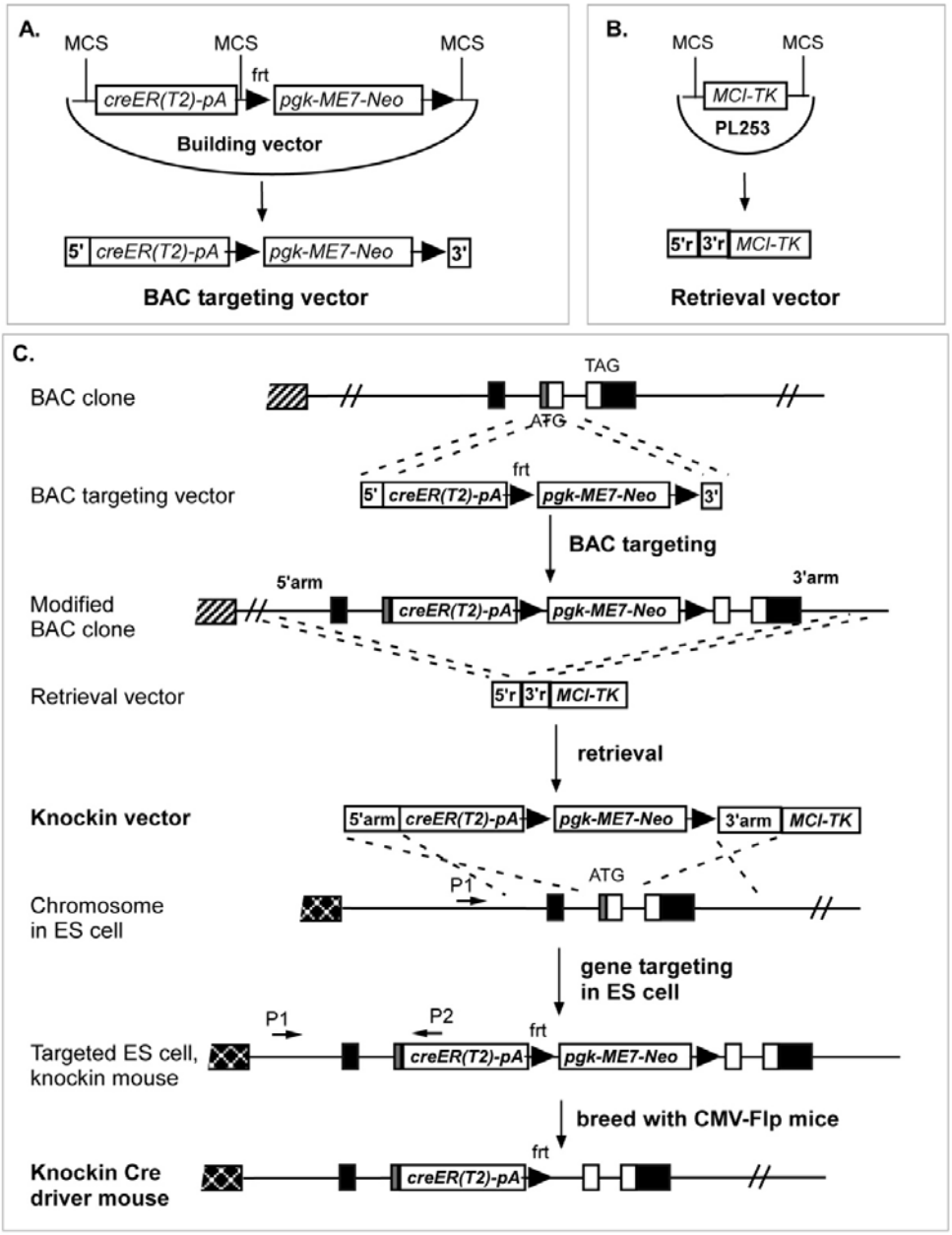

Figure 2.4 Scheme for the generation of GABA Cre drivers through recombineering and gene targeting.

(A) Example of a CreER^{T2} building vector and the generation of BAC targeting vector. pA: polyadenylation sequence; *pgk-ME7-Neo*: pgk and ME7 promoters driving the Neo gene; black arrow: frt site; MCS: multi-cloning sites; 5': 5' recombination arm; 3': 3' recombination arm.

(B) Generation of a retrieval vector. MC1-TK: MC1 promoter driving the TK gene. 5r': 5' retrieval arm; 3r': 3' retrieval arm.
(C) Recombineering scheme for generating a CreER^{T2} knockin vector. A CreER^{T2} expression cassette from the BAC targeting vector in (A) is first targeted into a selected BAC clone at the translation initiation site. This modified BAC is then used to generate a knockin vector by retrieving from it a DNA segment with defined 5' homology, CreER^{T2} expression cassette, and 3' homology into the retrieval vector in (B). Knockin vector is used to target ES cells and generate knockin mice. The final Cre knockin driver is generated by breeding with CMV-Flp transgenic mice to remove the *pgk-EM7-Neo* cassette from the germ line.

2.9.2 Characterization of Cre driver lines

Cre drivers were bred with the RCE or Ai9 or H2B-GFP reporter lines to assay recombination patterns. These mice usually contain mixed C57BL/6 and 129 genetic backgrounds carried from the various Cre and reporter lines. 50-μm thick vibratome sections from perfused brains were immunostained and imaged with confocal microscopy (Zeiss LSM510 and Zeiss LSM710) or with fluorescent microscopy equipped with a CCD camera.

2.9.3 Tamoxifen induction

Tamoxifen was prepared by dissolving in corn oil (20 mg/ml) at 37°C with constant agitation. Appropriate amount of tamoxifen was administered to mice by gavaging or intraperitoneal injection at a dose of 20mg/d every other day for 5 days. Animals were monitored for adverse effects, and if these became apparent, treatment was stopped. 9days after the last induction, mice were processed for analysis.

2.9.4 Immunohistochemistry and confocal microscopy

Postnatal animals were anaesthetized (avertin) and perfused with 4% paraformaldehyde (PFA) in 0.1 M PB. The brains were removed and post-fixed overnight at 4°C. Brain sections (50μm) were cut with a vibratome. Sections were blocked with 10% normal goat serum (NGS) or 10% normal donkey serum, and 0.1% Triton in PBS and then incubated with the following primary antibodies in the blocking solution at 4°C overnight: GFP (rabbit polyclonal antibody; 1:800; Rockland, chicken polyclonal antibody; 1:1000; abcam), RFP (rabbit polyclonal antibody; 1:1000; Rockland, parvalbumin (PV, mouse monoclonal antibody; 1:1000; Sigma, St. Louis, MO), somatostatin (SST; rat monoclonal antibody; 1:300; Millipore), VIP (rabbit polyclonal antibody; 1:600; Immunostar), nNOS (rabbit polyclonal antibody; 1:500; Zymed), lamin B(goat polyclonal antibody C-20;1:100; Santa Cruz Biotechnology). For immunostaining against Gad67 (mouse monoclonal antibody; 1:800; Millipore), no detergent was added in this and following steps, and incubation was done at room temperature for 2 days at the primary antibody step. For immunostaining against Camk2a (mouse monoclonal antibody sc-136212;1:200; Santa Cruz Biotechnology), sections were treated in boiling citrate buffer(10mM Citric Acid, pH 6.0) for antigen retrieval prior staining. Sections were then incubated with appropriate Alexa fluor dye-conjugated IgG secondary antibodies (1: 400; Molecular Probes) and mounted in Fluoromount-G (SouthernBiotech). In some experiments sections, were incubated with TOTO-3 (1:3000; Molecular Probes) together with secondary antibodies to visualize nuclei. Sections were imaged with confocal microscopy (Zeiss LSM510 and Zeiss LSM710) or with fluorescent microscopy equipped with a CCD camera.

Chapter 3. Cell-type based analysis of miRNA expression in the mouse brain

3.1 Introduction

In the mammalian brain, neural circuits often consist of diverse cells types characterized by their stereotyped location, connectivity patterns, and physiological properties. To a large extent, the identity and physiological state of neuron types are determined by their patterns of gene expression (Nelson, Hempel et al. 2006; Hobert, Carrera et al. 2010). Therefore, a comprehensive understanding of gene expression profiles in defined cell types not only provides a molecular explanation of cell phenotypes but also is necessary for establishing the link from gene function to neural circuit organization and dynamics. In addition to gene transcription which dictates mRNA production, the stability and translation of mRNAs are regulated by microRNAs (miRNAs), the class of 20~23nt small noncoding RNAs (Bartel 2004; He and Hannon 2004). miRNAs can also influence transcription by regulating the translation of transcriptional factors (Hobert 2008). Recent studies begin to reveal diverse role of miRNAs in the brain, such as in neural patterning (Ronshaugen, Biemar et al. 2005), neural stem cell differentiation (Kuwabara, Hsieh et al. 2004), cell type specification (Poole and Hobert 2006), synaptic plasticity (Schratt, Tuebing et al. 2006), and also in neuropsychiatric disorders (Shafi, Aliya et al. 2010; Xu, Karayiorgou et al. 2010). However, the mechanism and logic by which miRNAs regulate neuronal development, function, and plasticity are not well understood. A necessary step is a comprehensive

characterization of miRNA expression profiles at the level of distinct neuron types, because individual cell types are the building blocks of neural circuits as well as the basic units of gene regulation.

Analysis of gene expression, including miRNA expression, in the brain has posed a major challenge in genomics despite rapid advances in sequencing technology, because neuronal subtypes are highly heterogeneous and intermixed. Until recently, cell type based expression profiling in the brain has mainly relied on physical enrichment of target cell population such as laser capture microdissection (Meguro, Lu et al. 2004; Rossner, Hirrlinger et al. 2006), fluorescence-activated cell sorting (FACS) (Tomomura, Rice et al. 2001; Lobo, Karsten et al. 2006), or manual sorting (Sugino, Hempel et al. 2006). These methods are often labor intensive and of low yield. Furthermore, the physical damage and stress inherent to these procedures may alter the physiological state of cells and likely their gene expression. The recent invention of genetic tagging methods, such as TRAP (Heiman, Schaefer et al. 2008) and Ribo-tag (Sanz, Yang et al. 2009), begin to overcome these obstacles, but these strategies have been limited to the analysis of mRNA expression.

Here we present a novel miRNA tagging and Affinity Purification method, miRAP, which can be applied to genetically defined cell types in any complex tissues in mice. This method is based on the fact that mature miRNAs are incorporated into RNA-induced silencing complex (RISC), in which the Argonaute protein AGO2 directly binds miRNAs and their mRNA targets (Hammond, Boettcher et al. 2001). We demonstrate

that epitope tagging of Ago2 protein allows direct purification of miRNAs from tissue homogenates using antibodies against the engineered molecular tag. We further established a Cre-loxp binary expression system to deliver epitope-tagged AGO2 (tAGO2) to genetically defined cell types. To demonstrate the feasibility of this approach in the brain, we have analyzed miRNA profiles from five neuron types in mouse cerebral cortex and cerebellum by deep sequencing. Our study reveals the expression of a large fraction of known miRNAs (over 480) which show distinct profiles in glutamatergic and GABAergic neurons, and subtypes of GABAergic neurons. Our method further detects 22 putative novel miRNAs and also provides evidence for tissue-specific strand selection of miRNAs and miRNA editing in subset of neuron types. The miRAP method therefore enables a systematic analysis of miRNA expression and regulation in different neuron types in the brain and is generally applicable to other cell types and tissues in mice.

3.2 A genetically targeted microRNA tagging methodology

Our strategy for molecular tagging and affinity purification is based on the knowledge that mature miRNA is incorporated into the RNA–Induced Silencing Complex (RISC) where the miRNA and its mRNA target interact (Hammond, Boettcher et al. 2001). Argonaute (AGO) proteins are at the core of RISC complex and directly bind miRNAs. AGO immunoprecipitation has been successfully used to isolate miRNAs and their mRNA targets (Beitzinger, Peters et al. 2007; Easow, Teleman et al. 2007; Zhang, Ding et al. 2007; Hammell, Long et al. 2008; Hendrickson, Hogan et al. 2008). Among the four members in the AGO family in human and mouse, only AGO2 exhibits endoneuclase activity (Meister, Landthaler et al. 2004; Ikeda, Satoh et al. 2006) and is

indispensible for Dicer-independent miRNA biogenesis (Cheloufi, Dos Santos et al. 2010). We therefore chose to tag Ago2 by fusing GFP and MYC at its N-terminus (tAGO2) (Figure 3.1A). GFP allows visualization of tAgo2 expression and MYC allows efficient affinity purification of associated miRNAs.

In addition to confirming the functionality of tAGO2, it is essential to reliably and systematically deliver tAGO2 to different cell types at consistent levels. We achieved this using the Cre/loxp binary expression system (Figure 3.1A). We generated a knockin allele at the Gt(ROSA)26Sor (Rosa26) locus which expresses tAGO2 upon Cre/loxp recombination (R26-LSL- tAGO2). Combined with an increasing inventory of cell type-restricted Cre driver lines, this strategy would allow systematic analysis of miRNA expression in different cell types in mice.

To test the functionality of the LSL-tAgo2 allele, we first crossed the reporter mouse to a CMV-Cre line to activate tAgo2 expression in the germline. Offspring of CMV-Cre;LSL-tAgo2 were identified in which tAgo2 is ubiquitously expressed in all cells of the animal (the tAgo2 mouse) (Sppl Figure 3.1) . Using antibody against AGO2, a 100kD endogenous band was detected in whole brain homogenates from both the tAgo2 and LSL-tAgo2 mouse, while the higher molecular weight tAGO2 band is only detected in tAgo2 sample (Figure 3.1C). This result demonstrates the tight Cre-dependent activation of tAgo2 expression from the LSL-STOP cassette.

Using antibody to AGO2, GFP or MYC, tAGO2 can be efficiently immunoprecipitated (IP) from tAgo2 brain lysate (Figure 3.1C). To examine the identity

of co-precipitated RNAs, they were extracted from IP product, radio-labeled and visualized by denaturing urea-PAGE. Enrichment of RNAs corresponding to miRNAs (e.g. 20-23 nucleotides) was observed using AGO2, MYC or GFP antibody-conjugated Dynabeads, but not with IgG control (Figure 3.1D). In addition, miRNA Taqman PCR detected miRNAs that are known to be brain specific in these RNA extracts (e.g. miR-124) at much higher levels than others that are known to be absent (e.g. miR-122, data not shown).

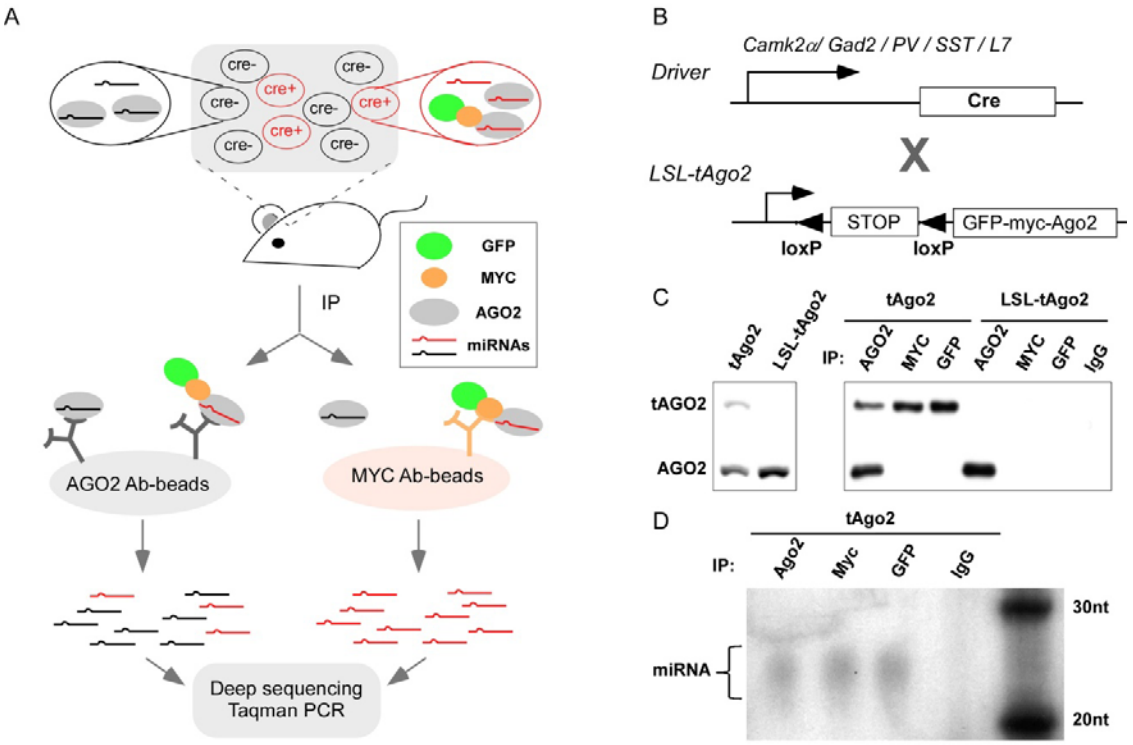

Figure 3.1 The miRAP methodology.

(A) The scheme of miRNA tagging and Affinity Purification (miRAP). tAGO2 (a GFP-MYC-AGO2 fusion protein) expression is activated by Cre recombinase in certain cell types in mouse brain. Using MYC antibody, miRNAs in Cre^{+} cells are co-precipitated with tAGO2. Using AGO2 antibody, miRNAs in all cells of the tissue are co-precipitated with AGO2 or tAGO2. RNAs prepared from immunoprecipitation (IP) product is subjected to deep sequencing or miRNA Taqman PCR.

(B) Cre-loxP binary system to achieve cell type specific delivery of tAGO2.

(C)Western analysis of tAGO2 expression and immunoprecipitation.

(D) Autoradiogram of ^{32}P-labelled RNA purified from *tAgo2* brain lysate by immunoprecipitation. RNAs ranging between 20-30nt were observed, corresponding to the size of miRNAs. (see also Sppl Figure 3.1)

3.3 miRNA profiling in several neuron types of the neocortex and cerebellum

We used the LSL-tAgo2 strategy to profile miRNA expression in glutamatergic, GABAergic, and subclasses of GABAergic neurons in P56 mouse neocortex and cerebellum. Cortical excitatory pyramidal neurons and inhibitory interneurons differ in their embryonic origin, neurotransmitters, and physiological function (Sugino, Hempel et al. 2006). GABAergic interneurons further consist of multiple subtypes characterized by distinct connectivity, physiological properties, and gene expression patterns (Markram, Toledo-Rodriguez et al. 2004; Ascoli, Alonso-Nanclares et al. 2008). In particular, the Ca2+-binding protein parvalbumin (PV) and neuropeptide somatostatin (SST) mark two major, non-overlapping subtypes (Gonchar, Wang et al. 2007; Xu, Roby et al. 2010; Rudy, Fishell et al. 2011). Whereas the PV interneurons innervate the soma and proximal dendrites and control the output and synchrony of pyramidal neurons, the SST interneurons innervate the more distal dendrites and control the input and plasticity of pyramidal neurons (Somogyi, Tamas et al. 1998; Di Cristo, Wu et al. 2004). Finally, Purkinje cells are GABAergic projection neurons which carry the sole output of cerebellar cortex.

We used well characterized transgenic or knockin Cre driver lines to activate tAgo2 in these cell types (Figure 3.1B, Sppl Table 3.1). The cell type specificity of tAGO2 was validated by dual immunostaining using antibodies against GFP and appropriate cell type markers (Figure 3.2, Sppl Figure 3.2, Sppl Table 3.1). Although not all neurons of a given classes expressed tAgo2, almost all GFP+ cells colocalized with corresponding cell type markers, proving the highly stringent specificity of our system.

tAGO2 predominantly localized to the cytoplasm in neuronal somata, but was also detected in neurites, with a particularly prominent example in the dendritic tree of Purkinje cells (Figure 3.2). miRAP was performed in cortical or cerebellar homogenates. Tissues from multiple mice were pooled as one IP sample when necessary. RNAs were immunopurified using a MYC antibody, extracted for construction of small RNA libraries which were analyzed by deep sequencing (Figure 3.1A). As a reference for these cell type specific miRNA profiles, we also sequenced miRNAs immunopurified by Ago2 antibody from neocortex and cerebellum and generated tissue-wide miRNA profiles. Consistent with previous reports, we observed that a group of miRNAs known to be brain specific, such as miR-124, miR-29b and miR-9, were highly enriched in all the samples. (Landgraf, Rusu et al. 2007; Bak, Silahtaroglu et al. 2008)

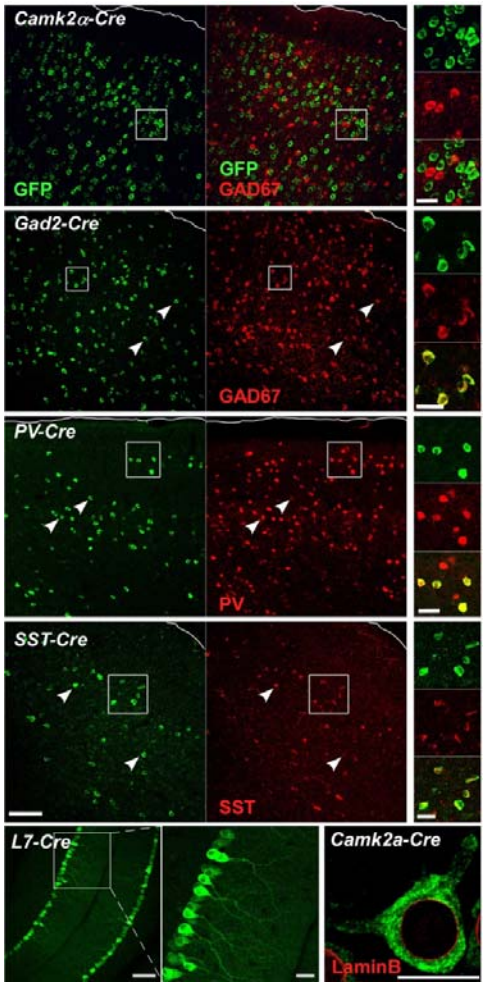

Figure 3.2 Cell type specific tAgo2 expression in the neocortex and cerebellum activated by Cre drivers.

Cre driver lines used are marked at top of each panel. tAgo2 expression was detected by GFP immunostaining. Pia of cortex is outlined. In the *Camk2α -Cre* line which labels pyramidal cells, GAD2 antibody was used due to the lack of appropriate Camk2α antibody; the lack of co-localization with GAD2 indicates tAgo2 expression in pyramidal neurons (also see sppl Figure 2 which demonstrates neuronal expression). In cortical GABA neuron drivers (*Gad2, Pv, Sst)*, GFP^{+} cells colocalized with corresponding cell type markers. In the *L7-cre* line, Purkinje cells were identified by their characteristic morphology and position. Note the prominent GFP signal in Purkinje dendrites. tAGO2 is predominantly localized in cell somata but not the nucleus, surrounded by LaminB (red) which labels nuclear envelop. Scale bar: 100μm in low magnification images, 20μm in high magnification images, 10μm in LaminB image. (see also Sppl Figure 3.2)

In total, we generated19 libraries and 291,164,604 raw reads. After removal of low-quality reads and those lacking 3' adaptor, 68.2% of the filtered reads equal or longer than 18nt were perfectly mapped to the mouse genome (mm9). 99.5% of all mapped reads can be aligned to known miRNA hairpins (miRbase 16). This percentage is higher than those from small RNA libraries constructed from size fractionated total RNA in most previous studies (commonly ranging 50%~80%), indicating that Ago2 immuno-precipitation is a more efficient way to enrich miRNAs while excluding other small RNAs such as degradation product of mRNAs (Table 3.1). In our experiments, the correlation coefficient of miRNA profiles from biological replicates within a group (the same cell or tissue type) were extremely high (>0.96, Sppl Table 3.1), indicating the high reproducibility of the miRAP method.

1.Total reads from Raw Data	291164604
2.Filtered total reads (>18nt)	188135991
Percentage of 2 in 1	64.6%
3. Reads perfectly mapped to genome	120186751
Percentage of 3 in2	63.9%
4. Reads map to miRNA precursor in miRbase 16	119551326
Percentage of 4 in3	99.5%
miRNA number in miRbase 16	672
miRNA detected (at least 1 read)	489

Table 3.1 Summary of deep sequencing

Hierarchical clustering based on the average linkage of Pearson Correlation (Eisen, Spellman et al. 1998) of miRNA profiles revealed non-random partition of the samples into two major branches, one containing all five individual neuron types and the other containing the two tissue types (Figure 3.3). This division is unlikely to be cause

by the use of different antibodies for IP, as in vitro studies show no difference of miRNA affinity between tagged and untagged Ago2 proteins (personal communication with Hannon lab). This result demonstrates the necessity and power of cell type based analysis. A common assumption is that brain specific or CNS specific miRNAs are likely to be neuron specific. Our findings suggest this is not always the case. For example, miR-143 was expressed at relatively high levels in both neocortex and cerebellum (ranking at 30 and 51 respectively, from highest to lowest in the normalized miRNA annotation profiles), but expressed at relatively low levels in all the examined neuron types (ranking after 160) (Sppl Table 3.2). It is likely that miR-143 and certain other brain enriched miRNAs may in fact be highly expressed in non-neuronal cells such as astrocytes. On the other hand, miRNAs that are enriched in specific but relatively rare neuron types are likely to be underrepresented and under-appreciated in miRNA profiles generated from the tissue homogenates. For example, miR-34a ranked at 14 in PV profiles, but only at 116 in neocortex profiles (Sppl Table 3.2). Together, these results highlight the critical importance of cell type-based approach in analyzing miRNA expression and function.

Although more similar to each other than to individual neuron types, difference in miRNA expression is observed between neocortex and cerebellum (Sppl Figure 3.3A and Sppl Table 3.3). This is consistent with results from different brain regions using miRNA microarray. For example, miR-128 is expressed ~4 folds higher in neocortex than in cerebellum, while miR-195 and miR-497 are expressed at >10 folds higher in cerebellum than in neocortex. In total, 221 out of 527 detected miRNAs and miRNA* were identified

as differentially expressed between these two brain regions in P56 mouse (P value <0.001, Sppl Figure 3.3A and Sppl Table 3.3), with differences as high as 55 fold.

Within the five neurons types, cortical Gad2, PV and SST neurons cluster together most closely, as expected from their common origin and transmitter phenotype. The miRNAs enriched in these groups, such as miR-34c and miR-130b, are likely to regulate functions that are common in all neocortical GABAergic interneurons. Others which show differential expression might serve as "finger prints" for subtypes of GABAergic neurons and regulate subtype specific functions. For example, both miR-133b and miR-187 are highly enriched in GABAergic neurons when compared to glutamatergic pyramidal neurons. However, miR-133b is significantly more enriched in PV cells, while miR-187 is more enriched in SST cells (Figure 3.4E). Interestingly, neocortical GABAergic neurons cluster more closely with Purkinje cells from cerebellum than with cortical glutamatergic neurons. This suggests that neurotransmitter phenotype, a major aspect of neuronal identity, is a more significant determinant than brain regional location in neuronal miRNA expression.

To compare expression levels of each miRNA in different libraries, we constructed relative miRNA expression profiles and arranged the miRNA according to their expression pattern (Figure 3.3). Many miRNAs have substantially stronger expression in one or more neuron types or tissue types than in others. This selective expression pattern suggests specificity in target regulation, and thus specific miRNA function, in different cell types and anatomical regions.

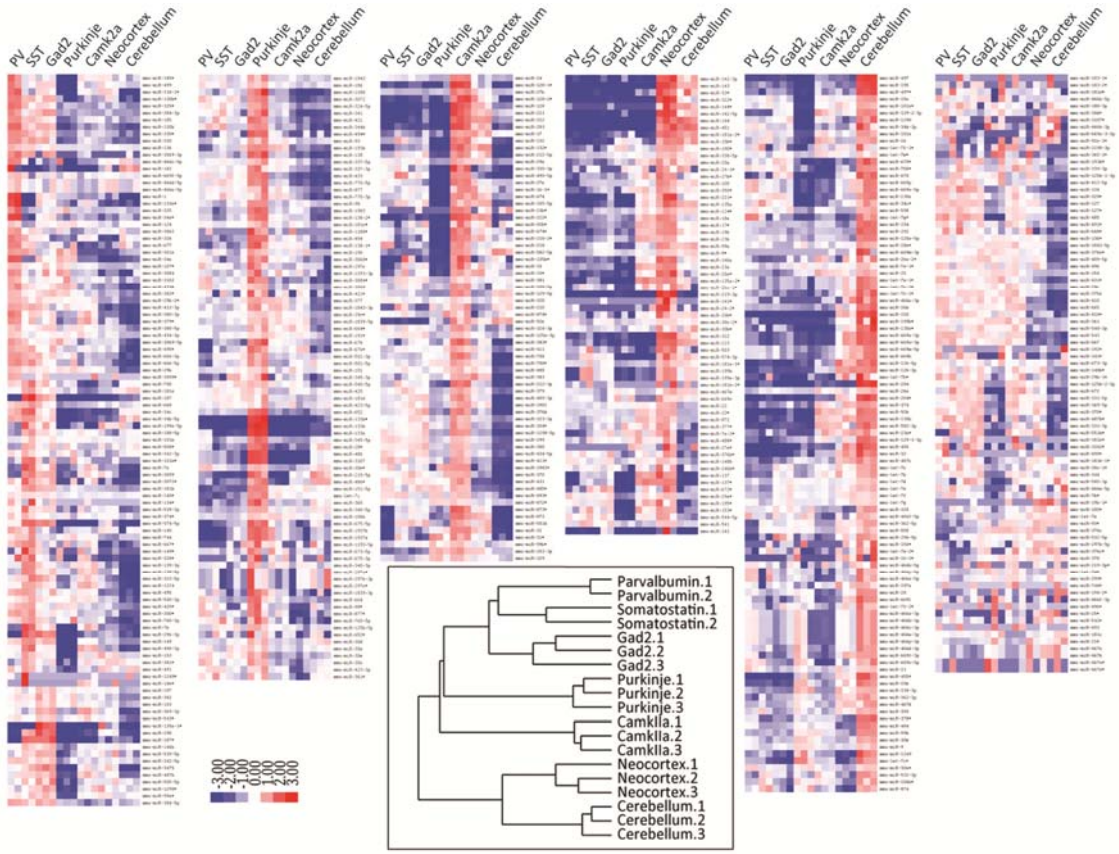

Figure 3.3 Relative miRNA expression profiles and hierarchical clustering of samples.

Relative expression profiles of mature miRNAs were constructed as follows: the raw reads counts of each miRNA are first normalized to the total number of reads that were mapped to all of the known mature miRNAs and miRNA* species, then log2 transformed, and mean centered. Inset: Hieratical clustering of miRNA expression of all the libraries. (see also Sppl Table 3.2)

3.4 Validation of deep sequencing results by miRNA Taqman PCR

To more closely examine differential miRNA expression in different cell types, we performed pair wise comparison between cortical glutamatergic and GABAergic neurons, and subtypes of GABAergic neurons. To validate the cell type differences revealed by deep sequencing, we used Taqman PCR to assess subsets of miRNAs from independent sets of samples. As the miRAP method enriches miRNAs but depletes other RNA species by design, we cannot use house-keeping mRNAs as endogenous control for normalization. Instead, difference for each miRNA between two cell types was calculated using the ΔΔCt method, ie. first normalized to the Ct value of miR-124, then compared between each other. In order to directly compare deep sequencing result with Taqman PCR result, the per million reads number of individual miRNAs in deep sequencing profiles are log2 transformed and normalized to the value of miR-124 as well. (Please note the choice of miRNA for normalization does not affect the results; in theory we could use any other miRNA beside miRNA-124 as internal reference, as the qPCR result is by no means an absolute quantification of miRNA abundance, but a way to allow the comparison between two cell types. The normalized value does not reflect actual differences of expression between one miRNA and the internal reference, in this case, miRNA-124. Only the relative differences of miRNA between two cell types are meaningful. Here we chose miR-124 as it is usually the most abundant one in neurons, exhibits relatively low Ct value in qPCR and therefore may introduce less experimental variance.)

We first examined the Camk2α and Gad2 group which represent the two cardinal neuron types in neocortex. 157 out of 523 detected miRNA or miRNA* were identified to have significant differential expression in deep sequencing profiles ($P<0.001$, Figure 3.4B and Sppl Table 3.4). We did Taqman PCR for 21 miRNAs, and found very high concordance between the two profiling techniques. Not only the trend of enrichment or depletion matched, but also the exact fold change value resembled closely (Figure 3.4D).

Next, we compared the PV and SST groups, which represent two major non-overlapping subtypes of cortical GABAergic interneurons. 125 out of 511 detected miRNA or miRNA* were identified to have significant differential expression in deep sequencing profiles ($P<0.001$, Figure 3.4C and Sppl Table 3.5). A set of 10 miRNAs were examined by Taqman PCR, which also validated the deep sequencing results very well (Figure 3.4E). Similarly, Taqman PCR validated the deep sequencing results in Purkinje cell vs cerebellum (Sppl Figure 3.3B and Sppl Table 3.6).

As an independent validation of the miRAP method, we performed FACS sorting to isolate Camk2α cells in neocortex and extracted RNA for Taqman PCR analysis. In order to label Camk2α neurons specifically, we generated a Rosa26-loxp-STOP-loxp-H2B-GFP reporter line which brightly labels cell nuclei upon Cre activation (Sppl Figure 3.3C). Breeding with the same Camk2α -Cre line used for miRAP, we were able to sort Camk2α cells at high purity. Most of miRNAs tested show very similar expression level between the two purification methods, proving miRAP as a reliable method to enrich cell type specific miRNAs (Figure 3.4F).

We also tried to validate in neocortical GABAergic neurons with the FACS sorting –qPCR method, but did not get results as consistent as the Camk2α case. (Sppl Figure 3.4). Only a subset of miRNAs tested show similar expression level between FACS sorting sample and miRAP samples, while the others show significant discrepancy. We believe the discrepancy can be largely explained by artifacts caused by FACS sorting and the inherent differences between two methods, rather than inaccurate profiling using miRAP.

We have noticed that the number of GFP positive cells collected from FACS sorting is much lower than one would predict based on theoretical calculation of cell density in the cortex, i.e., only a subset of neurons were retained from the initial population (usually 1% or less). This may not be a problem for pyramidal cells, as they are quite similar to each other compared to interneurons. This is why for Camk2α samples FACS and miRAP generate highly similar profiles. However, it could skew miRNA profiles in interneuron greatly. As discussed earlier, neocortical GABAergic neurons are very heterogeneous in many aspects, including gene expression patterns. Therefore the heterogeneity of miRNA expression among interneuron subtypes could also be very high. As FACS sorting has low efficiency, the composition of subtypes was not probably retained in the post-sorted samples. As different subtypes of interneurons have different miRNA profiles, the change of subtype composition will greatly affect the output profiles. This is probably why Gad2 samples show higher discrepancy than PV and SST samples, as Gad2 neurons are a much more heterogeneous population, encompassing PV and SST subtypes.

FACS sorting followed by RNA extraction purify miRNAs from the whole cell, representing the steady state of miRNA expression. The output of FACS depends on cell number and. On the other hand, miRAP purify miRNAs associated with RISC complex, representing the functional population of miRNA. The output of miRAP depends on not only cell number and cellular content of miRNAs, but also the functional state of miRNA, and the expression level of tAgo2 within each cell type. Even if we purify miRNA from exactly the same population of cells, as long as there is variation in the latter two conditions, one would expect somewhat different results from the two methods. In our immunostaining results, we have noticed the tAgo2 expression level in Camk2α neurons is in general higher than in GABAergic neurons, and more homogenous. Even within PV or SST subtypes, we have noticed different levels of tAgo2 expression. This could also contribute to the discrepancy we have observed in these neurons.

In the case of Purkinje cells, we have made two attempts of FACS sorting, and both got very inconsistent results among biological replicates of FACS samples and two batch of samples (data not shown). We wonder if adult Purkinje cells were particularly sensitive to FACS sorting procedure and changed their miRNAs drastically which led to uninterpretable results.

In addition to FACS sorting, we also tried miRNA in situ hybridization in mouse brain sections using LNA probes. We have tried two different protocols, one was using paraffin embedded sections and NBT-BCIP color deposit substrate (protocol 1); the other

was using cryosections and TSA fluorescence substrates (protocol 2), both modified from published protocols (Obernosterer, Martinez et al. 2007; Pena, Sohn-Lee et al. 2009).

Mouse cerebellum has very organized structure. It is easy to identify different cell types based on their layer localization without maker staining. Therefore we first focused on cerebellum staining pattern. We were able to detect positive signal for a subset of miRNAs (~1/4 of all probes tested) in cerebellum sections, but the results were not very consistent between two protocols. Some probes generate nice signal with one method, but has little or no signal with the other protocol; some even show different patterns with the two protocols. For example, miR187 can be detected by protocol 1, but not protocol 2; miR-298 is the opposite. For miR-149, protocol 1 shows similar expression level of miR-149 in Purkinje cells and granule cells, but protocol 2 shows higher expression in Purkinje cells than granule cells, while our profiling results imply lower expression in Purkinje cells than other cells types. Therefore we did not rely on miRNA in situ for validation, even though some of the in situ results were consistent with our miRAP results in cerebellum (miR-130b and miR-210 show similar expression level in Purkinje cells and other cell types in cerebellum; miR-133a and miR34a show higher expression level in Purkinje cells than other cell types; Sppl Figure 3.5 and 3.6).

For neocortex, it is difficult to identify specific neuron types without additional in situ or immunostaining for cell type markers, as different cell types are intermixed. We did not pursue further for this part considering the confusing result observed in cerebellum. However, I should note that whenever we observed signal in neocortex and

hippocampus, it seem to be present in all cells (similar pattern as U6 control), despite our profiling results indicate there should be some differences among different miRNA probes (data not shown). It is still possible that our miRNA in situ protocol is not optimized enough for proper assessment miRNA localization, but the current results we have are not suitable for validating our profiling results.

Although we hesitate to use miRNA in situ as proof of miRNA localization in neuron subtypes, we do find some published results being consistent with our miRAP result. For example, miRNA in situ showed more prominent expression of miR-134 and miR-370 in the Purkinje cell layer compared to other regions (Schaefer, O'Carroll et al. 2007; Pena, Sohn-Lee et al. 2009), which is consistent with our finding that these two miRNA are relatively enriched in Purkinje cells compared to whole cerebellum (~7 fold, Sppl table 3.6).

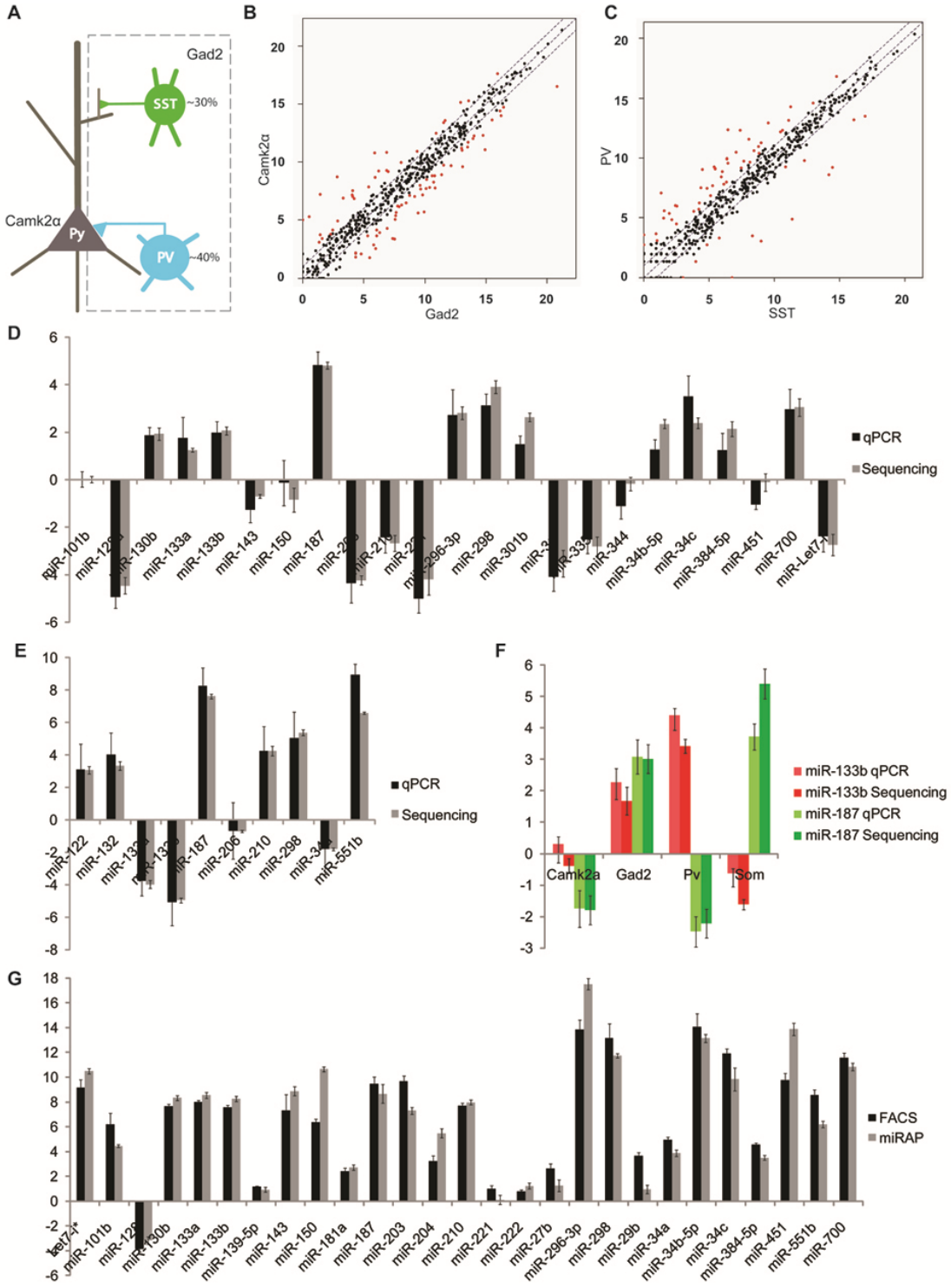

Figure 3.4 miRNA expression profiling in neocortical neurons.

(A) A simple schematic of neocortical neurons included in this study. The two major neuron types, glutamatergic projection neurons and GABAergic interneurons are targeted by Camk2α-cre and Gad2-cre lines, respectively. PV and SST interneurons are two non-overlapping subtypes of GABAergic neurons targeted by Pv-Cre and Sst-Cre, respectively.

(B) (C) Normalized expression values of miRNAs are plotted for Camk2α vs. Gad2 samples, and PV vs SST samples. The middle diagonal line represents equal expression, and lines to each side represent 2-fold enrichment in either cell population. The labels of axes are log 2 scaled. miRNAs with fold changes equal or larger than 2 and P values lower than 0.001 are represented in red.

(D) (E) miRNA Taqman PCR validation of deep sequencing. All miRNAs were normalized to miRNA-124 using the ΔΔCt method. Deep sequencing reads number were log2 transformed and then normalized to miRNA-124. (D) The value of Camk2α sample was compared to Gad2 sample. Values above 0 represent higher expression in Gad2 than Camk2α, and vice versa. n=3 for deep sequencing; n=4 for Taqman PCR. (E) The value of PV sample was compared to SST sample. Values above 0 represent higher expression in PV than SST, and vice versa. n=2 for deep sequencing; n=4 for Taqman PCR.

(F) miR-133b and miR-187 expression in four neocortical neuron types. The cell type specific data was normalized to data of neocortex homogenates in each case. Value above 0 indicates higher expression than neocortex sample, and vice versa.

(G) Comparison between RNAs purified from FACS sorting and miRAP using Taqman PCR in Camk2α neurons. n=4.Error bar: standard deviation. (see also Sppl Figure 3)

3.5 miRNA clusters and families

A large number of miRNAs reside in clusters in the genome (Altuvia, Landgraf et al. 2005), with miRNAs in the same cluster sharing the same promoter and polycistronic pri-miRNA transcript. Short distances between miRNA genes on the chromosome imply they may be located in a cluster, but it is not obvious what would be the appropriate distance to define a cluster and different standards have been used (Altuvia, Landgraf et al. 2005; Baskerville and Bartel 2005; Leung, Lin et al. 2008). Because miRNAs in the same cluster are co-transcribed, their expression should be more consistent with each other than those which are located in different clusters (Tanzer and Stadler 2004). We examined the relationship between genomic distance and pair-wise correlation coefficient of miRNAs on the same strand of the chromosome. The average correlation of paired miRNAs drops sharply at the genomic distance of 50kb (Figure 3.5), suggesting the average size of miRNA clusters may be approximately 50kb. This result agrees with those from Chiang et al which examined miRNA profiles in different tissue types (Chiang, Schoenfeld et al. 2010).

Based on primary sequence and secondary structure conservation, miRNAs can be grouped into different families. miRNAs from the same family evolved from a common ancestor and have high sequence homology. Therefore, family members may share mRNA targets and are involved in the similar aspects of biological function. As cell type is the basic unit of gene regulation in brain tissues, we examined whether miRNAs within a family have similar expression pattern. Information on miRNA families was obtained from miRBase. By examine the distribution of correlation coefficient, we

observed higher correlation of expression across the 5 cell types and 2 tissue types for miRNAs within the same family than ones between families (the family classification information of miRNAs is got from miRbase). This result indicates cooperation and co-regulation of homologous miRNAs (Figure 3.5B).

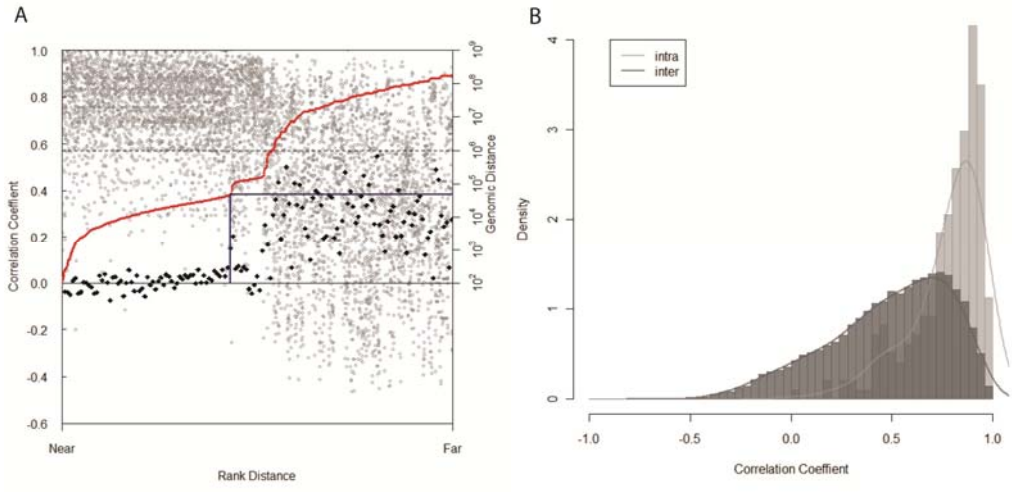

Figure 3.5 Correlation among miRNA gene expression, genomic organization and sequence similarity.

(A) Correlation of miRNA expression and the distance separating miRNA gene loci. Each miRNA gene was paired with every other miRNA lying in the same orientation on the same chromosome. For each pair, the distance between the two loci was ranked, and the correlation coefficient for their expression was plotted according this rank (grey circle). The red line indicates the relationship between rank and actual genomic distance. 50-point moving average of correlation coefficients was calculated. The difference of each moving average and the next was plotted according to the rank (black diamond). The blue line indicates the first point where this value deviates abruptly from the previous ones, i.e. where the average correlation coefficient beyond certain genomic distance changes abruptly.

(B) Correlation of expression among miRNA genes within a family (intra-family) and those that do not belong to the same family (inter-family). miRNA genes within the same family tend to have higher correlation coefficient than those that belong to different families. (see also Sppl Figure 3.7 and Sppl Table 3. 3-3.6)

3.6 Tissue-specific strand selection of miRNAs

Mature miRNAs can be processed from either the 5' arm or 3' arm of the precursor miRNA hairpin but in most cases are preferentially processed from only one arm. Overall, the discrimination of preferred strand (miRNA) over the other strand (miRNA*) is very high (Hu, Yan et al. 2009). Indeed, in our libraries the preferred stand comprises >90% of all the reads mapped to miRNA or miRNA* (Sppl Figure 3.4). In our data set, the preferred arm largely remained consistent across the cell and tissue types. However, a few miRNAs switched dominant arms in different libraries. For example, miR-544-3p was sequenced more frequently in Purkinje cell and cerebellum samples, while miR-544-5p was sequenced more frequently in the four neocortical cell samples and neocortex tissue sample. Because the two strands are expected to regulate different in mRNA targets, this brain regional difference in strand selection may have functional relevance in cellular phenotypes and physiology. In the case of miR-299 vs miR-299*, there were more reads of miR-299* in all libraries except in the two from SST cells. The case of miR-485 is more complicated: there is higher reads number for miR-485* in Purkinje cells, Camk2α cells and cerebellum, but similar reads number for miR-485 vs miR-485* in other libraries (Table 3.2).

	Pv	Som	Gad2	Purkinje	CamkIIa	Neocortex	Cerebellum
mmu-mir-544	0.088	1.132	0.119	-2.337	0.065	1.837	-0.224
mmu-mir-299	0.853	-0.105	0.893	1.915	1.097	1.507	3.543
mmu-mir-485	0.036	0.512	-0.246	-5.073	-0.991	0.514	-2.630

Table 3.2 Summary of tissue/cell type specific strand selection

Value in the table is the log 2 transformed ratio of 5' and 3' arm reads after adding pseudocount of one. Negative value means more reads from 5' arm than 3' arm of the miRNA precursor and vice versa.

3.7 Analysis of miRNA editing

RNA editing is the alteration of RNA sequence post transcription through nucleotide insertion, deletion or modification (Brennicke, Marchfelder et al. 1999). The most common type is adenosine (A) to inosine (I) base modification in dsRNA which is catalyzed by adenosine deaminases (ADAR). Pri-miRNAs and Pre-miRNAs are double stranded and can serve as ADAR substrate (Luciano, Mirsky et al. 2004; Blow, Grocock et al. 2006; Kawahara, Megraw et al. 2008). Such modification of miRNAs could affect their biogenesis and alter target specificity, thus affecting miRNA function (Yang, Chendrimada et al. 2006; Nishikura 2010).

Since the brain is a primary site of ADAR expression in mammals, we looked for evidence of miRNA editing in our samples. We first searched reads that have single nucleotide mismatches to miRNA and miRNA* but not perfectly matched to the mouse genome (mm9). To avoid considering untemplated 3'-terminal addition, we focused on mismatches that occurred at least 2 nucleotides from the 3' end. We observed substantially higher A-to-G base change above any other types of single nucleotide changes, indicating A-to-I modifications in miRNAs (Sppl Figure 3.8A). To look for specific sites of A-to-I editing in individual miRNAs, we calculated the rate of A-to-G changes at every genomic position of the sequenced reads. If the fraction of A-to-G modification at certain position exceeded 5% in any library, had a raw reads number above 10, and the same modification was detected in at least two libraries, it was considered as inferred A-to-I editing sites. Under these criteria, we discovered 18 editing sites in all the libraries. None of these sites corresponded to known SNPs. Some of them

have been reported before, such as miR-381 at position 4 and miR-376b/c at position 6, etc (Kawahara, Zinshteyn et al. 2007; Chiang, Schoenfeld et al. 2010). (Table 3.3)

One interesting phenomenon we have observed is that some of these inferred miRNA editing events seem to show cell/tissue type specificity, i.e. showing higher percentage of mismatch in libraries from some cell or tissue type than the others. At this point, we are not sure if this is due to biological reasons or experimental variation. We did not observe correlation of editing difference with genetic background of mouse strain, therefore it is unlikely the pattern is an artificial effect caused by SNPs.

One prominent example of mRNA editing in mammalian brain is editing of the mRNA encoding the 2C subtype of serotonin receptor (5-HT2CR). Five editing sites (A–E) have been identified within 5-HT2CR mRNA and the modified transcripts are present at different levels depending on the part of the brain analyzed (Burns, Chu et al. 1997; Niswender, Sanders-Bush et al. 1998), indicating these editing events occur at different rates in different brain region. However, why there is regional difference of editing on the same RNA given the broad expression patterns of ADAR enzymes is not fully understoon. Variations in expression levels of the editing enzyme, ADAR2, and/or from the variations in the ADAR2/ADAR1 ratio could partially explain some of these regional differences (Dracheva, Lyddon et al. 2009). Brain region difference of RNA editing has also been observed for GluR2 mRNA, and is associated with the expression level of ADAR2 mRNA (Kawahara, Ito et al. 2003).

As different brain region has different cell types, it is highly likely that the observed difference in the expression level of these modified transcripts derived from cell type specific bias of individual editing events. Therefore, it is not surprising to find similar situation for miRNA editing and maybe the cell/tissue type difference of miRNA editing we observed are real and have biological significance. The differential regulation of miRNA editing in cell/tissue types may also be partially explained by similar mechanisms. There are three highly conserved ADARs in vertebrates, ADAR1-3. ADAR1 and ADAR2 are detected in many tissues, whose enzyme activity has been demonstrated; whereas ADAR3 is expressed only in restricted regions of the brain and may not be enzymatically active, although the functional domain features are conserved(Nishikura 2010) (Chen, Cho et al. 2000). ADAR1 and ADAR2 have different substrate preference and efficiency (Wong, Sato et al. 2001; Dawson, Sansam et al. 2004), and seen to target different miRNAs (Kawahara, Megraw et al. 2008). ADAR3 could inhibit ADAR1/2 activity in vitro (Chen, Cho et al. 2000), and may serve as regulator of ADAR1/2 in vivo. Other factors, such as stability and functionality difference between unedited and edited miRNAs could also contribute to the detected cell/tissue type difference of miRNA editing.

Another interesting question worth investigating is if there are multiple editing events co-occurring in the same miRNA. We have not examined this question as the algorism we used for data processing filtered out sequences having more than one mismatches to miRNAs at the raw data processing step. We plan to modify the data analysis program to analyze reads alignments with up to three mismatches in order to

answer this question. Study in mouse brain by Chiang et al has shown that the vast majority of edited reads were edited at one position (Chiang, Schoenfeld et al. 2010), therefore we expect to see few miRNAs to be edited at multiple positions, if any.

As a control, we examined the background error rate of single mismatch in the two synthetic RNA oligos (M19 and M24) that we used during library construction. The total percentage of single mismatch is significantly lower than that from miRNAs, as is the rate of mismatch at each position of the oligos compared to the 5% filter criteria we set. In addition, A-to-G mismatch is not the highest kind of mismatches in the 12 possible single nucleotide mismatches found in the reads of control oligos (Sppl Figure 3.8B). This result indicates that the A-to-I editing events we observed in miRNA reads are most likely to be biological.

miRNA	A-to-I editing position	Percentage of edited reads
mmu-miR-100	1	0.2%
mmu-miR-1251	6	11.0%
mmu-miR-1274a	15	7.2%
mmu-miR-3099	7	72.5%
mmu-miR-337-3p	11	6.5%
mmu-miR-34b-5p	11	4.5%
mmu-miR-376b	6	72.9%
mmu-miR-376c	6	56.0%
mmu-miR-377	10	12.6%
mmu-miR-378	16	10.2%
mmu-miR-379	5	26.8%
mmu-miR-381	4	23.0%
mmu-miR-411	5	43.6%
mmu-miR-421	14	9.7%
mmu-miR-467c	3	10.2%
mmu-miR-467e	4	0.5%
mmu-miR-497	2	0.9%
mmu-miR-99a	1	6.1%

Table 3.3 Inferred A-to-I editing sites in miRNAs

3.8 Discovery of novel miRNAs

We sought to identify novel miRNAs from our deep sequencing data using a miRNA-discovery algorithm, miRDeep2 (Friedlander, Chen et al. 2008). We did prediction for each of the 19 libraries, and combine the results according to genomic position of the prediction. In total, 26 candidates passed the score cutoff of 6, which provided the highest signal-to-noise ratio (7.36) of the prediction, and had normalized read number larger than 1 per million in at least two libraries. These candidates were manually curated to remove highly palindromic precursors or redundant sequences resulting in a refined set of 23 miRNA candidates (Table 3.3). One of them has recently

been deposited into miRbase V17 (mmu-mir-3572) (Spierings, McGoldrick et al. 2011). Most of these predicted novel miRNAs have the same seed sequence as known miRNAs in other species, supporting the hypothesis that they are bona fide miRNAs. Among these, 15 predicted novel miRNAs reside in introns of other genes and 4 derive from small nucleolar RNAs(snoRNAs). Figure 3.6 shows the structure of one candidate miRNA precursor which derives from the SnoRNA H/ACA box 7A.

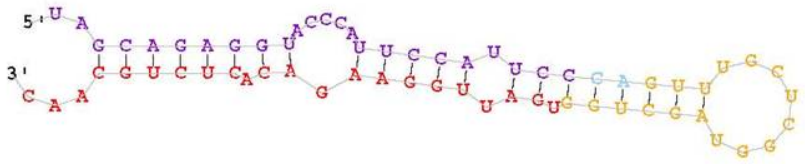

Figure 3.6 Secondary structure of one candidate novel miRNA

Red region: mature miRNA. Yellow region: loop. Purple region: miRNA*

3.9 Discussion

A necessary step towards understanding the regulatory function of miRNAs in the brain is gaining a comprehensive knowledge on their expression in the relevant cell types of the neural circuits and in the relevant physiological and developmental processes. However, to date, analysis of miRNA expression profiles in the brain has relied on tissue homogenates which completely erase cell type distinction. This approach not only cannot detect and quantify miRNAs in rare (and yet important) cell types but also makes

it nearly impossible to interpret results in the context of neural circuits that underlie the function under investigation. Physical enrichment of target cell population can significantly improve cell type resolution but suffer from several limitations. FACs (Arlotta, Molyneaux et al. 2005) or manual sorting (Sugino, Hempel et al. 2006) of fluorescence labeled cells and laser captured microdissection (Rossner, Hirrlinger et al. 2006) are often laborious and of low yield. The extensive manipulation of tissue causes cell damage and stress which alter gene expression. Here we establish a genetically targeted and affinity-based miRNA profiling method, miRAP, which largely overcomes these obstacles. miRAP is conceptually similar to TRAP and Ribo-Tag, which are designed for mRNA profiling, and presents several major advantages. First, miRAP captures miRNAs during their biogenesis and function within the cell in situ, thus bypassing cell enrichment and can be applied to tissues that are difficult to dissociate. Second, miRAP avoids physical damage and stress of cells. Third, miRAP procedure is simple and sensitive. Indeed, when estimated by the Ct value of miR-124 from two methods for the same cell type, the yield of RNA from miRAP samples is 70-400 times higher than FACS from the same amount of starting material, likely due to loss of fluorescence and cell death during FACS preparation and process. Together, these features of miRAP make it ideal for deep sequencing and Taqman PCR analysis in rare cell types when sample pooling is necessary.

Our implementation of miRAP using the Cre/loxP binary system is similar to Ribo-Tag (Sanz, Yang et al. 2009) which used Knock-in strategy to generate Cre responsitive epitope tagged ribosomal subunit, and has several advantages over bacTRAP

(Heiman, Schaefer et al. 2008) which used BAC transgenic method to express EGFP-tagged ribosomal protein L10a in specific cells for for immunepurification of mRNA. First, we can make use of well characterized Cre drivers which allow reliable and consistent expression of tAGO in genetically defines cell types in any tissue of interest, thus avoiding concerns about random insertion of BAC transgenes in the genome and ectopic expression in different transgenic lines. Second, Cre-dependent tAGO2 expression is well suited to study the effect of cell specific gene manipulations when combined with various floxed alleles. Third, because miRAP captures miRNA in situ under the physiological state of the cell, it allows meaningful assessment of miRNA profiles in the context of neuronal development, function, plasticity, pathology, and in mouse models of brain disorders. Finally, combined with other Cre dependent genetic tagging system, such as the Ribo-Tag, miRAP allows an integrated analysis of different molecular profiles in the same cell type using a defined drive line; this will facilitate a deeper understanding of the multi-level and multi-faceted gene regulatory mechanisms, such as those involving miRNA-mRNA interactions.

The Cre-activated expression of tAGO2 in our miRAP method is unlikely to significantly alter miRNA profile in the cells for the following reasons. In the tAgo2 mouse line in which tAGO2 is expressed in all cells of the animal, the expression level of tAGO2 is lower than the endogenous AGO2, assayed by western blot of whole brain homogenates (Figure 3.1C and Sppl Figure 3.1D). Interestingly, the combined level of tAGO2 and AGO2 in tAgo2 brain is comparable to, if not less than, the level of AGO2 in LSL-tAgo2 mouse brain (with no tAGO2 expression), suggesting a feedback regulation

of Ago2 expression. None of the Cre activated LSL-tAgo2 mouse lines show any notable phenotype in development and behavior. The epitode tag on AGO2 is also unlikely to change its affinity to miRNAs, as shown in in-vitro binding assays (?? G.H. unpublished result). In addition, in the validation experiment for Camk2α -Cre, the expression of miRNAs in two mouse lines harboring different transgenic allele, i.e. LSL-tAgo2 and LSL-H2B-GFP, showed the same expression level for the miRNAs examined. Together, these results indicate that the miRAP system is unlikely to affect the native miRNA profiles.

When comparing expression data obtained from miRAP and FACS, we detected discrepancy in expression levels of a few miRNAs (Figure 3.4E). This is likely due to the following factors. First, physical damage and stress during FACS sorting may alter miRNA profiles, because expression of certain miRNAs are sensitive to neuronal activity or respond to cellular stress. Second, FACS sorted neurons only retain cell body whereas most of their neuronal processes are lost, along with the miRNAs that are localized in dendrites (Tai and Schuman 2006) and synapses (Lugli, Torvik et al. 2008; Schratt 2009). miRAP, on the other hand, should capture miRNAs in neurites since AGO2 has been shown to localize in dendtrites (Lugli, Larson et al. 2005; Cougot, Bhattacharyya et al. 2008) and tAGO2 signal can be detected in dendrites (Figure 3). Third, not all mature miRNAs are incorporated into RISC complex. Profiles from miRAP likely represent "active" miRNAs which are associated with Ago2, while miRNA extraction from sorted cells harvests steady state miRNAs regardless of their functional status. Finally, within each major GLU and GABAergic neurons in our study, subtypes likely express tAgo2 at

different level and show different miRNA expression and regulation, including their response to stress and physical damage during FACS. The compounding effect of these factors will affect the miRNAs profiles obtained from these two methods. Another common method to validate RNA expression is in situ hybridization using LNA probes. Unfortunately, our extensive effort did not yield consistent and interpretable results, probably due to the relatively low expression of cell type specific miRNAs.

A potential caveat in a molecular tagging strategy to nucleic acid purification is the redistribution of the affinity tag to the un-tagged pool during homogenization and IP. This is more concerning when the tag is of low affinity and requires chemical cross linking. This issue is inherent to the tag and IP procedure itself and thus is common to all datasets; it would reduce the observed magnitude of differential expression among cell types. This issue is less of a concern for miRAP because AGO2-miRNA interaction is very stable and of high affinity (Tang, Hajkova et al. 2008). In addition, comparison of FACS with miRAP in the Camk2α-Cre line suggests that our method faithfully represent the miRNA profiles in this cell type.

Discovered less than two decades ago, miRNAs have since been implicated in the regulation of almost all aspects of cellular processes. Despite their prominent expression in the mammalian brain, the role of miRNAs in brain development, function, and plasticity remains poorly understood. A major challenge is to link miRNA activity in defined neuron types to specific aspects of neuronal specification, development and physiology; characterizing miRNA profiles in specific cell types is the first step. Using

miRAP, we have obtained the first set of miRNA expression profiles in defined neuron types in mouse brain. Our study reveals the expression of a large fraction of known miRNAs with distinct profiles in glutamatergic and GABAergic neurons, and subtypes of GABAergic neurons. We have further detected putative novel miRNAs, tissue or cell type- specific strand selection of miRNAs, and miRNA editing. This generally applicable miRAP method will facilitate a systematic analysis of miRNA expression and regulation in specific neuron types in the context of neuronal specification, development, physiology, plasticity, pathology and disease models. Targeting of rare cell types may further reveal novel, low abundant miRNAs, and link novel regulatory mechanisms such as miRNA editing to specific neuronal and circuitry function.

Identification of mRNA targets in defined cell types is key to understanding the biological function of miRNAs. As miRNA activity requires base-pairing with only 6-8 nucleotides of mRNA, target prediction through bioinformatics has proven to be challenging. Recently, Ago HITS-CLIP has been used to profile miRNA-mRNA targets in the mouse brain (Chi, Zang et al. 2009). Genetically targeted miRAP provides a possibility for cell type specific Ago2 HITS-CLIP using the MYC or GFP antibody.

3.10 Materials and methods

3.10.1 Mouse lines

To generate mouse line that conditionally express GFP –myc-Ago2, a cassette containing LoxP-STOP -LoxP-GFP-myc-Ago2 was cloned in to a Rosa26-CAG targeting vector which contains DTA negative selection marker. GFP-myc-Ago2 is a gift from Dr.

Richard M. Schultz in University of Pennsylvania. The STOP cassette contains Neo gene which confers G418 resistance. The targeting vector was linearized by PacI digestion and transfected into C57BL/6 mouse ES cell line. G418-resistant ES clones were screened by PCR first, then confirmed by southern blot of EcoRV digested DNA, which was probed by a 134bp genomic fragment upstream of the 5' targeting arm. Essentially all PCR positive clones are also positive for southern blot. Positive ES cell clones were injected into albino C57BL/6 blastocysts to obtain chimeric mice following standard procedures. Chimeric mice were bred with albino C57BL/6 mice to obtain germline transmission. To generate mouse line that conditionally express H2B-GFP, ZsGreen gene in Ai6 vector (Madisen, Zwingman et al. 2010) targeting vector was replaced with H2B-GFP gene. Ai6 vector is a gift from Dr. Hongkui Zeng from Allen Institute for Brain Science. 129SVj/B6 F1 hybrid ES cell line (V6.5, Open Biosystems) was transfected and screened using same strategy as Ai6 mice. Positive ES cell clones were used for tetroploid complementation to obtain male heterozygous mice following standard procedures. Heterozygous mice were bred with each other to obtain homozygotes. Homozygotes were bred with Cre driver lines for experiment.

CMV-cre (Stock NO 003465), *Camk2α –Cre* (Stock NO 005359) and two lines of *L7-Cre* mice(Stock NO 006207 and 004146; the first one was used for miRAP, the second one was used for immunostaining to show tAGO2 localization in Purkinje cells) were purchased from Jax laboratory. *Pv-ires-Cre* mice were gift from Dr Silvia Arber. *Gad2-ires-Cre* and *Som-ires-Cre* were generated in the Huang lab using 129SVj/B6 F1 hybrid ES cell line (V6.5, Open Biosystems) as described previously (Taniguchi, He et

al. 2011). ES cell transfections, blastocyst injections and tetroploid complementation were performed by the gene targeting shared resource center in Cold Spring Harbor Laboratory. The genetic backgrounds of other mouse driver lines used for miRAP library preparation are as following: *L7-cre* (C57BL/6 & black swiss), *Camk2 α-Cre* (C57BL/6 & BALB/c), *Pv-ires-Cre* (C57BL/6 & 129SVj).

3.10.2 Immunohistochemistry and confocal microscopy

Postnatal animals were anaesthetized (avertin) and perfused with 4% paraformaldehyde (PFA) in 0.1 M PB. The brains were removed and post-fixed overnight at 4°C. Brain sections (50μm) were cut with a vibratome. Sections were blocked with 10% normal goat serum (NGS) and 0.1% Triton in PBS and then incubated with the following primary antibodies in the blocking solution at 4°C overnight: GFP (rabbit polyclonal antibody; 1:800; Rockland), parvalbumin (Pv, mouse monoclonal antibody; 1:1000; Sigma), somatostatin (SOM; rat monoclonal antibody; 1:300; Millipore); lamin B(goat polyclonal antibody;1:100; Santa Cruz Biotechnology). Sections were then incubated with appropriate Alexa fluor dye-conjugated IgG secondary antibodies (1: 400; Molecular Probes) in blocking solution and mounted in Fluoromount-G (SouthernBiotech). For immunostaining against Gad67 (mouse monoclonal antibody; 1:800; Millipore), no detergent was added in any step, and incubation was done at room temperature for 2 days at the primary antibody step. In some experiments sections were incubated with TOTO-3 (1:3000; Molecular Probes) together with secondary antibodies to visualize nuclei. Sections were imaged with confocal microscopy (Zeiss LSM510 and Zeiss LSM710).

3.10.3 miRAP

Neocortex and cerebellum of P56 mouse brain were dissected on ice and flash frozen in liquid nitrogen, ground to a fine powder, and resuspend in 10 volume of ice-cold lysis buffer (10mM HEPES pH7.4, 100mM KCl, 5mM MaCl2, 0.5%NP-40, 1mM DTT, 100U/ml RNasin) containing Roche Complete proteinase inhibitors, EDTA-free. Tissue suspension was homogenized using glass douncer. Homogenates were centrifuged for 30min at 13,000g, 4ºC to pellet cell debris and unsolubilized material. Mouse-anti-c-Myc(sc-40, Santa Cruz Biotechnology), mouse-anti-Ago2(2E12-1C9, Abnova) or mouse IgG1(Molipore) conjugated protein G Dynabeads(Invitrogen) were added into supernatant, and the mixture was incubated in 4ºC with end-over-end rotation for 4 hours. Beads were washed twice with low salt NT2 buffer(50mM Tris.Hcl pH 7.5, 150mM NaCl, 1mM MgCl2, 0.5%NP-40, 1mM DTT, 100U/ml RNasin) and twice with high salt NT2 buffer(50mM Tris.Hcl pH 7.5, 600mM NaCl, 1mM MgCl2, 0.5%NP-40, 1mM DTT, 100U/ml RNasin) and treated with 0.6mg/ml proteinase K for 20min at 55 ºC. RNA was extracted by acid phenochloroform(Ambion), followed by chloroform, and precipitated with sodium acetate and glycoblue(Ambion) in ethanol overnight -80ºC. RNA pellet was washed once in 75% ethanol and resuspend in water for further application.

3.10.4 FACS sorting and RNA extraction

Neocortex and cerebellum were dissected and cut into small pieces on ice before dissociation. Tissue dissociation was performed using Papain Dissociation System(Worthington Biochemical Corporation, Lakewood, NJ) according to

manufacturer's instruction. Cells were washed once with FACS buffer(1%BSA in PBS, 50U/ml RNasin, 12.5U/ml DNase), resuspended in 2ml FACS buffer with 1μg/ml RNase-free propidium iodide for dead-cell discrimination. GFP positive PI negative single cells were FACS-sorted directly into Trizol-LS(Invitrogen) for RNA extraction according to manufacturer's instruction.

3.10.5 miRNA Taqman PCR

Real-time RT-PCR analyses of RNA purified by miRAP or from FACS sorted cells were carried out using Taqman MicroRNA Assays(Applied Biosystem) on 7900HT real time PCR machine (Applied Biosystem) according to the manufacturer's instruction. All reactions were run in triplicate. Data were normalized to miRNA-124. When deep sequencing data was compared with RT-q-PCR data, the per million reads number for each miRNA was log2 transformed and normalized to miRNA-124.

3.10.6 Small RNA library generation and sequencing

Libraries for deep sequencing were prepared from RNAs extracted from immonuprecipitation products as described (reference---can I say so if the reference were from another lab). Briefly, RNA was successively ligated to 3' and 5' adaptors, gel purified after each ligation, reverse transcribed and PCR amplified using Solexa sequencing primers. PCR product was gel purified, quantified , and sequenced for 36 cycles on Illumina Genome Analyzer II. Radiolabeled synthetic RNA oligos (M19: CGUACGGUUUAAACUUCGA and M24: CGUACGGUUUAAACUUCGAAAUGU) were spiked in to trace RNA on UREA-PAGE during library preparation, and were

depleted by PmelI digestion after PCR amplification. Significant amount of oligos were retained in the libraries, and were used as spike-in oligo control for RNA editing analysis.

3.10.7 Sequence processing, mapping and anotation

Raw Illumina sequencing reads were trimmed from 3' linker, filtered for low-quality reads, and collapsed to unique sequences retaining their individual read count information. Unique sequences 18nt or longer in length were mapped to the University of California at Santa Cruz mm9 assembly of the mouse genome using bowtie allowing no mismatch. miRNA annotations were made according to miRbase version 16. Raw data and annotated sequences of the small RNA libraries are uploaded in the GEO database (accession number GSE30286).

3.10.8 Data normalization and comparison

To quantify and compare miRNA expression across data sets, we performed normalization using EdgeR program which normalizes data by a weighted trimmed mean of the log expression ratios (trimmed mean of M values (TMM)). For pairwised comparison, edgeR "exact" Test was applied and a significance threshold of $P<0.001$ was used to identify differentially expressed miRNAs (Robinson, McCarthy et al. 2010; Robinson and Oshlack 2010). To generate the heatmap of miRNA expression across data set, we used the mean centered expression of each miRNA and miRNA*. For hierarchical clustering, the average linkage of Pearson Correlation was employed (Eisen, Spellman et al. 1998).

3.10.9 miRNA in situ hybridization

5’ dG labeled LNA–spiked oligodeoxynucleotide probes (LNAs) were purchased from Exiqon. For paraffine sections (6-10μm), the sections were deparaffinized with xylene or histoclear and rehydrated through a series of ethanol solution, treated with proteinase K and re-fixed with PFA before hybridization. For cryosections (10-15 μm), the sections were treated with H2O2 to quench endogenous HRP activity, treated with proteinase K and re-fixed with PFA before hybridization. Sections were prehybridizaed with hyb-buffer (50% Formamide, 5XSSC, %X Denhardt's, 250ug/ml yeast tRNA, 500ug/ml salmon sperm DNA, 2% Roche blocking reagent(1096176), 0.1% CHAPS, 0.1%Tween20) at 45 ºC for 2hours, then with DIG-labeled miRNA probes in hyb buffer (25nM-100nM) for at least 16 hours. Hybridization conditions were adjusted 20ºC below the LNA probe’s Tm. Sections were washed with 5XSSC, 2XSSC, 0.5XSSC and TBS, and blocked with blocking buffer (0.5% Blocking Reagent (Roche), 10% heat inactivated goat serum, and 0.1% Tween 20 in TBS) for 1 hour at room temperature. For probe dection, paraffin sections were incubated in anti-DIG- alkaline phosphatase (Roche) diluted 1:100 ~ 1:150, washed and developed using NBT/BCIP system according to the manufacturer’s protocol (Roche); cryosections were incubated in anti-DIG-FAB peroxidase (POD) (Roche) diluted1:500 in blocking solution for 1 h at R.T., washed and developed using TSA Plus Cy3 System according to the manufacturer’s protocol (PerkinElmer Life Sciences).

3.10.10 Novel miRNA prediction

Novel miRNAs were predicted by miReep2 uses a probabilistic model of miRNA biogenesis to score compatibility of the position and frequency of sequenced RNA with

the secondary structure of the miRNA precursor (Friedlander, Chen et al. 2008). Prediction was performed according to the manual of miRDeep2. Each library was processed separately, and the results were combined together according to genomic location. The signal-to-noise ration of the prediction was calculated according to the manual of miRDeep2.

3.10.11 Identification of arm switching miRNAs

To classify reads from 5' and 3' arms, we grouped reads from each library according to alignment with miRNA precursors. For each miRNA, we summarized the reads in libraries prepared from the same cell type or tissue type. The fold enrichment was calculated as the ratio of 5' and 3' arm reads after adding pseudocounts of one, and log2 transformed. Only miRNAs with unique precursor and five or more reads on either arm in at least 10 libraries were considered and reported.

3.10.12 RNA editing analysis

Each sequencing library was filtered for sequences that uniquely aligned to the genome with one mismatch >2nt from the 3' end of miRNA or miRNA*. The 12 possible mismatch types were then quantified at each position covered by the filtered reads. The individual editing fraction in each library was calculated as the number of reads containing a certain mismatch at a particular position divided by the number of filtered reads covering that position. To screen inferred A-to-I editing sites, A-to-G mismatches were filtered for editing fraction>5% at a particular position and reads number>10 for each library respectively, and then combined together to calculate the editing fraction in

all libraries. None of the inferred A-to-I editing sites was found to correspond to known SNPs by checking in the Perlegen SNP database and dbSNP. We also checked available genomic builds of other genetic background used in our studies except black swiss, as there is no genomic build for this strain. However, as we did not see correlation of any inferred miRNA editing site with the presence of any genetic background in our dataset, believe there is no false positive of editing sites caused by SNP in this strain.

3.11 Supplemental material

3.11.1 Supplemental figures

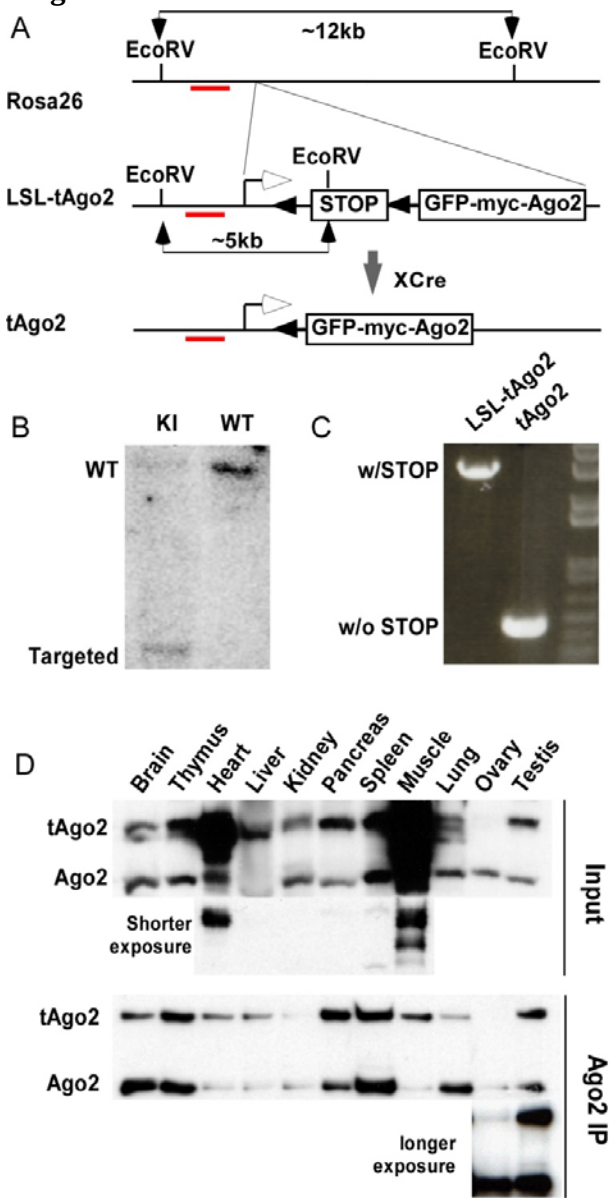

Figure 3.7 (Supplemental figure 3.1) Generation and characterization of *LSL-tAgo2* mouse line

(A) Targeting and screening strategy. Red bar: southern probe
(B) Southern blot confirmation of targeted ES cell.
(C) PCR confirmation of the deletion of STOP cassette.

(D) Western blotting anaylsis of tAGO2 expression in different organs of *tAgo2* mouse

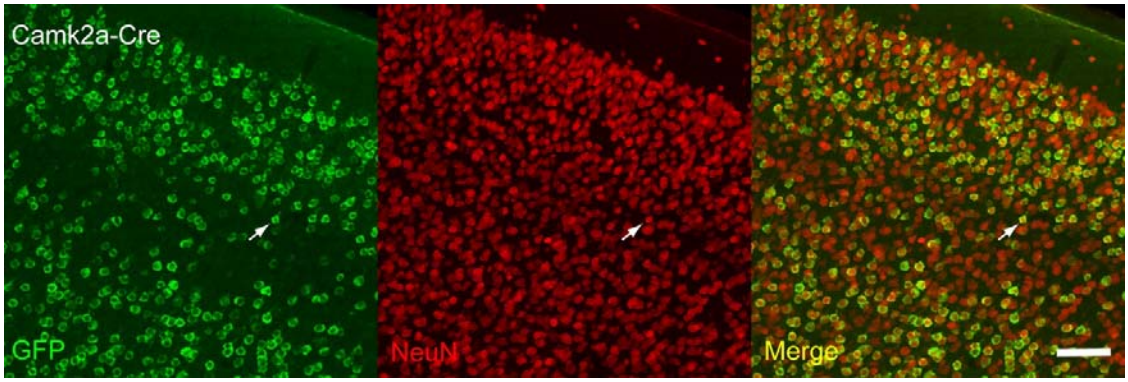

Figure 3.8 (Supplemental figure3.2) The neuronal identity of labeled cells in the cortex of *Camk2α-Cre; LSL-tAgo2* mice.

Immunofluoresence of GFP in adult brain sagittal sections from a *Camk2α-Cre; LSL-tAgo2* mouse. All GFP signals colocalize with NueN, a pan-neuronal marker. No colocalization with GAD67 was observed (Figure 3.2), indicating these neurons are glutermatergic. Scale bar:100 μm

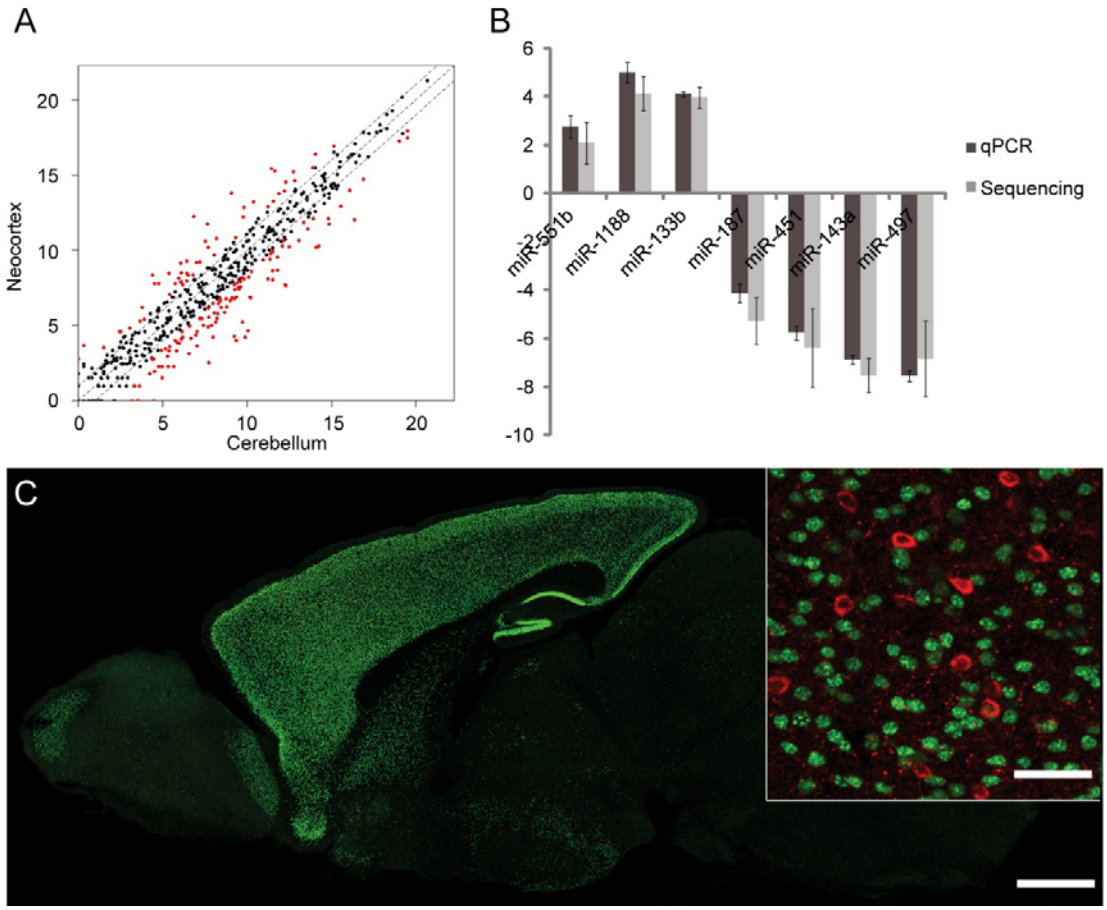

Figure 3.9 (Supplemental figure 3.3)

(A) Comparison of neocortex and cerebellum miRNA profiles. Dashed line: fold change=2 or -2. Red dots: P value<0.001

(B) Taqman PCR validation of deep sequencing results in Purkinje cell vs. whole cerebellum. Value above 0 represents higher expression in Purkinje cells. n=3 for deep sequencing data. n=4 for Taqman PCR. Error bar: standard deviation.

(C) The Camk2α-cre;LSL-H2B-GFP mouse labels pyramidal cell nuclei. Low magnification image: overview of direct GFP fluorescence in a adult brain sagittal section from the Camk2α-cre;LSL-H2B-GFP mouse. Scale bar:1mm. High magnification image: merge of GFP and immunostaining of GAD67. No colocalization was observed. Scale bar: 50 μm

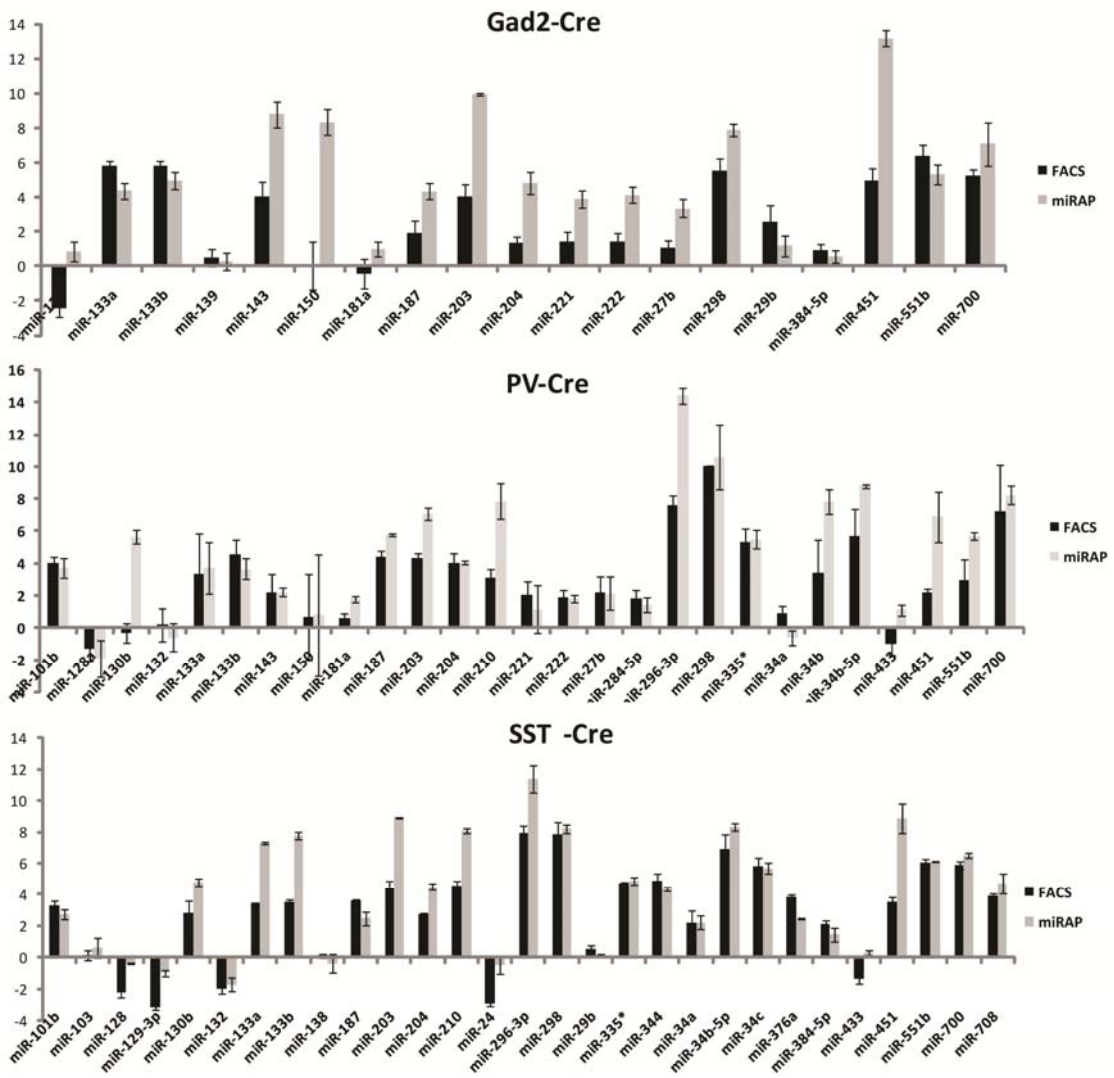

Figure 3.10 (Supplemental figure 3.4) miRNA Taqman PCR validation of deep sequencing in Gad2, PV and SST cells.

All miRNAs were normalized to miRNA-124 using the ΔΔCt method. Deep sequencing reads number were log2 transformed and then normalized to miRNA-124. n=3 for all samples. Error bar: standard deviation.

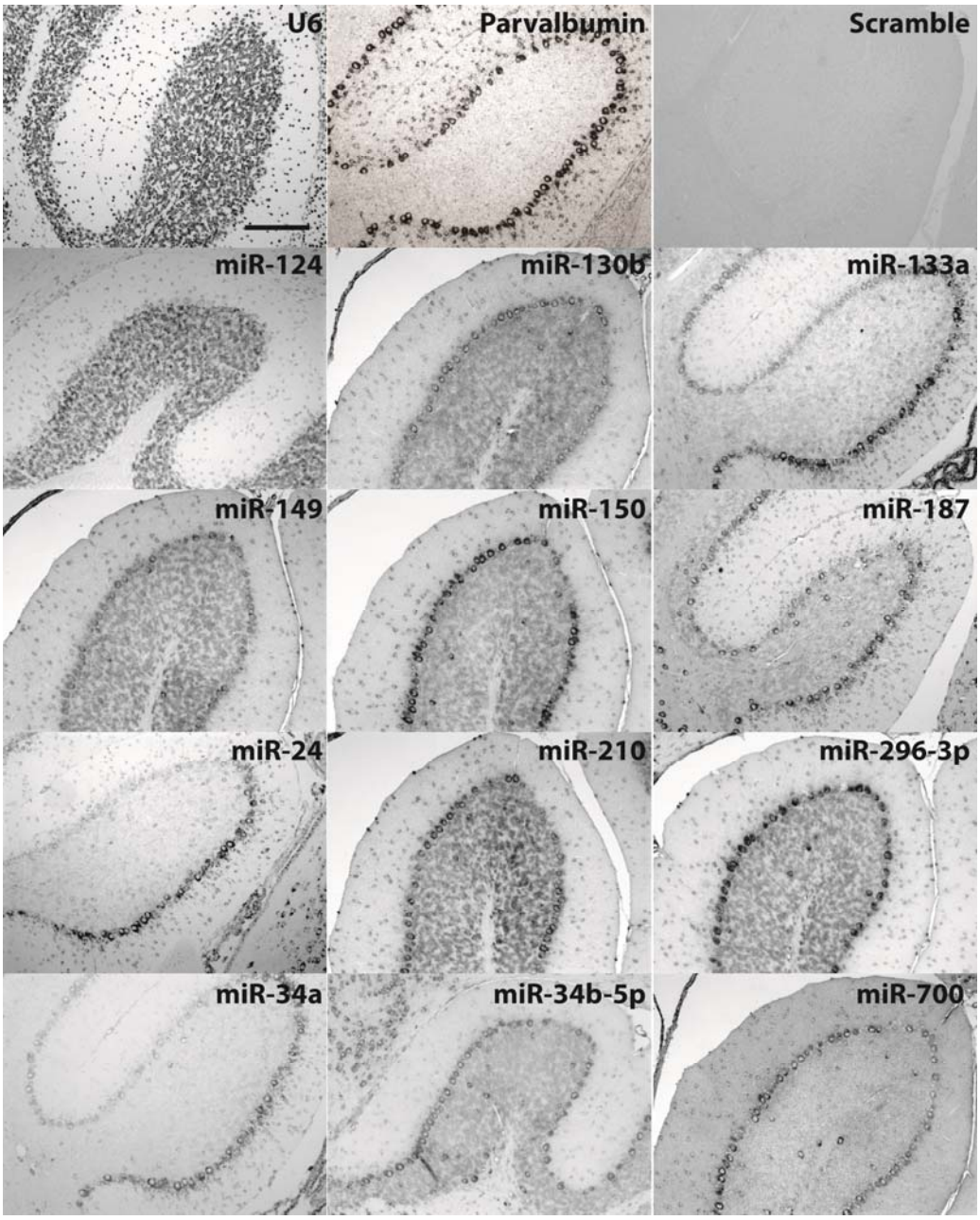

Figure 3.11 (Supplemental figure 3.5) miRNA in situ hybridization in cerebellum using paraffin section and NBT/BCIP substrate. Scale bar: 200μm.

Among these miRNAs, miR-124, miR-130b,miR-24,miR-210 and miR-700 shows no significant difference between Purkinje cell and whole cerebellum profiles according to miRAP result; miR-133a and miR-34a are relatively enriched in Purkinje cells; miR-149, miR-150, miR-187, miR-296-3p and miR-34b-5p are relatively depleted in Purkinje cells.

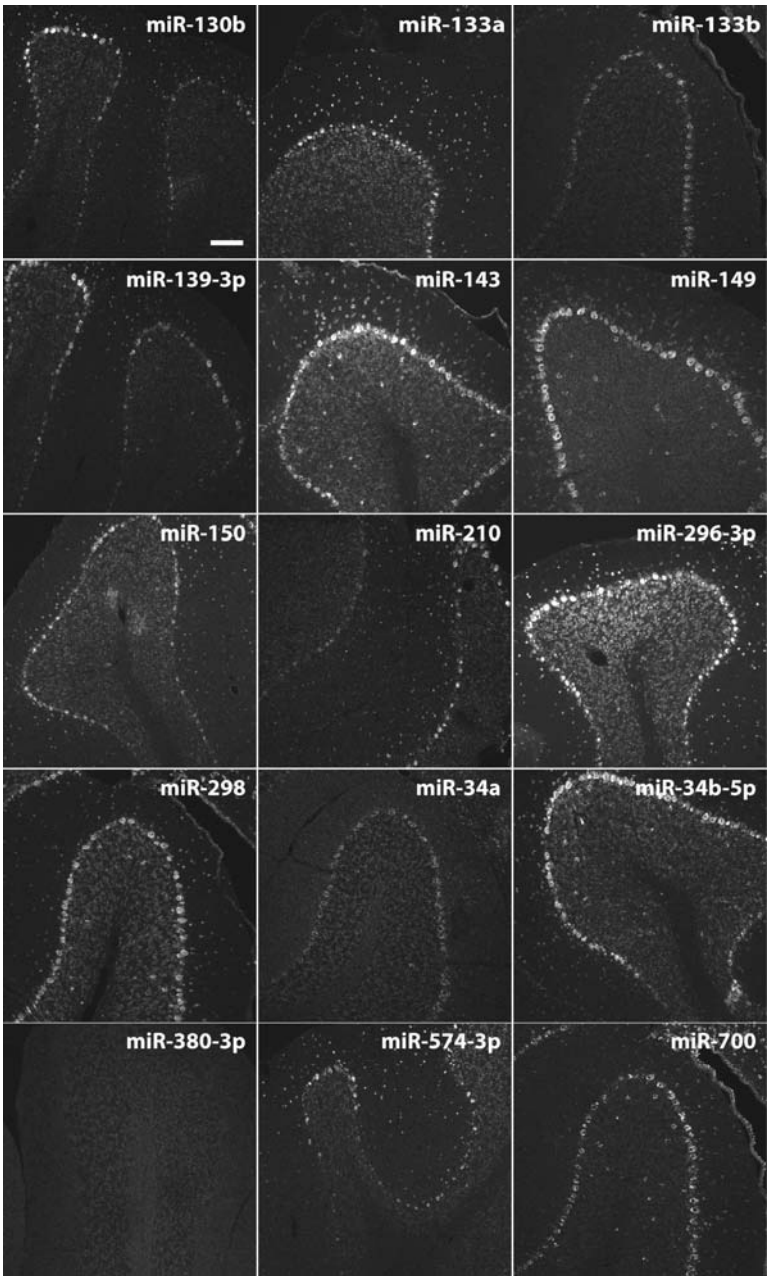

Figure 3.12 (Supplemental figure 3.6) miRNA in situ hybridization in cerebellum using cryosection section and TSA Plus Cy3 system. Scale bar: 100μm.

Among these miRNAs, miR-130b, miR-210 and miR-700 shows no significant difference between Purkinje cell and whole cerebellum profiles according to miRAP result; miR-133a, miR-133b, miR-139-3p, miR-34a and miR-380-3p are relatively enriched in Purkinje cells; miR-143,miR-149, miR-150, miR-296-3p, miR-298, miR-34b-5p and miR-574-3p are relatively depleted in Purkinje cells.

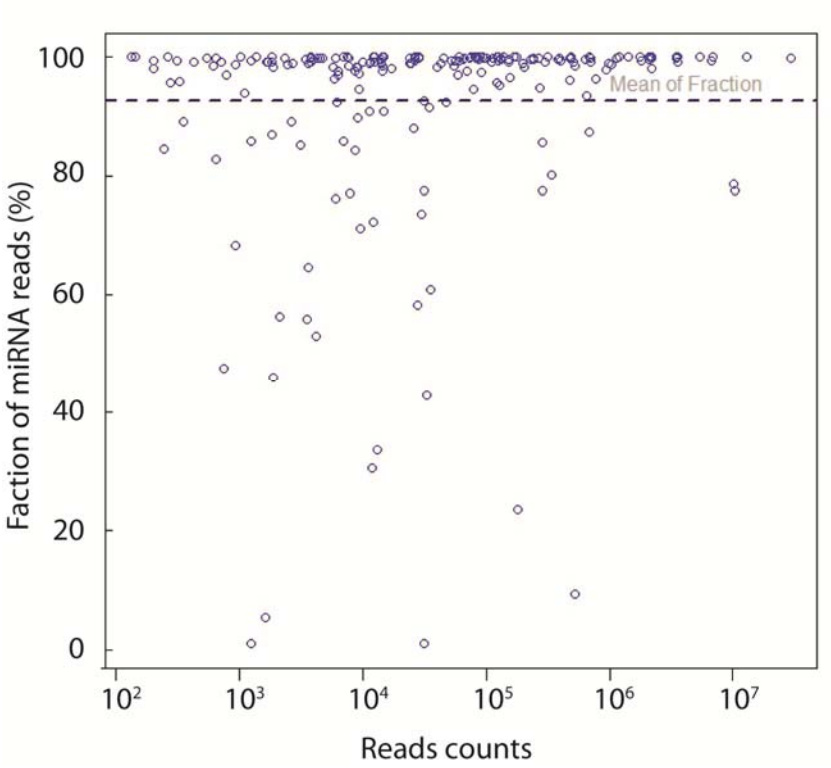

Figure 3.13 (Supplemental figure 3.7) Fraction and abundance of miRNA reads from each miRNA hairpin.

To calculate the fraction, the miRNA reads were divided by the total number of miRNA and miRNA*reads. The dashed lines indicate the mean fraction of miRNA reads.

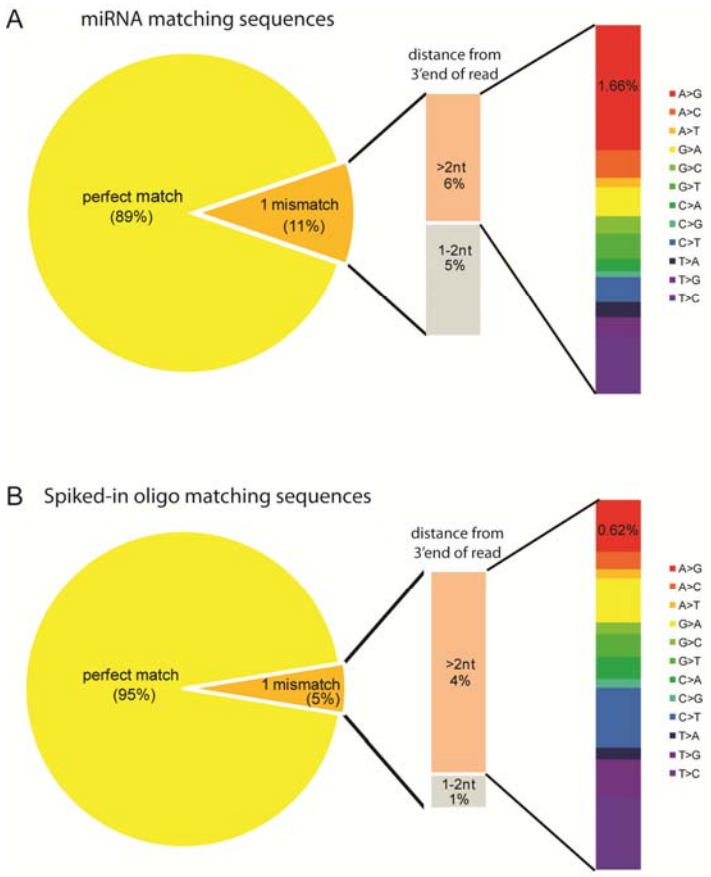

Figure 3.14 (Supplemental figure 3.8) Overview of mismatches from miRNA and spike-in oligo controls.

(A) In miRNA-mapping small RNA sequences from brain, mismatches were concentrated in the last 2 nt of theread, probably due to cellular terminal-transferase activity. . A-to-G mismatches are the most abundant kind.

(B) In the two spiked-in synthetic RNAs of known sequence, mismatches were distributed throughout the length of the sequence, with no preference forA-to-G mismatches

3.11.2 Supplemental tables

Supplemental table 3.1: Summary and annotation of experiments

Supplemental table 3.2: Normalized per million reads by edgeR.

Supplemental table 3.3-3.6: Pairwise comparision of neocortex vs. cerebellum, Camk2α vs. Gad2, PV vs. SST and Purkinje vs. cerebellum.

Supplemental table3. 7: Predicted novel miRNAs

(Please see attached excel files)

Chapter 4. Investigating miRNAs function in cortical interneurons development and physiology by conditional Dicer inactivation

4.1 Introduction

Dicer is an indispensable enzyme in the multistep miRNA biogenesis process (He and Hannon 2004). Recent studies have shown conditional ablation of Dicer in specific cell types cause cell death for Purkinje neurons (Schaefer, O'Carroll et al. 2007), dopaminergic neurons (Kim, Inoue et al. 2007), excitatory neocortical and hippocampal neurons (Davis, Cuellar et al. 2008), while leads to a smaller cell body in striatal neurons in the absence of neurodegeneration (Cuellar, Davis et al. 2008). However, there has been no such study on neocortical GABAergic interneurons.

By breeding a conditional Dicer line with different Cre drivers, I disrupted miRNA production in three major and non-ovelapping subtypes of neocortical GABAergic interneurons. In this conditional Dicer line, a large part of the two RNAseIII domains in the Dicer gene were flanked by two loxP sites with same orientation(Murchison, Partridge et al. 2005). Upon Cre expression, the loxP-flanking part will be deleted and Dicer expression will be inactivated. This is a rather rough method to disrupt miRNA function, as the inactivation of Dicer abolished normal production of almost all miRNAs. Therefore, any phenotype we see will be a combinatorial effect due to the disruption of the miRNA biogenesis pathway, not attributing to specific miRNAs. Nonetheless, it is still possible to get some perspectives on potential aspects of miRNA functions by

looking into the details of phenotypic abnormalities, which will hopefully facilitate future studies of individual miRNA in specific cell types.

4.2 Dicer KO in PV neurons

The large majority of Parvalbumin expressing cells in the neocortex are fast-spiking basket interneurons which innervate the soma and proximal dendrites of pyramidal neurons and control the output and synchrony of pyramidal cells (de Lecea, del Rio et al. 1995). They are a predominant subtype, accounting for ~40% of the total neocortical interneuron population. I used PV-ires-Cre (Hippenmeyer, Vrieseling et al. 2005) to inactivate Dicer in this subtype of interneurons. However, as PV is also in other brain regions, some endocrine tissue and fast contracting muscle, Dicer could be inactivated in these cells as well.

Compared to Pv-Cre; $Dicer^{flox/+}$ (Het) littermates, most Pv-**Cre;** $Dicer^{flox/flox}$ (Homo) mice had shorter life spans and died 3-4 months after birth (fig4.1A). These mice weighed less as early as postnatal 2 weeks when I first started the measurement, and started to lose weight from week10 (fig4.1B).

Visual examination indicated behavior abnormalities starting from ~postnatal week 4. These mice had constant head dipping behavior, and it could be aggravated by exogenous stimuli such as shaking the cage. When suspended by the tail, they seemed to have shorter immobility duration and could bend backwards to a greater angle. At ~8 weeks, their hindlimbs are partially paralyzed, incapable of supporting their bodies.

These phenotypes manifest at slightly different pace in different individuals, probably due to impure genetic background.

Some aspects of these phenotypes seem to be neurological, however, the broad expression pattern of PV gene makes it difficult to attribute certain phenotypes to the miRNA loss in neocortical PV-class interneurons. To further investigate the effect of Dicer deletion in these cells, I examined their cellular phenotypes.

It has been reported that loss of Dicer in certain types of neurons leads to neuron apoptosis. To examine if cell death occurs in the neocortical PV-class GABAergic cells after Dicer deletion, I did TUNEL staining at different developmental stages (week4-16). In neocortex, there was no TUNEL signal observed in PV cells in any developmental stage, suggesting miRNAs are dispensable for their survival. On the contratry, TUNEL positive signals were observed from week10 in Purkinje cells and cerebellar basket cells in the cerebellum, consistent with published result. In addition, immunostaining showed lower Gad2 and VGAT signal at the pinceau synapse region prior cell death, indicating abnormality of the basket-Purkinje cell connection.

Even though Dicer deletion did not seem to cause cell death in neocortical PV neurons, it could still have other minor effect. To check this possibility, we examined their electrophysiology characteristics. Intrinsic properties of PV fast spiking cells and pyramid neurons were recorded at P15-16, P28-29, P42-43(table 4.1) and P60-65(data not shown); miniEPSP and miniIPSP on PV fast spiking cells, and miniIPSP on pyramidal neurons were recorded at P42-43(table 4.2) in mouse visual cortex. No

significant differences were observed between the experiment group and control group in any of these recordings. This suggests that the basic electrophysiological properties of PV fast spiking cells and their connection with pyramidal neurons in these animals are not affected by Dicer deletion up to the age of 2 months.

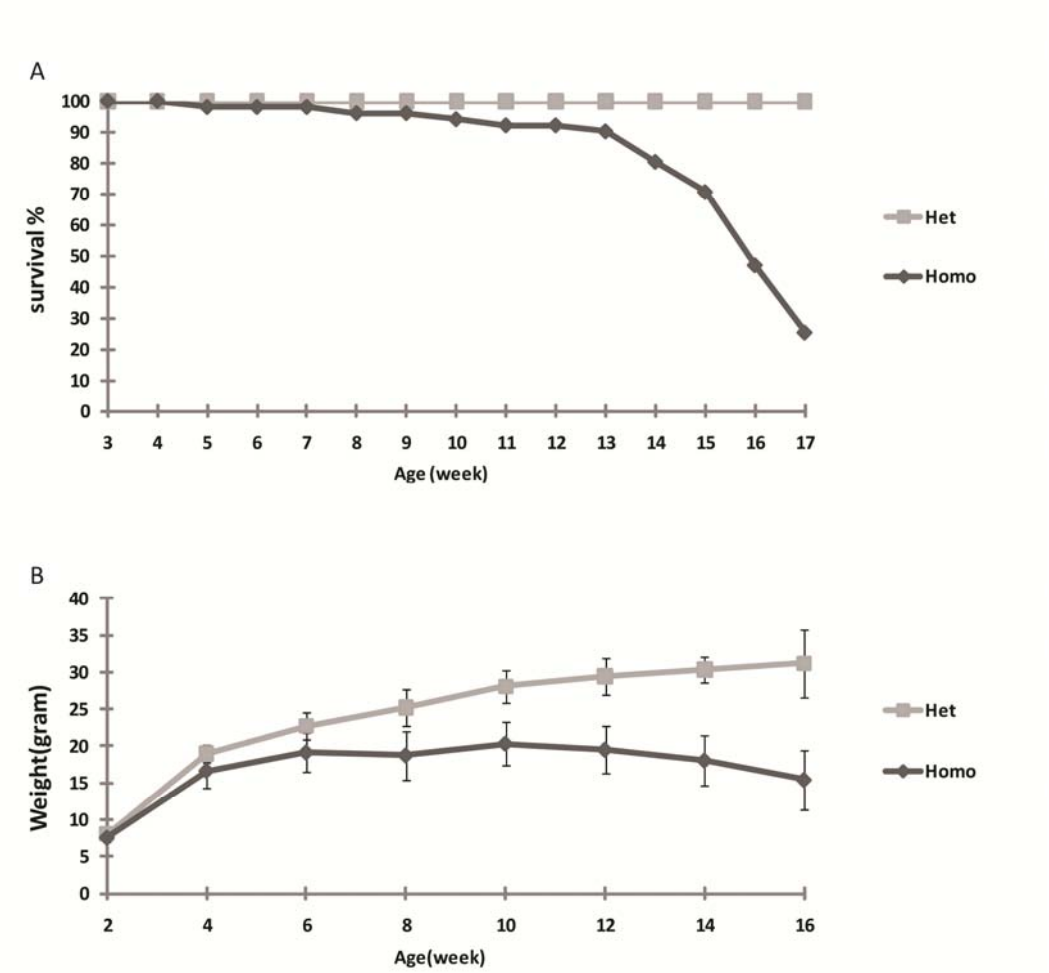

Figure 4.1 Dicer deficiency in Pv cells causes weight loss and death

(A) Kalpan-Meier plot of survival shows that most PvCre/+; Dicerflox/flox mice die around 14-17 weeks after birth. n=51.

(B) Weight plot shows that PvCre/+; Dicerflox/flox (n=10) mice are usually lighter than PvCre/+; Dicerflox/+ mice (n=9). error bar: standard deviation. $P<0.05$ for every pair of data points between the two genotypes.

	p15-16 FS cells			p28-29 PV cells			p42-43 PV cells		
	con (*19*)	ko (*20*)	p	con (*21*)	ko (*18*)	p	con (*21*)	ko (*22*)	p
Cm (pF)	71.4±3.1	69.9±2.5	*0.42*	66.7±2.8	65.0±3.2	*0.68*	59.6±2.6	59.4±2.5	*0.84*
Rm (Mohm)	97.5±8.6	98.4±6.4	*0.68*	88.3±10.3	83.4±9.5	*0.44*	98.5±4.5	89.9±6.2	*0.07*
Vm (-mV)	74.4±1.6	78.5±1.1	*0.07*	79.2±0.7	77.5±0.9	*0.07*	76.6±0.9	75.3±1.1	*0.74*
AP threshold (-mV)	40.2±1.1	40.9±0.7	*0.5*	35.4±0.9	35.5±0.8	*0.72*	35.8±0.9	37.4±1.0	*0.25*
AP amplitude (mV)	69.0±1.4	70.9±1.2	*0.47*	48.9±1.6	53.6±1.6	*0.07*	64.0±1.4	67.2±1.2	*0.11*
AP half-width (ms)	0.561±0.015	0.535±0.009	*0.23*	0.456±0.016	0.464±0.009	*0.15*	0.373±0.010	0.372±0.006	*0.57*
FI slope (Hz/pA)	0.295±0.026	0.306±0.021	*0.42*	0.517±0.040	0.448±0.020	*0.18*	0.530±0.036	0.587±0.035	*0.31*
adaptation index	1.125±0.017	1.103±0.021	*0.15*	1.151±0.043	1.145±0.029	*0.69*	1.145±0.020	1.116±0.016	*0.28*
maximal firing (Hz)	219.4±14.9	234.8±9.9	*0.2*	365.0±22.9	327.8±13.6	*0.1*	360.0±13.7	376.8±11.9	*0.39*
	p15-16 PyNs			p28-29 PyNs			p42-43 PyNs		
	con (16)	ko (14)	p	con (14)	ko (13)	p	con (18)	ko (19)	p
Cm (pF)	112.5±4.8	117.7±4.4	0.51	158.4±3.9	161.2±4.5	0.54	154.5±4.7	167.9±5.8	0.09
Rm (Mohm)	343.8±29.6	297.4±29.4	0.17	163.7±8.1	179.6±12.8	0.65	183.8±12.9	156.9±7.4	0.1
Vm (-mV)	82.3±1.7	83.1±1.0	0.83	86.4±1.1	87.6±0.6	0.83	84.9±1.1	84.9±1.0	0.92
AP threshold (-mV)	39.2±0.8	39.3±0.9	0.65	37.2±0.7	37.0±0.6	0.94	35.8±0.6	35.5±0.7	0.95
AP amplitude (mV)	94.5±1.0	95.7±1.0	0.24	100.0±1.9	97.4±1.8	0.25	97.9±0.9	97.0±0.7	0.42
AP half-width (ms)	0.966±0.021	0.861±0.017	7E-04	0.822±0.023	0.814±0.018	0.94	0.691±0.010	0.690±0.016	0.73
FI slope (Hz/pA)	0.047±0.004	0.058±0.004	0.17	0.039±0.004	0.049±0.003	0.1	0.055±0.006	0.044±0.005	0.17
adaptation index	2.35±0.20	1.700.005	2E-04	1.89±0.09	1.88±0.09	0.98	2.02±0.13	2.11±0.09	0.35
maximal firing (Hz)	43.8±2.3	43.7±1.9	0.99	48.5±1.8	51.4±1.3	0.11	56.3±1.8	57.2±3.1	0.57

Table 4.1 Intrinsic properties of parvalbumin positive cells and pyramidal neurons in visual cortex L2/3

mini-EPSCs on PV cells	Dicer KO (n=23)	control (n=33)	p
frequency (Hz)	70.7 ± 2.8	70.3 ± 3.5	0.91
amplitude (pA)	14.4 ± 0.4	14.3 ± 0.3	0.93
rise time 10-90% (ms)	0.24 ± 0.003	0.24 ± 0.004	0.64
decay time 90-37% (ms)	0.80 ± 0.04	0.83 ± 0.03	0.55

mini-IPSCs on PV cells	Dicer KO (n=13)	control (n=13)	p
frequency (Hz)	55.1 ± 3.8	56.3 ± 3.9	0.96
amplitude (pA)	18.9 ± 1.2	20.3 ± 1.5	0.44
rise time 10-90% (ms)	0.35 ± 0.01	0.36 ± 0.01	0.74
decay time 90-37% (ms)	1.45 ± 0.04	1.38 ± 0.05	0.31

mini-IPSCs on Pyr cells	Dicer KO (n=12)	control (n=9)	p
frequency (Hz)	49.5 ± 4.8	46.1 ± 3.5	0.75
amplitude (pA)	15.8 ± 1.1	19.6 ± 1.8	0.10
rise time 10-90% (ms)	0.42 ± 0.02	0.38 ± 0.02	0.12
decay time 90-37% (ms)	2.45 ± 0.09	2.49 ± 0.11	0.52

Table 4.2 mini events of P42-43 PV neurons and Pyramidal neurons

4.3 Dicer KO in SST interneurons

The SST cells consist of regular-spiking interneurons which innervate the dendrites and spines of pyramidal neurons derived from the MGE. Dendrite-targeting interneurons control the input and integration of pyramidal neurons, and also the back-propagating action potential activated Ca+ spiking in dendrites. These interneurons have been implicated both in feedforward and feedback inhibitions. Furthermore, dendrite-targeting inhibitory synapses are regulated by sensory experience. Using *SST-ires-Cre* developed in our lab, I did Dicer KO in this class of interneurons by breeding with Dicer flox animals. No obvious abnormalities were observed in the mice in terms of their weight, life span and fertility. Similar to the case of PV interneurons, electrophysiology

recordings of SST interneurons in 2 month old mice did not reveal any significant changes in intrinsic properties in these neurons.

	Rm (Mohm)	AP threshold (-mV)	AP amplitude (mV)	halfwidth (ms)	AHP(mV)
SST Ctr	277.8±24.5	-40.0±2.5	58. 3±1.9	0.488±0.013	-14.59±0.50
SST KO	262.8±32.9	-39.8±1.5	62.1±3.9	0.494±0.017	-15.14±0.97
P value	0.71	0.96	0.29	0.82	0.67

Table 4.3 Intrinsic properties of SST cells in visual cortex L2/3

4.4 Dicer KO in VIP interneurons

Vasoactive intestinal peptide (VIP) is expressed in a subset of cortical GABAergic neurons that are derived from the caudal ganglionic eminence (CGE) and do not overlap with SST or PV interneurons(Miyoshi, Hjerling-Leffler et al. 2010). Both the dendrites and axons of VIP cells extend largely vertically and thus are suited for mediating translaminar inhibition. A prominent feature of some VIP interneurons is their preferential innervation of other inhibitory interneurons, such as PV, SST, VIP interneurons(David, Schleicher et al. 2007). VIP neurons may also regulate cortical blood flow and metabolism since its receptors appear to localize to blood vessels as well as neurons(Cauli, Tong et al. 2004).

Using *VIP-ires-Cre* line developed in our lab, I deleted Dicer in these populations of interneurons in the cortex. some of the KO animals died before 2 months, the remaining ones survive longer and seem to be fertile. Preliminary results of electrophysiology recordings in 2 month old animals revealed significant changes in the action potential threshold in these interneurons, implying changes in their ion channel compositions. Further validations are needed to confirm this phenotype. (Table 4.4)

	Rm (Mohm)	AP threshold (-mV)	AP amplitude (mV)	halfwidth (ms)	AHP(mV)
VIP Ctr (n=15)	336.6±32.8	37.6±1.2	63.1±1.5	0.569±0.023	-10.87±1.01
VIP KO	417.7± 37.0	45.5±0.8	73.4±2.0	0.613±0.017	-5.47±0.60
P value	0.12	0.0002	0.0009	0.11	0.0009

Table 4.4 Intrinsic properties of VIP cells in visual cortex L2/3

4.5 Discussion

The lack of phenotype in PV and SST interneurons in the neocortex could be cause by several reasons. First, incomplete ablation of Dicer leads to failure of miRNA inactivation. I have tried extensively immunostaining and in situ hybridization to examine Dicer expression in these animals, but both antibody and in situ probes did not work. In the case of PV neurons, I did PCR using primers flanking the two loxP sites to check Dicer ablation. Under appropriate PCR conditions, PCR products will be observed only when deletion happens. Using this method, I did observe Dicer deletion event in PV cells of neocortex as early as P15, but it is not enough to prove Dicer is knocked out in all neocortical PV neurons. In the case of SST cells, SST starts to express in embryonic stages. Therefore it is unlikely Dicer is still active in late postnatal age. Therefore, incomplete ablation of Dicer is less likely to be the reason of negative results, although not impossible.

Second, subsets miRNAs may be very stable and stayed in the neurons even when Dicer stopped producing new miRNAs. miRNAs are much more stable than mRNAs (Gantier, McCoy et al. 2011). Study in Dicer1 KO MEF culture modeled an average half life of ~5days, but the half life of individual miRNAs probably varies according to their identity and cellular environment. It is possible miRNAs essential for cell survival and

intrinsic properties are extremely stable in PV and SST neurons, therefore no defect were observed at the time point we examined.

Third, miRNA function may be context dependent, ie. even the same miRNAs can function differently in different cell type. It is not totally unexpected that Dicer deletion, even if it completely abolished miRNA function, can cause different outcome in different neurons. Although Dicer deletion can lead to progressive cell loss and neurodegeneration in many other neuron types, our results suggest this is not a general rule. For neocortical PV, SST and VIP neurons, miRNAs seem to be dispensable for their survival. For VIP neurons, miRNA may regulate ion channel expression, therefore affect their intrinsic properties.

Future experiments could be designed to systematically assess the morphology, connectivity and plasticity of GABAergic neurons when Dicer is inactivated. With the knowledge of miRNA profiles, we could also look at signature miRNAs in specific cell type, which will be more informative.

4.6 Materials and methods

4.6.1 Mouse lines

For PV cell specific Dicer KO experiment, $Dicer^{flox/flox}$ (Murchison, Partridge et al. 2005)and *Pv-ires-Cre* were intercrossed to generate *Pv-ires-Cre*;$Dicer^{flox/flox}$ mice. For SST and VIP cell specific Dicer KO experiment, $Dicer^{flox/flox}$, *Sst-ires-Cre* or *Vip-ire-Cre*

, and *Ai9* reporter were intercrossed to generate *Pv-ires-Cre*;*Dicer*$^{flox/flox}$;*Ai9* or *Vip-ires-Cre*;*Dicer*$^{flox/flox}$;*Ai9* mice. Mice were housed under standard laboratory conditions at The Cold Spring Harbor Laboratory Animal facility. All experimental procedures were approved by the Institutional Animal Care and Use Committee (IACUC) of CSHL in accordance with NIH guidelines.

4.6.2 Immunostaining and confocal microscopy

Postnatal animals were anaesthetized (avertin) and perfused with 4% paraformaldehyde (PFA) in 0.1 M PB. The brains were removed and post-fixed overnight at 4°C. Brain sections (50μm) were cut with a vibratome. Sections were blocked with 10% normal goat serum (NGS) or 10% normal donkey serum, and 0.1% Triton in PBS and then incubated with the following primary antibodies in the blocking solution at 4°C overnight: GFP (rabbit polyclonal antibody; 1:800; Rockland, chicken polyclonal antibody; 1:1000; abcam), RFP (rabbit polyclonal antibody; 1:1000; Rockland, parvalbumin (PV, mouse monoclonal antibody; 1:1000; Sigma, St. Louis, MO), somatostatin (SST; rat monoclonal antibody; 1:300; Millipore), VIP (rabbit polyclonal antibody; 1:600; Immunostar), Sections were then incubated with appropriate Alexa fluor dye-conjugated IgG secondary antibodies (1: 400; Molecular Probes) and mounted in Fluoromount-G (SouthernBiotech). In some experiments sections, were incubated with TOTO-3 (1:3000; Molecular Probes) together with secondary antibodies to visualize nuclei. Sections were imaged with confocal microscopy (Zeiss LSM510 and Zeiss LSM710) or with fluorescent microscopy equipped with a CCD camera.

4.6.3 TUNEL staining

6μm paraffin sections of mouse brain were deparaffinized using Xylene. The In Situ Cell Death Detection kit (TMR red; Roche) was used according to the manufacturer's instructions. To identify PV cells in neocortex or cerebellum, pressure cooker method was used for antigen retrieval and followed by regular immunostaining method described in last section.

4.6.4 Electrophysiological recording in cortical slice

4.6.5 Labeling of interneurons

For *Pv-ires-Cre* mice, AAV-LSL-GFP virus was injected into V1 region of visual cortex brain at least 2 weeks prior recording to label PV cells. Kuhlman and Huang (2008) have developed Cre-activated adeno-associated viral vectors (AAV) which confer cell type specific and high level gene expression in Cre knockin mice. Briefly, animals with different genotypes and ages as indicated throughout the text were anesthetized with an intraperitoneal injection of ketamine/xylazine mixture (0.1 mg/g, 0.01mg/g body weight). A small hole in the skull was made using a dental drill (Henry Schein), 3.5 mm posterior from Bregama, and 3 mm form the midline in the adult mice. As for younger mice, scaled dimension was used according to that in adult. The dura was slightly punctured and virus was delivered by pressure injection using a glass micropipette (tip size of roughly 10 μm) attached to a Picrospritzer (General Valve). The virus was AAV-LSL-GFP vector and 0.5 μl solution (concentration?) in each pipette. The glass pipette was lowered to 0.35 mmm below the pia surface. To inject virus into the brain, 40 air

puffs were delivered (25 psi, 10 ms duration) at a frequency of 0.4 Hz, the pipette was then retracted 20-30 microns towards to the surface, and pressure injection repeated. This sequence was repeated until the pipette tip reached a depth of -200 micrions below the surface. The pipette was then held in place for approximately 5 minutes before completely retracting out of the brain. During the process of surgery and injection, ketamine (0.05 mg/g body weight) would be injected intraperitoneally to keep animal anaesthetizing when animals showed awake behaviors (whisker shaking, tail moving). Usually, the animals would be dissected for electrophysiological experiments more than 4 days after viral injection. But in some cases, animals were used 2 days after the injection.

For SST-ires-cre and VIP-ires-cre, Ai9 reporter was used to label SST and VIP cells.

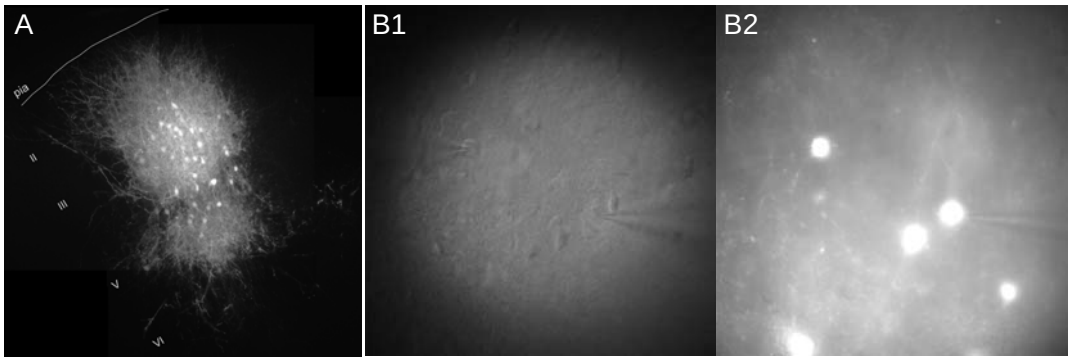

Figure 4.4.2 Recording setup.

(A) Pv-cre driver mouse injected with AAV-loxSTOPlox-GFP reporter. All GFP+ cells are PV basket interneurons (data not shown). Image taken with regular fluorescence microscope at 20X. Presynaptic boutons are readily discernable. Pia and cortical layers are indicated. Infection at P21, analyzed at P33.

(B) Whole-cell recordings at two GFP-labeled Pv cells in V1 slices (P75, cortical injection at P60). Two cells exhibited fast-spiking firing pattern and coupled with electrical synapses (data no shown). B1, under IR-DIC image; B2, under normal fluorescence microscope. Both at 60X.

4.6.6 Preparation of cortical slices

Mice were anesthetized with sodium pentobarbital (50 mg/kg) and quickly decapitated. Visual cortical slices (350 μm) were prepared from P15 to adult mice. All animals were anesthetized with ketamine/xylazine mixture (0.1 mg/g, 0.01mg/g body weight) before decapitated. The brain was rapidly dissected and transferred into ice-cold oxygenated artificial cerebrospinal fluid (section ACSF; composition in mM: 110 choline-Cl, 2.5 KCl, 4 MgSO4, 1 CaCl2, 1.25 NaH2PO4, 26 NaHCO3, 11 D-glucose, 10 Na-ascorbate, 3.1 Na-pyruvate, pH 7.35, ~300 mOsm) for 2 min. Coronal slices were dissected with a vibratome (HM 650 V, Microm, Germany) at 1-2 °C and further incubated with oxygenated ACSF (working ACSF; composition in mM: 124 NaCl, 2.5 KCl, 2 MgSO4, 2 CaCl2, 1.25 NaH2PO4, 26 NaHCO3, 11 D-glucose, pH 7.35, ~300 mOsm) at 34 °C for 20-30 min, and then transferred to ACSF at room temperature (25 °C) for > 30 min before use. The anatomical locations of these recordings were assessed with reference to Franklin and Paxinos (1997), using the shape of subcortical whiter matter and hippocampus as the primary landmarks. The anterior/posterior position of visual cortical slices corresponded to plates 54-66. For experiments, slices were transferred to the recording chamber and perfused with oxygenated ACSF at 32-34 °C.

4.6.7 Electrophysiology

Single whole-cell recordings from pyramidal cells (PCs) or fluorescent labeled cells (PV, SST and VIP cells) in layer 2/3 was made with Axopatch 200B or 700B amplifiers (Molecular Devices, Union City, CA), using an upright microscope (Olympus, BX51) equipped with infrared-differential interference contrast (IR-DIC) optics and

fluorescence excitation source. Both IR-DIC image and fluorescence image are captured with a digital camera (Microfire, Optronics, CA).

Examination of intrinsic properties. The internal solution of the recording pipette contained (in mM): 130 K-gluconate, 15 KCl, 10 Na-phosphocreatine, 10 HEPES, 4 ATP-Mg, 0.3 GTP and 0.3 EGTA, adjusted to pH 7.3 with KOH and to ~300 mOsmol.

Examination of mini-EPSCs on Pv cells. The internal solution of the recording pipette contained (in mM): 140 K-gluconate, 5 KCl, 10 Na-phosphocreatine, 10 HEPES, 4 ATP-Mg, 0.3 GTP and 0.3 EGTA, adjusted to pH 7.3 with KOH and to ~294 mOsmol. External solution was working ACSF contained 1 μM TTX and 100 μM Picrotoxin.

Examination of mini-IPSCs on Pv cells. The internal solution was the same with that in examination of intrinsic properties. External solution was working ACSF contained 1 μM TTX, 100 μM (DL)-APV and 20 μM CNOX. The pipette resistance was 4 - 6 MΩ. Signals were recorded and filtered at 2 kHz, digitalized at 10 or 20 kHz (DIGIDATA 1322A, Molecular Devices) and further analyzed using the pClamp 9.0 software (Molecular Devices) for intrinsic properties and MiniAnalysis for mini-events. Data are presented as mean ± s.e.m.. The comparison of results before and after treatments was done by Mann-Whitney test.

Chapter 5. Discussion and future directions

5.1 Significance of thesis work

To understand how brain works has been one of the most important and intriguing questions a scientist could ask. However, this is probably also the one of the most difficult question to answer. Emerson M. Pugh once said, “If the brain were so simple that we could understand it, we would be so simple we couldn't.” The structure, functional and dynamic complexity of the brain created numerous difficulties for neuroscience researchers.

A great portion of the structure complexity of the brain comes from its cellular heterogeneity. In the mammalian brain, neural circuits often consist of diverse cells types characterized by their stereotyped location, connectivity patterns, and physiological properties. To a large extent, the identity and physiological state of neuron types are determined by their patterns of gene expression. Therefore, a comprehensive understanding of gene expression and regulation in defined cell types not only provides a molecular explanation of cell phenotypes but also is necessary for establishing the link from gene function to neural circuit organization and dynamics.

Until recently, most genomic studies of the brain use tissue homogenates where the distinction among cell types is completely lost; thus both the detection and interpretation of gene expression changes are very problematic. Our lab has been aiming for a systematic survey of genomic and epigenomic information on a cell type specific level within the brain. However, analysis of gene expression, including miRNA expression, in

the brain has posed a major challenge in genomics despite rapid advances in sequencing technology, because neuronal subtypes are highly heterogeneous and intermixed.

GABAergic interneurons, as numerical minority in mouse neocortex compared to pyramidal neurons, contribute to a greater part of the cellular heterogeneity. The Cre driver lines developed in our lab is critical to the establishment of experimental systems that allow precise and reliable identification and manipulation of distinct interneuron cell types. These GABA drivers set the stage for a systematic and comprehensive analysis of cortical GABAergic circuits, from cell fate specification, migration, connectivity, to their functions in network dynamics and behavior. Beyond this, as GABAergic neurons are basic components of neural circuits throughout the mammalian brain, these GABA drivers will also prove useful for analyzing many other brain systems and circuits.

Besides contributing to the generation of GABAergic driver mouse lines, my thesis research has been mainly focused on cell type specific miRNA analysis, which is an essential component of our "grand plan" of cell type specific genomic and epigenomic analysis in the brain. miRNA is a class of 20-23nt small non-coding RNA which could regulate mRNA stability and translation on a sequence specific manner. Along with transcriptional factors, they constitute the largest family of cis-acting gene expression regulators. miRNAs can also influence transcription by regulating the translation of transcriptional factors. miRNAs are expressed at diverse patterns and involved in various developmental and physiological processes. The mammalian brain is a prominent site for

miRNAs expression, and recently studies begin to reveal their critical role from synaptic level to system level.

In order to enable cell type specific miRNA expression analysis, I have developed a miRNA affinity purification system (miRAP) and illustrated its utility by profiling five specific neuron types within mouse neocortex and cerebellum. Our comparative analysis among these cell types reveals distinct expression of a large number of miRNAs in glutamatergic and GABAergic neurons, and subtypes of GABAergic neurons. This provided basis for future studies of miRNA function in these neurons and demonstrate our method is an an enabling technology for studies of the miRNA biology of specific cell types in even the most heterogeneous cell populations, such as those that occur in the brain. This method will also enable systematic analysis of miRNA expression on a cell type specific level in any other complex tissues in mice giving appropriate cre driver lines.

The data from the last part of my thesis study, Dicer inactivation in specific subtype of neocortical interneurons, was less encouraging, as the results were mostly negative. However, this does not mean miRNAs were not important for interneuron function. Besides the experiment caveats and possible explanations I have discussed in last chapter, the functional complexity of neuronal system has made it rather difficult to fully assess the phenotype of Dicer knock out. With a better understanding of miRNA expression pattern on the cell type level gained through my profiling study, it will be more interesting to assess individual candidate miRNA's function in specific cell types.

5.2 Future directions

5.2.1 Profiling across development stages

The construction of the cortical GABAergic system begins during embryonic and early postnatal period, when genetic programs direct the generation of diverse cell types (Wonders and Anderson, 2006), the appropriate distribution of these cell types in defined cortical areas (Marin and Rubenstein 2001) and the specific wiring of the input and output of each cell type (Huang, Di Cristo et al. 2007). The subsequent developmental maturation of inhibitory interneurons is a prolonged process, often extending into adolescence, and involves the acquisition of characteristic innervation patterns, the sharpening of distinct physiological properties, and the emergence of various network dynamics (Huang, Di Cristo et al. 2007).

Purkinje cells in the cerebellum also go through a postnatal maturation process. At birth, Purkinje cells arranged in clusters with immature neuronal morphology rudimentary synaptic innervation. During the first three weeks, they undergo a robust outgrowth of their dendrites, form elaborate arborizations and acquire characteristic synapitic connections.

The genetic blueprint for cellular development should be mirrored by their gene expression profiles. In order for this series of postnatal development events to proceed smoothly, expression of specific genes and gene groups must be controlled in a timely way at each developmental stage. miRNAs are important regulators of gene expression, therefore could play critical roles during these processes.

In order to study miRNA function in GABAergic neuron development, I plan to perform miRAP and deep sequencing in cortical PV, SST, VIP neurons, and cerebellar Purkinje cells across development (at P7, P14, P21, P28, P35 and P56). Currently, I have finished collecting samples for cortical SST neurons and Purkinje cells. Data is waiting for bioinformatic analysis. miRNAs which are highly expressed in specific cell type and show interesting developmental changes will be our focus of future studies.

5.2.2 Integrated analysis of cell type specific miRNA and mRNA profiles

Molecular approaches to understanding the function of the nervous system promise new insights into the relationship between genes, circuits, behavior, and plasticity. miRNA profiles alone, although informative, are insufficient to direct functional studies of individual miRNAs, mainly because it is difficult to accurately predict miRNA targets by bioinformatic analysis alone without extensive experimental validation. However, simultaneous analysis of mRNA and miRNA profiles will facilitate the discovery of physiological miRNA-mRNA pairs and portrait the gene regulatory network in specific cell types.

There are two approaches to do so. The easier one is to obtain miRNA profiles and mRNA profiles from the same cell type at different developmental stages separately, and then analyze them together. The changes in miRNA expression will induce corresponding changes of their target mRNA in an opposite direction. By looking at the pattern during development, one may be able to fish out mRNA targets for certain miRNAs. Anirban Paul in our lab has generated mRNA profiles from manually sorted Purkinje cells during

postnatal development at the same time line with the miRNA samples I collected with miRAP. We propose to analyze these two data sets together. The other appraoche is to obtain miRNA and mRNA target profiles simultaneously by Ago2-CLIP (Chi, Zang et al. 2009). In theory, with the *LSL-tAgo2* mice I could perform cell type specific Ago2-CLIP using antibody recognizing the epitope tag. It is not clear yet if the amount of tAGO2 in defined cell types is sufficient for CLIP experiment, as the efficiency of UV-crosslinking is low. Nonetheless, we would like to test it for abundant cell types in the brain.

5.2.3 miRNA profiling studies in animal models

The use of Cre-loxP system in our miRAP method makes it easy to plug our method into animal models of disease and genetic, pharmacological or environmental perturbations.

Accumulating evidence indicates that microRNAs play crucial roles in human disease development, progression, prognosis, diagnosis and evaluation of treatment response (Nicolas and Lopez-Martinez 2010). Although studies in cancer field are leading the way, dysfunction of miRNAs is also commonly implicated in the pathogenesis of central nervous system (Eacker, Dawson et al. 2009). These include genetic disorders such as fragile X mental retardation(Jin, Alisch et al. 2004), Huntington disease(Lee, Chu et al. 2011) and Alzheimer disease(Maes, Chertkow et al. 2009), as well as other more complex conditions such as autism(Miller and Wahlestedt 2010), schizophrenia, neurodegeneration(Eacker, Dawson et al. 2009) and addiction(Dreyer 2010). It will be interesting to examine miRNA profiles in a cell type specific manner in

mouse models of these neurological diseases. This will help to identify the roles of miRNAs and their target genes and signaling pathways in neurological disorders and provide a novel class of therapeutic targets.

Neuronal activity can regulate miRNA function by affecting their production (Lugli, Larson et al. 2005; Nudelman, DiRocco et al. 2010) or their association with effector complex (Lugli, Larson et al. 2005; Ashraf, McLoon et al. 2006); on the other hand, miRNAs can work as modulators of neuron activity and plasticity (Schratt 2009). At mature synapse, miRNA could fine tune local protein expression and regulate receptor concentration transiently. During development, miRNA can regulate dendritogenesis, synapse formation and synapse maturation, exerting long lasting effect. Profiling studies under functional manipulations, such as sensory deprivation or stress, will help to elucidate the relationship and logic between miRNA and neuronal activity in different subsets of neurons.

List of Reference

Abu-Elneel, K., T. Liu, et al. (2008). "Heterogeneous dysregulation of microRNAs across the autism spectrum." Neurogenetics **9**(3): 153-161.

Allman, J. (1999). "Evolving Brains." Scientific American Library, HPHLP, New York.

Altuvia, Y., P. Landgraf, et al. (2005). "Clustering and conservation patterns of human microRNAs." Nucleic acids research **33**(8): 2697-2706.

Arlotta, P., B. J. Molyneaux, et al. (2005). "Neuronal subtype-specific genes that control corticospinal motor neuron development in vivo." Neuron **45**(2): 207-221.

Asada, H., Y. Kawamura, et al. (1997). "Cleft palate and decreased brain gamma-aminobutyric acid in mice lacking the 67-kDa isoform of glutamic acid decarboxylase." Proc Natl Acad Sci U S A **94**(12): 6496-6499.

Ascoli, G. A., L. Alonso-Nanclares, et al. (2008). "Petilla terminology: nomenclature of features of GABAergic interneurons of the cerebral cortex." Nat Rev Neurosci **9**(7): 557-568.

Ashraf, S. I., A. L. McLoon, et al. (2006). "Synaptic protein synthesis associated with memory is regulated by the RISC pathway in Drosophila." Cell **124**(1): 191-205.

Baehrecke, E. H. (2003). "miRNAs: micro managers of programmed cell death." Curr Biol **13**(12): R473-475.

Bak, M., A. Silahtaroglu, et al. (2008). "MicroRNA expression in the adult mouse central nervous system." RNA **14**(3): 432-444.

Bartel, D. P. (2004). "MicroRNAs: genomics, biogenesis, mechanism, and function." Cell **116**(2): 281-297.

Bartos, M., I. Vida, et al. (2007). "Synaptic mechanisms of synchronized gamma oscillations in inhibitory interneuron networks." Nat Rev Neurosci **8**(1): 45-56.

Baskerville, S. and D. P. Bartel (2005). "Microarray profiling of microRNAs reveals frequent coexpression with neighboring miRNAs and host genes." Rna **11**(3): 241-247.

Batista-Brito, R. and G. Fishell (2009). "The developmental integration of cortical interneurons into a functional network." Curr Top Dev Biol **87**: 81-118.

Beitzinger, M., L. Peters, et al. (2007). "Identification of human microRNA targets from isolated argonaute protein complexes." RNA Biol **4**(2): 76-84.

Berezikov, E., W. J. Chung, et al. (2007). "Mammalian mirtron genes." Mol Cell **28**(2): 328-336.

Berger, T. K., R. Perin, et al. (2009). "Frequency-dependent disynaptic inhibition in the pyramidal network: a ubiquitous pathway in the developing rat neocortex." J Physiol **587**(Pt 22): 5411-5425.

Bernstein, E., S. Y. Kim, et al. (2003). "Dicer is essential for mouse development." Nat Genet **35**(3): 215-217.

Blow, M. J., R. J. Grocock, et al. (2006). "RNA editing of human microRNAs." Genome biology **7**(4): R27.

Bourgin, P., V. Fabre, et al. (2007). "Cortistatin promotes and negatively correlates with slow-wave sleep." Eur J Neurosci **26**(3): 729-738.

Bredt, D. S. and S. H. Snyder (1994). "Transient nitric oxide synthase neurons in embryonic cerebral cortical plate, sensory ganglia, and olfactory epithelium." Neuron **13**(2): 301-313.

Brennecke, J., A. Stark, et al. (2005). "Principles of microRNA-target recognition." PLoS Biol **3**(3): e85.

Brennicke, A., A. Marchfelder, et al. (1999). "RNA editing." FEMS microbiology reviews **23**(3): 297-316.

Burmistrova, O. A., A. Y. Goltsov, et al. (2007). "MicroRNA in schizophrenia: genetic and expression analysis of miR-130b (22q11)." Biochemistry (Mosc) **72**(5): 578-582.

Burns, C. M., H. Chu, et al. (1997). "Regulation of serotonin-2C receptor G-protein coupling by RNA editing." Nature **387**(6630): 303-308.

Bushati, N. and S. M. Cohen (2008). "MicroRNAs in neurodegeneration." Current opinion in neurobiology **18**(3): 292-296.

Buzsaki, G. (2001). "Hippocampal GABAergic interneurons: a physiological perspective." Neurochem Res **26**(8-9): 899-905.

Buzsaki, G., C. Geisler, et al. (2004). "Interneuron Diversity series: Circuit complexity and axon wiring economy of cortical interneurons." Trends Neurosci **27**(4): 186-193.

Calin, G. A. and C. M. Croce (2006). "MicroRNA signatures in human cancers." Nat Rev Cancer **6**(11): 857-866.

Cauli, B. and E. Hamel (2010). "Revisiting the role of neurons in neurovascular coupling." Front Neuroenergetics **2**: 9.

Cauli, B., X. K. Tong, et al. (2004). "Cortical GABA interneurons in neurovascular coupling: relays for subcortical vasoactive pathways." J Neurosci **24**(41): 8940-8949.

Celio, M. R. and C. W. Heizmann (1981). "Calcium-binding protein parvalbumin as a neuronal marker." Nature **293**(5830): 300-302.

Chan, J. A., A. M. Krichevsky, et al. (2005). "MicroRNA-21 is an antiapoptotic factor in human glioblastoma cells." Cancer Res **65**(14): 6029-6033.

Chang, S., R. J. Johnston, Jr., et al. (2004). "MicroRNAs act sequentially and asymmetrically to control chemosensory laterality in the nematode." Nature **430**(7001): 785-789.

Chattopadhyaya, B., G. Di Cristo, et al. (2004). "Experience and activity-dependent maturation of perisomatic GABAergic innervation in primary visual cortex during a postnatal critical period." J Neurosci **24**(43): 9598-9611.

Cheloufi, S., C. O. Dos Santos, et al. (2010). "A dicer-independent miRNA biogenesis pathway that requires Ago catalysis." Nature **465**(7298): 584-589.

Chen, C. X., D. S. Cho, et al. (2000). "A third member of the RNA-specific adenosine deaminase gene family, ADAR3, contains both single- and double-stranded RNA binding domains." RNA **6**(5): 755-767.

Cheng, H. Y., J. W. Papp, et al. (2007). "microRNA modulation of circadian-clock period and entrainment." Neuron **54**(5): 813-829.

Chi, S. W., J. B. Zang, et al. (2009). "Argonaute HITS-CLIP decodes microRNA-mRNA interaction maps." Nature **460**(7254): 479-486.

Chi, S. W., J. B. Zang, et al. (2009). "Argonaute HITS-CLIP decodes microRNA–mRNA interaction maps." Nature.

Chiang, H. R., L. W. Schoenfeld, et al. (2010). "Mammalian microRNAs: experimental evaluation of novel and previously annotated genes." Genes & development **24**(10): 992-1009.

Christensen, M. and G. M. Schratt (2009). "microRNA involvement in developmental and functional aspects of the nervous system and in neurological diseases." Neurosci Lett **466**(2): 55-62.

Cogswell, J. P., J. Ward, et al. (2008). "Identification of miRNA changes in Alzheimer's disease brain and CSF yields putative biomarkers and insights into disease pathways." Journal of Alzheimer's disease : JAD **14**(1): 27-41.

Cohen, S. M., J. Brennecke, et al. (2006). "Denoising feedback loops by thresholding--a new role for microRNAs." Genes Dev **20**(20): 2769-2772.

Cougot, N., S. N. Bhattacharyya, et al. (2008). "Dendrites of mammalian neurons contain specialized P-body-like structures that respond to neuronal activation." J Neurosci **28**(51): 13793-13804.

Cuellar, T. L., T. H. Davis, et al. (2008). "Dicer loss in striatal neurons produces behavioral and neuroanatomical phenotypes in the absence of neurodegeneration." Proc Natl Acad Sci U S A **105**(14): 5614-5619.

David, C., A. Schleicher, et al. (2007). "The innervation of parvalbumin-containing interneurons by VIP-immunopositive interneurons in the primary somatosensory cortex of the adult rat." Eur J Neurosci **25**(8): 2329-2340.

Davis, T. H., T. L. Cuellar, et al. (2008). "Conditional loss of Dicer disrupts cellular and tissue morphogenesis in the cortex and hippocampus." J Neurosci **28**(17): 4322-4330.

Dawson, T. R., C. L. Sansam, et al. (2004). "Structure and sequence determinants required for the RNA editing of ADAR2 substrates." The Journal of biological chemistry **279**(6): 4941-4951.

de Lecea, L. (2008). "Cortistatin--functions in the central nervous system." Mol Cell Endocrinol **286**(1-2): 88-95.

de Lecea, L., J. R. Criado, et al. (1996). "A cortical neuropeptide with neuronal depressant and sleep-modulating properties." Nature **381**(6579): 242-245.

de Lecea, L., J. A. del Rio, et al. (1997). "Cortistatin is expressed in a distinct subset of cortical interneurons." J Neurosci **17**(15): 5868-5880.

de Lecea, L., J. A. del Rio, et al. (1995). "Developmental expression of parvalbumin mRNA in the cerebral cortex and hippocampus of the rat." Brain Res Mol Brain Res **32**(1): 1-13.

De Pietri Tonelli, D., J. N. Pulvers, et al. (2008). "miRNAs are essential for survival and differentiation of newborn neurons but not for expansion of neural progenitors during early neurogenesis in the mouse embryonic neocortex." Development **135**(23): 3911-3921.

Di Cristo, G., C. Wu, et al. (2004). "Subcellular domain-restricted GABAergic innervation in primary visual cortex in the absence of sensory and thalamic inputs." Nat Neurosci **7**(11): 1184-1186.

Dracheva, S., R. Lyddon, et al. (2009). "Editing of serotonin 2C receptor mRNA in the prefrontal cortex characterizes high-novelty locomotor response behavioral trait." Neuropsychopharmacology : official publication of the American College of Neuropsychopharmacology **34**(10): 2237-2251.

Dreyer, J. L. (2010). "New insights into the roles of microRNAs in drug addiction and neuroplasticity." Genome medicine **2**(12): 92.

Dymecki, S. M. and J. C. Kim (2007). "Molecular neuroanatomy's "Three Gs": a primer." Neuron **54**(1): 17-34.

Eacker, S. M., T. M. Dawson, et al. (2009). "Understanding microRNAs in neurodegeneration." Nature reviews. Neuroscience **10**(12): 837-841.

Easow, G., A. A. Teleman, et al. (2007). "Isolation of microRNA targets by miRNP immunopurification." RNA **13**(8): 1198-1204.

Eisen, M. B., P. T. Spellman, et al. (1998). "Cluster analysis and display of genome-wide expression patterns." Proceedings of the National Academy of Sciences of the United States of America **95**(25): 14863-14868.

Eulalio, A., E. Huntzinger, et al. (2009). "Deadenylation is a widespread effect of miRNA regulation." RNA **15**(1): 21-32.

Faller, M. and F. Guo (2008). "MicroRNA biogenesis: there's more than one way to skin a cat." Biochim Biophys Acta **1779**(11): 663-667.

Fiore, R., S. Khudayberdiev, et al. (2009). "Mef2-mediated transcription of the miR379-410 cluster regulates activity-dependent dendritogenesis by fine-tuning Pumilio2 protein levels." The EMBO journal **28**(6): 697-710.

Friedlander, M. R., W. Chen, et al. (2008). "Discovering microRNAs from deep sequencing data using miRDeep." Nature biotechnology **26**(4): 407-415.

Fuentealba, P., R. Begum, et al. (2008). "Ivy cells: a population of nitric-oxide-producing, slow-spiking GABAergic neurons and their involvement in hippocampal network activity." Neuron **57**(6): 917-929.

Gantier, M. P., C. E. McCoy, et al. (2011). "Analysis of microRNA turnover in mammalian cells following Dicer1 ablation." Nucleic acids research.

Gehrke, S., Y. Imai, et al. (2010). "Pathogenic LRRK2 negatively regulates microRNA-mediated translational repression." Nature **466**(7306): 637-641.

Gelman, D. M. and O. Marin (2010). "Generation of interneuron diversity in the mouse cerebral cortex." Eur J Neurosci **31**(12): 2136-2141.

Gerashchenko, D., J. P. Wisor, et al. (2008). "Identification of a population of sleep-active cerebral cortex neurons." Proc Natl Acad Sci U S A **105**(29): 10227-10232.

Giraldez, A. J., R. M. Cinalli, et al. (2005). "MicroRNAs regulate brain morphogenesis in zebrafish." Science **308**(5723): 833-838.

Gonchar, Y., Q. Wang, et al. (2007). "Multiple distinct subtypes of GABAergic neurons in mouse visual cortex identified by triple immunostaining." Front Neuroanat **1**: 3.

Gregory, R. I., T. P. Chendrimada, et al. (2006). "MicroRNA biogenesis: isolation and characterization of the microprocessor complex." Methods Mol Biol **342**: 33-47.

Grimson, A., K. K. Farh, et al. (2007). "MicroRNA targeting specificity in mammals: determinants beyond seed pairing." Mol Cell **27**(1): 91-105.

Hammell, M., D. Long, et al. (2008). "mirWIP: microRNA target prediction based on microRNA-containing ribonucleoprotein-enriched transcripts." Nat Methods **5**(9): 813-819.

Hammond, S. M., S. Boettcher, et al. (2001). "Argonaute2, a link between genetic and biochemical analyses of RNAi." Science **293**(5532): 1146-1150.

Haubensak, W., P. S. Kunwar, et al. (2010). "Genetic dissection of an amygdala microcircuit that gates conditioned fear." Nature **468**(7321): 270-276.

Hawkins, P. G. and K. V. Morris (2008). "RNA and transcriptional modulation of gene expression." Cell Cycle **7**(5): 602-607.

Hayashi, S. and A. P. McMahon (2002). "Efficient recombination in diverse tissues by a tamoxifen-inducible form of Cre: a tool for temporally regulated gene activation/inactivation in the mouse." Developmental biology **244**(2): 305-318.

He, L. and G. J. Hannon (2004). "MicroRNAs: small RNAs with a big role in gene regulation." Nat Rev Genet **5**(7): 522-531.

Hebert, S. S., K. Horre, et al. (2009). "MicroRNA regulation of Alzheimer's Amyloid precursor protein expression." Neurobiol Dis **33**(3): 422-428.

Heiman, M., A. Schaefer, et al. (2008). "A Translational Profiling Approach for the Molecular Characterization of CNS Cell Types." Cell **135**(4): 738-748.

Heiman, M., A. Schaefer, et al. (2008). "A translational profiling approach for the molecular characterization of CNS cell types." Cell **135**(4): 738-748.

Hendrickson, D. G., D. J. Hogan, et al. (2008). "Systematic identification of mRNAs recruited to argonaute 2 by specific microRNAs and corresponding changes in transcript abundance." PLoS One **3**(5): e2126.

Hernandez-Miranda, L. R., J. G. Parnavelas, et al. (2010). "Molecules and mechanisms involved in the generation and migration of cortical interneurons." ASN Neuro **2**(2): e00031.

Hernando, E. (2007). "microRNAs and cancer: role in tumorigenesis, patient classification and therapy." Clinical & translational oncology : official publication of the Federation of Spanish Oncology Societies and of the National Cancer Institute of Mexico **9**(3): 155-160.

Higo, S., K. Akashi, et al. (2009). "Subtypes of GABAergic neurons project axons in the neocortex." Front Neuroanat **3**: 25.

Hippenmeyer, S., E. Vrieseling, et al. (2005). "A developmental switch in the response of DRG neurons to ETS transcription factor signaling." PLoS Biol **3**(5): e159.

Hobert, O. (2004). "Common logic of transcription factor and microRNA action." Trends Biochem Sci **29**(9): 462-468.

Hobert, O. (2008). "Gene regulation by transcription factors and microRNAs." Science **319**(5871): 1785-1786.

Hobert, O., I. Carrera, et al. (2010). "The molecular and gene regulatory signature of a neuron." Trends in neurosciences **33**(10): 435-445.

Hodges, A., A. D. Strand, et al. (2006). "Regional and cellular gene expression changes in human Huntington's disease brain." Human molecular genetics **15**(6): 965-977.

Hollander, J. A., H. I. Im, et al. (2010). "Striatal microRNA controls cocaine intake through CREB signalling." Nature **466**(7303): 197-202.

Hu, H. Y., Z. Yan, et al. (2009). "Sequence features associated with microRNA strand selection in humans and flies." BMC Genomics **10**: 413.

Huang, Z. J., G. Di Cristo, et al. (2007). "Development of GABA innervation in the cerebral and cerebellar cortices." Nat Rev Neurosci **8**(9): 673-686.

Ikeda, K., M. Satoh, et al. (2006). "Detection of the argonaute protein Ago2 and microRNAs in the RNA induced silencing complex (RISC) using a monoclonal antibody." J Immunol Methods **317**(1-2): 38-44.

Jin, P., R. S. Alisch, et al. (2004). "RNA and microRNAs in fragile X mental retardation." Nat Cell Biol **6**(11): 1048-1053.

Jinno, S. and T. Kosaka (2002). "Patterns of expression of calcium binding proteins and neuronal nitric oxide synthase in different populations of hippocampal GABAergic neurons in mice." J Comp Neurol **449**(1): 1-25.

Johnston, R. J. and O. Hobert (2003). "A microRNA controlling left/right neuronal asymmetry in Caenorhabditis elegans." Nature **426**(6968): 845-849.

Johnston, R. J., Jr., S. Chang, et al. (2005). "MicroRNAs acting in a double-negative feedback loop to control a neuronal cell fate decision." Proc Natl Acad Sci U S A **102**(35): 12449-12454.

Jonas, P., J. Bischofberger, et al. (2004). "Interneuron Diversity series: Fast in, fast out--temporal and spatial signal processing in hippocampal interneurons." Trends Neurosci **27**(1): 30-40.

Karres, J. S., V. Hilgers, et al. (2007). "The conserved microRNA miR-8 tunes atrophin levels to prevent neurodegeneration in Drosophila." Cell **131**(1): 136-145.

Kash, S. F., L. H. Tecott, et al. (1999). "Increased anxiety and altered responses to anxiolytics in mice deficient in the 65-kDa isoform of glutamic acid decarboxylase." Proc Natl Acad Sci U S A **96**(4): 1698-1703.

Kawahara, Y., K. Ito, et al. (2003). "Low editing efficiency of GluR2 mRNA is associated with a low relative abundance of ADAR2 mRNA in white matter of normal human brain." The European journal of neuroscience **18**(1): 23-33.

Kawahara, Y., M. Megraw, et al. (2008). "Frequency and fate of microRNA editing in human brain." Nucleic Acids Res **36**(16): 5270-5280.

Kawahara, Y., B. Zinshteyn, et al. (2007). "Redirection of silencing targets by adenosine-to-inosine editing of miRNAs." Science **315**(5815): 1137-1140.

Kilduff, T. S., B. Cauli, et al. (2011). "Activation of cortical interneurons during sleep: an anatomical link to homeostatic sleep regulation?" Trends Neurosci **34**(1): 10-19.

Kim, J., K. Inoue, et al. (2007). "A MicroRNA feedback circuit in midbrain dopamine neurons." Science **317**(5842): 1220-1224.

Klausberger, T. (2009). "GABAergic interneurons targeting dendrites of pyramidal cells in the CA1 area of the hippocampus." Eur J Neurosci **30**(6): 947-957.

Klausberger, T. and P. Somogyi (2008). "Neuronal diversity and temporal dynamics: the unity of hippocampal circuit operations." Science **321**(5885): 53-57.

Krichevsky, A. M., K. C. Sonntag, et al. (2006). "Specific microRNAs modulate embryonic stem cell-derived neurogenesis." Stem Cells **24**(4): 857-864.

Kubota, Y., N. Shigematsu, et al. (2011). "Selective Coexpression of Multiple Chemical Markers Defines Discrete Populations of Neocortical GABAergic Neurons." Cereb Cortex.

Kuwabara, T., J. Hsieh, et al. (2004). "A small modulatory dsRNA specifies the fate of adult neural stem cells." Cell **116**(6): 779-793.

Landgraf, P., M. Rusu, et al. (2007). "A mammalian microRNA expression atlas based on small RNA library sequencing." Cell **129**(7): 1401-1414.

Lee, R. C., R. L. Feinbaum, et al. (1993). "The C. elegans heterochronic gene lin-4 encodes small RNAs with antisense complementarity to lin-14." Cell **75**(5): 843-854.

Lee, S. T., K. Chu, et al. (2011). "Altered microRNA regulation in Huntington's disease models." Experimental neurology **227**(1): 172-179.

Leung, W. S., M. C. Lin, et al. (2008). "Filtering of false positive microRNA candidates by a clustering-based approach." BMC Bioinformatics **9 Suppl 12**: S3.

Li, Y., F. Wang, et al. (2006). "MicroRNA-9a ensures the precise specification of sensory organ precursors in Drosophila." Genes Dev **20**(20): 2793-2805.

Lim, L. P., N. C. Lau, et al. (2005). "Microarray analysis shows that some microRNAs downregulate large numbers of target mRNAs." Nature **433**(7027): 769-773.

Ling, K. H., P. J. Brautigan, et al. (2011). "Deep sequencing analysis of the developing mouse brain reveals a novel microRNA." BMC Genomics **12**(1): 176.

Liu, J., F. V. Rivas, et al. (2005). "A role for the P-body component GW182 in microRNA function." Nat Cell Biol **7**(12): 1261-1266.

Liu, N. K., X. F. Wang, et al. (2009). "Altered microRNA expression following traumatic spinal cord injury." Exp Neurol **219**(2): 424-429.

Liu, N. K. and X. M. Xu (2011). "MicroRNA in Central Nervous System Trauma and Degenerative Disorders." Physiological genomics.

Lobo, M. K., S. L. Karsten, et al. (2006). "FACS-array profiling of striatal projection neuron subtypes in juvenile and adult mouse brains." Nat Neurosci **9**(3): 443-452.

Lu, C., B. C. Meyers, et al. (2007). "Construction of small RNA cDNA libraries for deep sequencing." Methods **43**(2): 110-117.

Lu, D. P., R. L. Read, et al. (2005). "PCR-based expression analysis and identification of microRNAs." Journal of RNAi and gene silencing : an international journal of RNA and gene targeting research **1**(1): 44-49.

Lu, J., G. Getz, et al. (2005). "MicroRNA expression profiles classify human cancers." Nature **435**(7043): 834-838.

Luciano, D. J., H. Mirsky, et al. (2004). "RNA editing of a miRNA precursor." RNA **10**(8): 1174-1177.

Lugli, G., J. Larson, et al. (2005). "Dicer and eIF2c are enriched at postsynaptic densities in adult mouse brain and are modified by neuronal activity in a calpain-dependent manner." J Neurochem **94**(4): 896-905.

Lugli, G., V. I. Torvik, et al. (2008). "Expression of microRNAs and their precursors in synaptic fractions of adult mouse forebrain." J Neurochem **106**(2): 650-661.

Lund, E. and J. E. Dahlberg (2006). "Substrate selectivity of exportin 5 and Dicer in the biogenesis of microRNAs." Cold Spring Harb Symp Quant Biol **71**: 59-66.

Luo, L., E. M. Callaway, et al. (2008). "Genetic dissection of neural circuits." Neuron **57**(5): 634-660.

Madisen, L., T. A. Zwingman, et al. (2010). "A robust and high-throughput Cre reporting and characterization system for the whole mouse brain." Nat Neurosci **13**(1): 133-140.

Maes, O. C., H. M. Chertkow, et al. (2009). "MicroRNA: Implications for Alzheimer Disease and other Human CNS Disorders." Curr Genomics **10**(3): 154-168.

Marin, O. and J. L. Rubenstein (2001). "A long, remarkable journey: tangential migration in the telencephalon." Nat Rev Neurosci **2**(11): 780-790.

Markram, H., M. Toledo-Rodriguez, et al. (2004). "Interneurons of the neocortical inhibitory system." Nat Rev Neurosci **5**(10): 793-807.

Meguro, R., J. Lu, et al. (2004). "Static, transient and permanent organization of GABA receptor expression in calbindin-positive interneurons in response to amygdala kindled seizures." J Neurochem **91**(1): 144-154.

Meister, G., M. Landthaler, et al. (2004). "Human Argonaute2 mediates RNA cleavage targeted by miRNAs and siRNAs." Mol Cell **15**(2): 185-197.

Miller, B. H. and C. Wahlestedt (2010). "MicroRNA dysregulation in psychiatric disease." Brain Res **1338**: 89-99.

Minones-Moyano, E., S. Porta, et al. (2011). "MicroRNA profiling of Parkinson's disease brains identifies early downregulation of miR-34b/c which modulate mitochondrial function." Human molecular genetics **20**(15): 3067-3078.

Miska, E. A., E. Alvarez-Saavedra, et al. (2004). "Microarray analysis of microRNA expression in the developing mammalian brain." Genome Biol **5**(9): R68.

Miyoshi, G., S. J. Butt, et al. (2007). "Physiologically distinct temporal cohorts of cortical interneurons arise from telencephalic Olig2-expressing precursors." J Neurosci **27**(29): 7786-7798.

Miyoshi, G., J. Hjerling-Leffler, et al. (2010). "Genetic fate mapping reveals that the caudal ganglionic eminence produces a large and diverse population of superficial cortical interneurons." J Neurosci **30**(5): 1582-1594.

Monyer, H. and H. Markram (2004). "Interneuron Diversity series: Molecular and genetic tools to study GABAergic interneuron diversity and function." Trends in neurosciences **27**(2): 90-97.

Mourelatos, Z., J. Dostie, et al. (2002). "miRNPs: a novel class of ribonucleoproteins containing numerous microRNAs." Genes Dev **16**(6): 720-728.

Murchison, E. P., J. F. Partridge, et al. (2005). "Characterization of Dicer-deficient murine embryonic stem cells." Proc Natl Acad Sci U S A **102**(34): 12135-12140.

Nave, K. A. (2010). "Oligodendrocytes and the "micro brake" of progenitor cell proliferation." Neuron **65**(5): 577-579.

Nelson, P. T., D. A. Baldwin, et al. (2004). "Microarray-based, high-throughput gene expression profiling of microRNAs." Nature methods **1**(2): 155-161.

Nelson, P. T., W. X. Wang, et al. (2008). "MicroRNAs (miRNAs) in neurodegenerative diseases." Brain pathology **18**(1): 130-138.

Nelson, S. B., C. Hempel, et al. (2006). "Probing the transcriptome of neuronal cell types." Curr Opin Neurobiol **16**(5): 571-576.

Nicolas, F. E. and A. F. Lopez-Martinez (2010). "MicroRNAs in human diseases." Recent patents on DNA & gene sequences **4**(3): 142-154.

Nishikura, K. (2010). "Functions and regulation of RNA editing by ADAR deaminases." Annual review of biochemistry **79**: 321-349.

Niswender, C. M., E. Sanders-Bush, et al. (1998). "Identification and Characterization of RNA Editing Events within the 5-HT2C Receptora." Annals of the New York Academy of Sciences **861**(1): 38-48.

Nudelman, A. S., D. P. DiRocco, et al. (2010). "Neuronal activity rapidly induces transcription of the CREB-regulated microRNA-132, in vivo." Hippocampus **20**(4): 492-498.

Obernosterer, G., J. Martinez, et al. (2007). "Locked nucleic acid-based in situ detection of microRNAs in mouse tissue sections." Nature protocols **2**(6): 1508-1514.

Olah, S., M. Fule, et al. (2009). "Regulation of cortical microcircuits by unitary GABA-mediated volume transmission." Nature **461**(7268): 1278-1281.

Packer, A. N., Y. Xing, et al. (2008). "The bifunctional microRNA miR-9/miR-9* regulates REST and CoREST and is downregulated in Huntington's disease." J Neurosci **28**(53): 14341-14346.

Papagiannakopoulos, T., A. Shapiro, et al. (2008). "MicroRNA-21 targets a network of key tumor-suppressive pathways in glioblastoma cells." Cancer Res **68**(19): 8164-8172.

Pena, J. T., C. Sohn-Lee, et al. (2009). "miRNA in situ hybridization in formaldehyde and EDC-fixed tissues." Nat Methods **6**(2): 139-141.

Perkins, D. O., C. D. Jeffries, et al. (2007). "microRNA expression in the prefrontal cortex of individuals with schizophrenia and schizoaffective disorder." Genome Biol **8**(2): R27.

Pillai, R. S. (2005). "MicroRNA function: multiple mechanisms for a tiny RNA?" RNA **11**(12): 1753-1761.

Pinal, C. S. and A. J. Tobin (1998). "Uniqueness and redundancy in GABA production." Perspect Dev Neurobiol **5**(2-3): 109-118.

Poole, R. J. and O. Hobert (2006). "Early embryonic programming of neuronal left/right asymmetry in C. elegans." Current biology : CB **16**(23): 2279-2292.

Pratt, A. J. and I. J. MacRae (2009). "The RNA-induced silencing complex: a versatile gene-silencing machine." The Journal of biological chemistry **284**(27): 17897-17901.

Redell, J. B., Y. Liu, et al. (2009). "Traumatic brain injury alters expression of hippocampal microRNAs: potential regulators of multiple pathophysiological processes." Journal of neuroscience research **87**(6): 1435-1448.

Redell, J. B., A. N. Moore, et al. (2010). "Human traumatic brain injury alters plasma microRNA levels." Journal of neurotrauma **27**(12): 2147-2156.

Reinhart, B. J., F. J. Slack, et al. (2000). "The 21-nucleotide let-7 RNA regulates developmental timing in Caenorhabditis elegans." Nature **403**(6772): 901-906.

Robinson, M. D., D. J. McCarthy, et al. (2010). "edgeR: a Bioconductor package for differential expression analysis of digital gene expression data." Bioinformatics **26**(1): 139-140.

Robinson, M. D. and A. Oshlack (2010). "A scaling normalization method for differential expression analysis of RNA-seq data." Genome Biol **11**(3): R25.

Ronshaugen, M., F. Biemar, et al. (2005). "The Drosophila microRNA iab-4 causes a dominant homeotic transformation of halteres to wings." Genes Dev **19**(24): 2947-2952.

Rossner, M. J., J. Hirrlinger, et al. (2006). "Global transcriptome analysis of genetically identified neurons in the adult cortex." The Journal of neuroscience : the official journal of the Society for Neuroscience **26**(39): 9956-9966.

Rudy, B., G. Fishell, et al. (2011). "Three groups of interneurons account for nearly 100% of neocortical GABAergic neurons." Developmental neurobiology **71**(1): 45-61.

Sanz, E., L. Yang, et al. (2009). "Cell-type-specific isolation of ribosome-associated mRNA from complex tissues." Proceedings of the National Academy of Sciences **106**(33): 13939-13944.

Sauer, B. and N. Henderson (1989). "Cre-stimulated recombination at loxP-containing DNA sequences placed into the mammalian genome." Nucleic acids research **17**(1): 147-161.

Schaefer, A., D. O'Carroll, et al. (2007). "Cerebellar neurodegeneration in the absence of microRNAs." The Journal of experimental medicine **204**(7): 1553-1558.

Schratt, G. (2009). "microRNAs at the synapse." Nature reviews. Neuroscience **10**(12): 842-849.

Schratt, G. M., F. Tuebing, et al. (2006). "A brain-specific microRNA regulates dendritic spine development." Nature **439**(7074): 283-289.

Sen, G. L. and H. M. Blau (2005). "Argonaute 2/RISC resides in sites of mammalian mRNA decay known as cytoplasmic bodies." Nat Cell Biol **7**(6): 633-636.

Shafi, G., N. Aliya, et al. (2010). "MicroRNA signatures in neurological disorders." Can J Neurol Sci **37**(2): 177-185.

Siva, A. C., L. J. Nelson, et al. (2009). "Molecular assays for the detection of microRNAs in prostate cancer." Mol Cancer **8**: 17.

Skalsky, R. L. and B. R. Cullen (2010). "Viruses, microRNAs, and host interactions." Annual review of microbiology **64**: 123-141.

Smith, P., A. Al Hashimi, et al. (2011). "In vivo regulation of amyloid precursor protein neuronal splicing by microRNAs." Journal of neurochemistry **116**(2): 240-247.

Soghomonian, J. J. and D. L. Martin (1998). "Two isoforms of glutamate decarboxylase: why?" Trends Pharmacol Sci **19**(12): 500-505.

Somogyi, P., G. Tamas, et al. (1998). "Salient features of synaptic organisation in the cerebral cortex." Brain Res Brain Res Rev **26**(2-3): 113-135.

Spierings, D. C., D. McGoldrick, et al. (2011). "Ordered progression of stage specific miRNA profiles in the mouse B2 B cell lineage." Blood.

Sugino, K., C. M. Hempel, et al. (2006). "Molecular taxonomy of major neuronal classes in the adult mouse forebrain." Nat Neurosci **9**(1): 99-107.

Tai, H. C. and E. M. Schuman (2006). "MicroRNA: microRNAs reach out into dendrites." Curr Biol **16**(4): R121-123.

Tan, Y., B. Zhang, et al. (2009). "Transcriptional inhibiton of Hoxd4 expression by miRNA-10a in human breast cancer cells." BMC Mol Biol **10**: 12.

Tang, F., P. Hajkova, et al. (2008). "MicroRNAs are tightly associated with RNA-induced gene silencing complexes in vivo." Biochemical and biophysical research communications **372**(1): 24-29.

Taniguchi, H., M. He, et al. (2011). "Towards a Genetic Dissection of GABAergic Circuitry in Cerebral Cortex

" Neuron **In press**.

Tanzer, A. and P. F. Stadler (2004). "Molecular evolution of a microRNA cluster." J Mol Biol **339**(2): 327-335.

Tomioka, R., K. Okamoto, et al. (2005). "Demonstration of long-range GABAergic connections distributed throughout the mouse neocortex." Eur J Neurosci **21**(6): 1587-1600.

Tomomura, M., D. S. Rice, et al. (2001). "Purification of Purkinje cells by fluorescence-activated cell sorting from transgenic mice that express green fluorescent protein." Eur J Neurosci **14**(1): 57-63.

Wang, Y., M. Toledo-Rodriguez, et al. (2004). "Anatomical, physiological and molecular properties of Martinotti cells in the somatosensory cortex of the juvenile rat." J Physiol **561**(Pt 1): 65-90.

Wienholds, E., W. P. Kloosterman, et al. (2005). "MicroRNA expression in zebrafish embryonic development." Science **309**(5732): 310-311.

Wong, S. K., S. Sato, et al. (2001). "Substrate recognition by ADAR1 and ADAR2." RNA **7**(6): 846-858.

Wu, H., J. Tao, et al. (2010). "Genome-wide analysis reveals methyl-CpG-binding protein 2-dependent regulation of microRNAs in a mouse model of Rett syndrome." Proceedings of the National Academy of Sciences of the United States of America **107**(42): 18161-18166.

Xu, B., M. Karayiorgou, et al. (2010). "MicroRNAs in psychiatric and neurodevelopmental disorders." Brain Res **1338**: 78-88.

Xu, Q., L. Guo, et al. (2008). "Sonic hedgehog signaling confers ventral telencephalic progenitors with distinct cortical interneuron fates." Neuron **65**(3): 328-340.

Xu, X. M., K. D. Roby, et al. (2010). "Immunochemical Characterization of Inhibitory Mouse Cortical Neurons: Three Chemically Distinct Classes of Inhibitory Cells." Journal of Comparative Neurology **518**(3): 389-404.

Yang, W., T. P. Chendrimada, et al. (2006). "Modulation of microRNA processing and expression through RNA editing by ADAR deaminases." Nat Struct Mol Biol **13**(1): 13-21.

Yang, Z., H. J. Edenberg, et al. (2005). "Isolation of mRNA from specific tissues of Drosophila by mRNA tagging." Nucleic Acids Res **33**(17): e148.

Yoo, A. S., A. X. Sun, et al. (2011). "MicroRNA-mediated conversion of human fibroblasts to neurons." Nature.

Zhang, L., L. Ding, et al. (2007). "Systematic identification of C. elegans miRISC proteins, miRNAs, and mRNA targets by their interactions with GW182 proteins AIN-1 and AIN-2." Mol Cell **28**(4): 598-613.

Zhao, X., X. He, et al. (2010). "MicroRNA-mediated control of oligodendrocyte differentiation." Neuron **65**(5): 612-626.